



Radboud Universiteit

Learning to self-regulate the balance of stress-related large-scale brain networks: Effects on brain activation during tasks of higher cognitive functions & vigilance

Rengin Yoldas

s1064374

MSc Thesis

Supervisor: Dr. Florian Krause

Second Reader: Dr. Nils Kohn

Cognitive Neuroscience, Faculty of Social Science

Radboud University, Nijmegen

26th August, 2022

ABSTRACT	1
1. INTRODUCTION	2
2. METHODS	5
2.1. Participants	5
2.2. Design	5
2.3. Procedure	6
2.4. Physiological Recordings	12
2.5. MRI Data Acquisition	13
2.6. Data Analysis	13
3. RESULTS	17
3.1. Random-effects whole-brain voxel-wise analysis	17
3.2. Fixed-effects whole-brain voxel-wise analysis	20
4. DISCUSSION	22
4.1. Self-regulation	23
4.2. Task-related activation	24
4.3. Self-regulation dependent changes in activation during tasks blocks	24
4.4. Limitations	26
4.5. Conclusion and Outlook	26
5. REFERENCES	28
7. SUPPLEMENTARY MATERIAL	34

Abstract

The dynamic activation balance in large-scale brain networks such as the executive control network (ECN) and the salience network (SN), in response to stress seem to be maladapted in stress-related psychopathologies. This led to the idea to train individuals in voluntary neurofeedback-based self-regulation of the activation balance in the SN and ECN. This approach could teach them a skill that can be used to influence those networks' dynamic activation shifts during and after stress. Using neurofeedback training with real-time functional Magnetic Resonance Imaging (rtfMRI), the current study implemented a paradigm teaching participants to voluntarily self-regulate the activation balance of the SN and ECN. Neural activation patterns during cognitive task performance after self-regulation periods were analysed, in order to assess if the effects of the self-regulation influence not only neural activation during the regulation but also afterwards during performance in various cognitive tasks. The involvement of the ECN in higher-order executive cognitive functions lead to the hypothesis that previous regulation to ECN would enhance task-related neural activation during a working memory task (n-back). The same effect was hypothesized for regulation to SN with respect to task-related neural activation during the oddball task, due to the increases in regions associated with the SN during the highly vigilant state in the initial response-phase to stress. The results of the random-effects analysis showed that participants were able to self-regulate the activation balance towards especially SN, without receiving any feedback. Further activation patterns during the tasks resembled activation patterns that were found in previous fMRI studies of the oddball and n-back task. However, no results supporting a modulation effect on neural activation during the tasks was observable for either task. Assuming that the size of the desired effect is smaller than expected, a follow-up fixed-effects analysis was performed. The results for this analysis, indicated amongst others 1) that prior regulation towards ECN as well as SN resulted in higher task-related activation patterns in comparison to prior resting phases, 2) that the regulation towards ECN resulted in more task-related activation during the n-back task and 3) that the regulation towards SN resulted in more task-related activation during the oddball task. Although, the results of the second analyses provided more support of the hypotheses they are only valid for the current sample. Nevertheless, they provide evidence that prior self-regulation of activation balance in stress-related brain networks affects cognitive performance. These findings support the potential of neurofeedback training as a tool to build resilience as well as targeting the maladapted activation balance of large-scale brain networks in stress-related psychopathologies.

1. Introduction

In recent years, the burden of various psychological disorders on affected individuals but also on our society has become increasingly clear (Rehm & Shield, 2019). Stress-related psychological disorders in particular, result in a decreased life quality and pose an increased risk of developing comorbid psychiatric disorders (Tian et al., 2022). Nevertheless, the human response to acute stress in itself should not be regarded as something negative (McEwen & Akil, 2020). When we encounter a “stressor” our body’s homeostatic state is disrupted (Kloet et al., 2005). As a rapid response to the stressor, we experience a heightened vigilant state during which salient stimuli are processed and an adequate plan of action to the stressor is developed and executed (Hermans et al., 2014; van Marle et al., 2009). To return to homeostasis after acute stress, this alert state is reversed and an increase in goal-directed behaviours and higher cognitive functions is observable, which all aid in this later adaptive phase (Corr et al., 2022; Hermans et al., 2014; Russell & Lightman, 2019). However, if the acute stress response is inadequate or prolonged, for example due to chronic stress exposure, the triggering of a response to stress, as well as the termination of this response can be dysfunctional (Kloet et al., 2005; Qin et al., 2009). This maladaptation of the elicited processes to stress, has been proposed as one of the reasons for the development of stress-related disorders including anxiety disorder or post-traumatic stress disorder (PTSD) (Kalisch et al., 2015; Kloet et al., 2005; McEwen & Akil, 2020; Russell & Lightman, 2019).

To understand how exactly this maladaptation manifests on a neural level, research shifted from looking into single brain regions towards investigating large-scale brain networks (Menon, 2011). Motivated by this, Menon (2011) introduced the Triple Network Model that is based on large-scale brain networks including the salience network (SN), the executive control network (ECN) and the default mode network (DMN). This model suggests that abnormal functional connectivity and activation patterns of these networks compose a crucial factor in neurological and psychological. Considering that those three networks were observed to interact within multiple cognitive functions, their involvement in various disorders that affect our cognition and behaviour is not surprising (Menon, 2011).

Investigating the role of these large-scale brain networks specifically in stress, focusing on the SN and the ECN, Hermans et al. (2014) proposed a model that describes the dynamic activation changes of large-scale brain networks in response to stress. According to this model, the activation of the SN and the ECN seem to be affected by stress-related changes in neuromodulators (Hermans et al., 2014). The neuromodulators that are involved in the reaction to a stressor, include different neurotransmitters and hormones which act in a spatially and temporally specific manner, with an initial involvement of catecholamines and neuropeptides and a later surge of corticosteroids (Hermans et al., 2014; Joëls & Baram, 2009). Spatially, these neuromodulators act on different brain regions that are connected to the SN and the ECN. Considering this and the functions assigned to each network, the observed activation-

and connectivity-shift of the SN and ECN throughout the stress response, seems to partially explain stress-related behavioural and cognitive changes (Hermans et al., 2014; Kloet et al., 2005; van Oort et al., 2017). The functions assigned to the SN are directing attention to salient internal or external stimuli as well as to further integrate this information and other preparations to yield enough energy for an appropriate response (Hermans et al., 2014; Menon, 2011). Therefore, it has been suggested that the SN supports the increased vigilant state observed in the initial phase of the stress response (Hermans et al., 2014; van Marle et al., 2009). The main regions connected to the SN include the amygdala (AMG), the thalamus (TH), the temporal poles (TP), the insular cortex (IC) and the dorsal anterior cingulate cortex (dACC) (Hermans et al., 2014; Menon, 2011; van Oort et al., 2017). The ECN has been associated with higher-order cognitive functions, including goal-directed decision making and working memory (WM) (Qin et al., 2009; van Oort et al., 2017). The observed later activation of the ECN is therefore thought to be involved in the integration of more complex behaviours that are part of the adaptation processes in the later stress response, which aims to restore a state of homeostasis (Hermans et al., 2014; Menon, 2011). The regions connected to the ECN include the posterior parietal cortex (PPC), frontal eye fields (FEF), the dorsolateral and parts of the dorsomedial prefrontal cortex (dlPFC, dmPFC) (Barrett & Satpute, 2013; Hermans et al., 2014; Menon, 2011; van Oort et al., 2017). In the context of stress-related psychopathologies, this balanced activation shift between the SN and ECN has been suggested to be out of balance, with indications of a hyperactive SN and a hypoactive ECN (Menon, 2011; Qin et al., 2009; Young et al., 2017). This suggests, that targeting this dynamic activation shift between the ECN and the SN, might therefore provide a strategy in counteracting the manifestations or the development of stress-related psychological disorder. More specifically, such a strategy could help build stress resilience by adapting the activation shift between these two networks (Krause et al., 2021).

Building resilience to stress became of increasing importance, since regardless of progress in understanding aspects of the overall response to stress (Joëls & Baram, 2009), the number of individuals affected by stress-related psychopathologies did not subside over the years (Kalisch et al., 2015; Kalisch et al., 2017). Therefore, stress research also has to focus on preventive strategies, such as increasing stress resilience in individuals (Kalisch et al., 2015). Resilience to stress can be defined as the attribute of successful adaptation or reaction to an adverse or stressful situation, without any lasting negative effects on one's mental health (Herrman et al., 2011). Thus, understanding why some individuals remain mostly unaffected by an environment that results in the development of stress-related psychopathologies in other individuals, is a core question in resilience research (Kalisch et al., 2017; Mary et al., 2020). Understanding what contributes to stress resilience and building on it, can help in developing preventive strategies and thus hopefully minimize incidences of stress-related disorders for individuals at higher risk (Kalisch et al., 2015; Kalisch et al., 2017; Krause et al., 2021). The current study aimed to explore a potential method building resilience as a preventive measure, by implementation of a real-time fMRI (rtfMRI) neurofeedback training paradigm. The aim of this training was to teach participants in voluntarily self-regulation of the activation balance between the SN and ECN, a method that has already

been successfully tested in a proof-of-concept study by Krause et al. (2021). Within that study, it was shown that participants were able to learn mental self-regulation strategies and to apply them even in the absence of any feedback on their self-regulation performance. In addition, participants effectively self-regulated in the presence of an acute stressor, which was applied via a mild but uncomfortable electrical stimulation, showing that the activation shift of the stress-related networks was possible in an experimentally induced stressful situation (Krause et al., 2021).

Building on the previous study by Krause et al. (2021), this neurofeedback training paradigm was again implemented in the current study in order to observe effects of the self-regulation on cognitive and affective functions. More specifically, the aim was to explore possible modulatory effects of cognitive performance as a result of the self-regulation (Tursic et al., 2020) within cognitive functions that are affected by stress, including vigilance and higher cognitive functioning (Hermans et al., 2014; Kloet et al., 2005). In order to do so, a sample of healthy participants was trained to voluntarily self-regulate the balance in activation of the SN and ECN, by application of mental strategies. The main aim of this thesis was, to investigate if the self-regulation resulted in changes in cognitive performance on the neural level. Therefore, participants that successfully learned to self-regulate, performed in several cognitive tasks while also applying their learned self-regulation strategies. In the following thesis, I will report and discuss the results of a full-brain analysis of the fMRI data collected during two of the implemented cognitive tasks in this study. To assess, if the self-regulation was applied effectively during the tasks, I expected that during regulation towards SN, overall brain activation was balanced towards SN and towards ECN, when participants regulated towards ECN. As mentioned above the brain regions included in the ECN are often associated with higher order cognitive functions including also WM (Daniel et al., 2016; van Oort et al., 2017; Voogd, Hermans, & Phelps, 2018). Therefore, one of the cognitive tasks included was the n-back task, which was shown to recruit cognitive resources for WM, and is thus often used to assess WM (Schoofs et al., 2008; Schoofs et al., 2013; Soveri et al., 2017). Based on the aim of the study, I expected that prior brain activation regulation towards ECN might result in stronger task-related neural activation. Since the SN's functions are associated with detecting salient stimuli (Menon, 2011), an oddball task was used to assess effects of self-regulation towards SN on the neural level. The oddball task is often used to investigate individual's ability to direct their attention towards salient stimuli and react fast to this detection (Linden et al., 1999; Rusiniak et al., 2013). The cognitive demand for the detection of and reaction to salient stimuli is comparable to the vigilant state during the rapid stress response (Kloet et al., 2005), during which the SN shows heightened activation patterns (Hermans et al., 2014). Therefore, I expected that a prior shift in activation balance towards the SN might increase task-related neural activation during the oddball task.

2. Methods

2.1. Participants

Participants for this study were recruited at Radboud University, Radboudumc and HAN University of Applied Sciences (Nijmegen, The Netherlands). The recruitment was done via an online research participation system. The study was approved by the local ethics committee. Before the participants started their participation in the study, they gave written informed consent. Exclusion criteria covered the presence of mental disorders including, psychotic disorders, personality disorders, substance use disorders or intellectual disability. At the first visit, participants filled out a screening form for MRI scans, to check for further exclusion criteria specific to MRI studies. For participation in the complete study, participants were reimbursed with €190-225. The reimbursement covered all sessions of the study, including a potential fourth neurofeedback training session, as well as an extra €25 for the three participants that were best in self-regulation of brain activation. Participants that could not complete the study received partial reimbursement. Before each session, participants were reminded to refrain from consuming caffeinated or alcoholic drinks as well as stop smoking up to six hours before the session. Additionally, a good night of sleep and rest before the session were advised.

Recruitment included 37 healthy volunteers. Out of these, four dropped out of the study, two of them because of personal reasons and two because of problems going into the MRI scanner, due to e.g. discomfort. A total of 7 participants (4 females, 3 males), aged between 18 and 29 ($M = 23.14$, $SD = 4.91$) did not learn self-regulation after neurofeedback training i.e., are *non-learners*. If participants did not learn to self-regulate their brain activity after the fourth neurofeedback training session, they were excluded. Thus, these 7 participants were excluded from the study. This resulted in 26 participants (12 females, 14 males), aged between 19 and 47 ($M = 23.65$, $SD = 6.08$), who completed the study and were therefore included in the data analysis.

2.2. Design

Overall, the study consisted of eight to nine sessions and three weeks of at-home sessions (see Fig. 1). Participants received an overview of all sessions at the start of their participation and more detailed instructions for each session right before the respective session started. After the initial visit (Localizer), participants underwent three, or if needed four, neurofeedback training sessions in the MRI scanner (Neurofeedback Training). After successful training, participants had another MRI session (Transfer 1). The last training session and Transfer 1 had a minimum of 2 and a maximum of 6 full days between them ($M = 4.65$, $SD = 1.57$). The main aim of Transfer 1 was to analyse if the application of self-regulation had any effects on neural or behavioural task-related changes, within different integrated cognitive tasks. Another aim, was to answer if participants could still self-regulate their brain activity outside of a training session i.e., without receiving any feedback on their performance. Testing this was important in order to assess, if the training success in self-regulation of brain activation was still apparent

outside of training situations (Sulzer et al., 2013; Thibault et al., 2018). The next two behavioural sessions were conducted on two consecutive days (Behavioural 1 & 2). These sessions included, similar to Transfer 1, different cognitive tasks that were intermixed with blocks of self-regulations. The aim of these sessions was again to observe possible effects on cognition and affect due to the application of self-regulation strategies prior to the task blocks. The last MRI session of the study (Transfer 2) aimed to investigate if participants were able to self-regulate their brain activity without any feedback on their performance, after a longer time period post neurofeedback training. Given various meta-analyses on neurofeedback studies, this transfer effect after a longer time period is rarely included in neurofeedback-based paradigms that target the voluntary control of brain activation (Thibault et al., 2018; Tursic et al., 2020). However, it is a relevant aspect to analyse in order to assess if the self-regulation is a skill that can be maintained over time (Thibault et al., 2018). At the start and the end of the study, participants conducted several weeks of Ecological Momentary Assessment (EMA) at home. The EMA questionnaires aimed to acquire real-time assessments of subjective stress during participants' normal life routines (Vaessen et al., 2015). Physiological measures during these at-home phases of the study, were obtained with the E4 wristband including skin conductance, heart rate, movement and body temperature (<https://www.empatica.com/en-eu/research/e4/>). These wristbands were used to measure stress-related physiological changes during real-life scenarios, which has already been implemented in other studies as well (Tutunji et al., 2021). The focus of this thesis, including the data analysis, will be on the data acquired during Transfer 1.

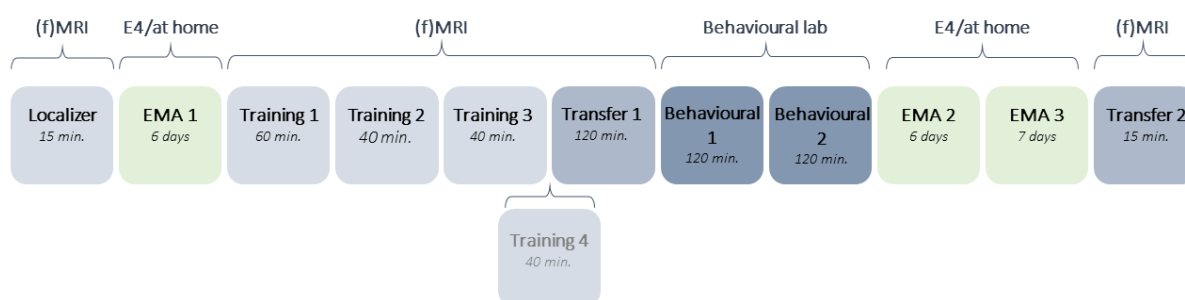


Fig. 1. Overview of the complete study paradigm, including all sessions. Overall, sessions occurred either in the MRI scanner, the behavioural lab (Behavioural) or at home (EMA/E4). For every session, the approximate duration is given below the session description.

2.3. Procedure

In the following the procedure of each session will be described, focusing on Neurofeedback Training and Transfer 1. These are explained in more detail since the neurofeedback training was the main component of the whole study, and the fMRI data of Transfer 1 was included in the data analysis.

2.3.1. Localizer

The first session (Localizer) included the intake of the participants and a high-resolution anatomical scan as well as a short functional run (192 volumes) and a resting state run (300 volumes). The Localizer session was an important step for the rtfMRI neurofeedback set-up (see Supplementary Material A). The resulting anatomical and resting-state scans from this session were used to acquire participant-specific brain network masks. These brain-network masks were important to calculate the neurofeedback signal (see Supplementary Material B) during the neurofeedback training sessions. These individualized masks were created using a custom *Nipype* (version 1.4.2; Gorgolewski et al., 2011; Gorgolewski et al., 2018) pipeline (IndNet version 0.2.0, <https://github.com/can-lab/IndNet>).

2.3.2. EMA week 1

At the evening after the first visit, the first Ecological Momentary Assessment (EMA) week started during which participants wore an E4 wristband and answered several short EMA questionnaires per day. Each day, eight EMA questionnaires arrived on the participant's phone in 2-hour intervals, with additional questions in the morning and the evening (see Supplementary Material C). The last questionnaire arrived on the evening before the first training session and the participants were asked to stop wearing the E4 wristband the morning after. Additionally, the participants filled out a set of different questionnaires (see Supplementary Material D) before their first Neurofeedback Training session.

2.3.3. Neurofeedback Training

At least one week after the Localizer session, the first Neurofeedback Training session took place. Neurofeedback Training sessions were performed in the MRI scanner. Each session started with a low-resolution anatomical scan (AA-HeadScout), which was followed by four (or in case of the first training session six) neurofeedback runs (each 600 volumes), which lasted around 10 minutes each. Each neurofeedback run included multiple single regulation blocks. Each regulation block included variations of the main stimulus ("rest", "regulation", "feedback"), which was a smaller grey disc at the centre of a larger black circle (see Fig. 2). A single regulation block always started with a "rest" stimulus (10s), followed by a "regulation" stimulus (16s), and a second "rest" stimulus (6s), ending with the "feedback" stimulus (4s). At the beginning of each run the "rest" stimulus was presented for a longer time once (34s). During all "rest" stimulus presentations, participants were instructed to disengage from the task and to not think of anything specific. There were two types of "regulation" stimuli, one of them indicating to make the grey disc "smaller" and the other to make it "larger". To change the size of the grey disc, participants were instructed to apply different mental strategies. The instructions to the participants included non-specific examples of mental strategies that might be used to change the size of the grey disc: "The examples of strategies you might consider are: thinking of something specific, performing some mental task internally, or getting into a certain emotion, feeling, mood or state of

mind”. They were non-specific since participants needed to discover themselves which strategy worked best for them. Importantly, participants were instructed to not use any physical strategies (e.g. change of breathing patterns or eye movements). The changed size of the grey disc after self-regulation was shown to the participants with the “feedback” (4s) stimulus, which always came last in a single regulation block. The feedback served as orientation for the participants on the success of their self-regulation strategy. The “feedback” stimulus is based on the calculation of the neurofeedback signal, which is obtained in parallel during the second “rest” stimulus presentation in a regulation block (see details on the neurofeedback signal calculation in Supplementary Material B).

Each training session consisted of four neurofeedback runs and each run had multiple regulation blocks with occurrences of both “regulation” stimuli (i.e. “larger” and “smaller”). The first training session included two practice runs at the beginning, which only included regulation towards “larger” or “smaller”, respectively. Primarily, these extra runs were implemented for the participants to get used to the neurofeedback paradigm. Based on the received feedback participants got a feeling for possible strategies. After each run, participants had to rate their performance and their perceived difficulty of the regulation towards both directions. At the end of each training session, participants also answered several open-ended questions (see Supplementary Material E). With their answers they reflected on their used strategies and how confident they were in them. In addition, female participants had to indicate the first day of their current menstrual cycle. Previous research indicated differences in female stress response depending on menstrual cycle phase (Rohleder et al., 2003), which is why this measure was included for possible effects that might emerge in future analyses.

As already mentioned, participants applied the self-regulation in order to shift their neural activation balance towards the SN or the ECN. Depending on the achieved brain activation, the size of the grey disc was changed. The “larger” regulation stimulus required shifting the balance of their brain network activation towards ECN (even participant number) or towards SN (uneven participant number), and vice versa for the “smaller” stimulus. Participants were unaware of the connection between their regulation and the different brain-network activations.

2.3.3.1. Self-regulation Stimuli

All the tasks and stimuli used for this study were created and presented via *Python* (version 3.7.9; van Rossum & Drake, 2009) scripts using *Experiment* (version 0.10.0; Krause & Lindemann, 2014). The stimuli used for the self-regulation (see Fig. 2) had a black outer circle (red = 0, green = 0, blue = 0, visual angle of radius = 5.96°, visual angle of thickness = 0.07°) with a grey disc inside of the black circle (red = 128, green = 128, blue = 128, visual angle of radius = 3.06°). A dot in the centre of the grey disc functioned as fixation point for the participants. Depending on the stimulus condition, the colour of the fixation point changed. During “rest” the dot was black (red = 0, green = 0, blue = 0, visual angle of radius = 0.16°), during “regulation” periods it was green (red = 0, green = 255, blue = 0) and during “feedback” stimuli presentation it was orange (red = 255, green = 128, blue = 0). The size of the

grey disc changed only during the “feedback” stimulus presentation, based on the calculations of the neurofeedback signal (Supplementary Material B). The possible minimum size of the grey disc was as small as the fixation dot and the maximum as large as the outer black circle. During “regulation” stimulus presentation the circle had 4 additional arrows, either pointing outwards (“larger”) or inwards (“smaller”) and were positioned on the top, bottom, left and right sites (visual angle of width = 0.77° , visual angle of height = 0.98° , visual angle of distances between top and bottom as well as left and right arrows = 6.99°).

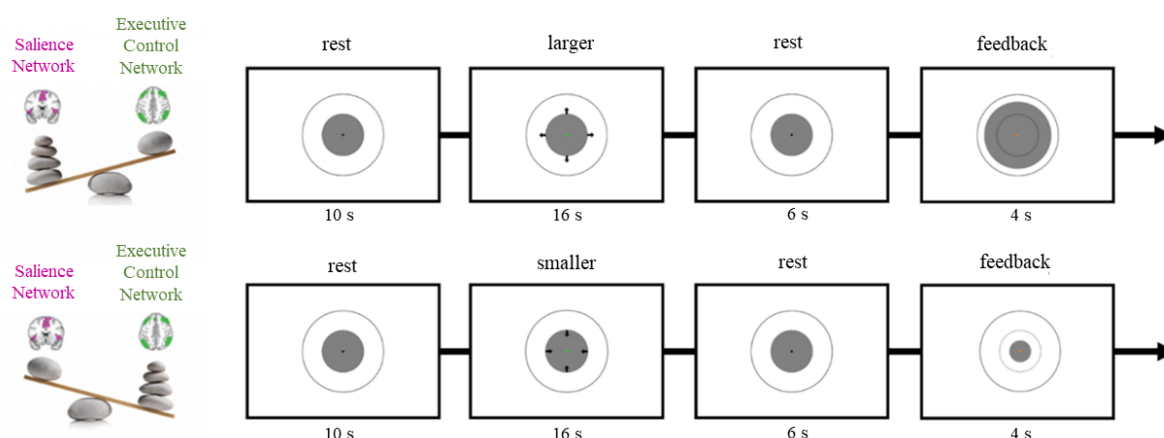


Fig. 2. Overview of the different stimuli used in the Neurofeedback Training session. On the left the balancing shift of network activation can be seen for a case where a “regulation” stimulus towards “larger”, indicates an activation shift towards ECN, and towards SN for a “regulation” stimulus towards “smaller” (even participant number). The stimulus sequence for both directions can be seen right next to it, respectively. The two sequences presented here show the structure of a single regulation block, which were intermixed within regular Neurofeedback Training runs. The stimulus sequence was the same for self-regulation periods outside of Neurofeedback Training sessions, with only the feedback stimulus missing (Krause et al., 2021).

2.3.4. Transfer 1

Transfer 1 included an fMRI scan with three different cognitive tasks. Each task included self-regulation blocks known to the participants from the training sessions. Participants had to self-regulate by using their learned strategies. Each task included “regulation” stimuli (“larger” and “smaller”) or “rest” stimuli (each 16s) that were presented before each task block of the currently running task (27s).

Prior to the session, participants were informed about the details of the tasks and that they would not receive any feedback on their self-regulation. The session started with a low-resolution anatomical scan (AA-HeadScout). The first task was the 2-back task, which is based on the n-back task paradigm (cf. Schoofs et al., 2008), followed by the Emotional face/shape matching task (cf. Hariri et al., 2002). Afterwards, participants had a small break outside of the scanner, before finishing the session with the Emotional Faces Oddball task, which is based on the oddball paradigm (cf. Krebs et al., 2018). Lastly, they had to answer some questions outside of the scanner (see Supplementary Material F). This paper

will only focus on the 2-back and Emotional Faces Oddball task (see Fig.3), which are explained in more detail below. Additional measurements inside the scanner included heart rate, respiration, skin conductance, and recordings of the left eye.

2.3.4.1. 2-back task

During the 2-back task (cf. Schoofs et al., 2008), participants saw a series of numbers that appeared successively on the screen. The participants had to respond whenever the current number on the screen was the same as the number two steps earlier (target) in the presented sequence. The participants had to respond to this target as fast as possible, by pressing a button on the MRI compatible button box (Current Designs, Philadelphia, USA) with their right index finger. The task took approximately 35 minutes (2084 volumes in total). The task started with a “regulation” block (16s) which alternated with task blocks throughout the whole task. Each task block was randomized and included 15 task trials (each 27s) with two or three targets. Overall, the task included 48 “regulation” or “rest” blocks, followed by task blocks. The “regulation” or “rest” blocks were also randomized, including also the control for occurrence frequency of each condition.

The stimuli in this task included the self-regulation stimuli (see Fig. 2) and the task specific stimuli. The task specific stimuli included numbers, presented in black at the centre of the screen for 850 ms, followed by a black fixation cross (950ms) which was also at the centre of the screen.

2.3.4.2. Emotional Faces Oddball task

The Emotional Faces Oddball task (cf. Krebs et al., 2018) had the same neutral face as the regular stimulus and different emotional faces as the target stimuli. When a target stimulus appeared, the participants had to press the button on the button box with their right index finger as fast as possible. The task took approximately 35 minutes (2084 volumes in total). The task started with a “regulation” block (16s) which alternated with task blocks throughout the whole task. Each task block included a randomized occurrences of 15 task trials (each 27s) with two or three targets. Overall, the task included 48 “regulation” or “rest” blocks, followed by task blocks. The “regulation” or “rest” blocks were also randomized, including the control for occurrence frequency of each condition.

The stimuli in this task included the self-regulation stimuli (see Fig. 2) and the task specific stimuli. The task specific stimuli included the neutral face and different variations of faces with emotional expressions. The faces were presented at the centre of the screen for 850 ms, followed by a black fixation cross (950ms) which was also at the centre of the screen.

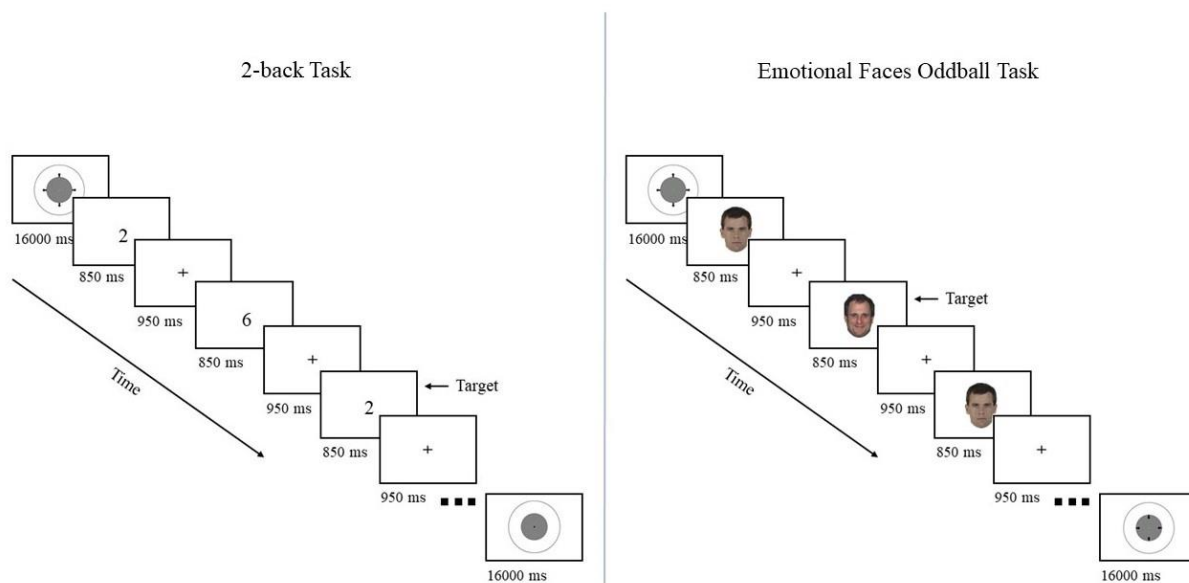


Fig. 3. Overview of the stimuli sequence within the 2-back task (left) and the Emotional Faces Oddball task (right). Task stimuli were presented for 850ms followed by a 950ms fixation cross presentation. Before each task block a regulation stimulus was presented for 16s, without any following feedback on the regulation performance.

2.3.5. Behavioural 1 & 2

The following two behavioural sessions were set on two consecutive days and included in total five tasks. During task performance, participants had to again apply their self-regulation strategies during “regulation” stimulus presentation, without receiving any feedback. These were, similar to the design in Transfer 1, mixed with the task blocks. The first day included an Oddball Recall task, during which participants had to indicate if they recalled the presented faces from the Emotional Faces Oddball task, to assess recall performance of emotional stimuli (cf. Krebs et al., 2018). The other two tasks during the first behavioural session included an Emotional Conflict task, to assess participants ability to suppress emotional stimuli that are irrelevant to the task (cf. Etkin et al., 2006) and a Fear Conditioning/Extinction task, which assessed if memory consolidation was stronger for fear-coupled stimuli, and if the learned threat could be unlearned after removing the fearful stimulus (i.e. the mild electrical shock) (cf. Voogd et al., 2016). The second day included a Reinstatement/Re-extinction task based on the paradigm of a Conditioning/Extinction task (cf. Voogd et al., 2016), a Situation-focused Reappraisal task, which assessed the influence of neutral and adverse images on the participant’s mood (cf. Kanske & Kotz, 2011) and an Effort/Reward task, which aimed detect possible effects of reward anticipation as well as increasing cognitive effort on behavioural results (cf. Vassena et al., 2019). Additional to the behavioural data, physiological measures, including skin conductance and heart rate, as well as pupil size and eye movement of the left eye were recorded.

2.3.6. EMA Week 2 & 3

After Behavioural 2, participants completed EMA weeks 2 & 3 during two consecutive weeks. The participants received the instructions for EMA week 2 at the end of Behavioural 2. They started wearing their E4 wristbands on the evening after Behavioural 2 and received the first EMA questionnaire the morning after. EMA week 2 was the same as EMA week 1 and halfway through EMA week 2, participants received more detailed instructions for EMA week 3. The last EMA week included self-regulation reminders that arrived on the participant's phone three times per day, additional to the EMA questionnaires and E4 measures. In these reminders, participants were asked to open a video, which included a short self-regulation run without feedback. Importantly, the at-home regulation only included "regulation" stimuli indicating self-regulation towards ECN and not towards SN. This had ethical reasons, asking participants to apply mental strategies that induce potentially stressful mental states outside of a controlled lab environment should be avoided. Therefore, participants with an even participant number received a video that only included "regulation" stimuli asking to make the grey disc "larger", and participants with an uneven participants received the video with the "smaller" stimuli. The last EMA questionnaire arrived on the evening before Transfer 2 and participants stopped wearing the E4 wristbands the morning before Transfer 2.

2.3.7. Transfer 2

Lastly, the participants came back for Transfer 2, which was a short MRI session during which participants had apply their learned self-regulation strategies without receiving any feedback. The participants were informed about this and the 15 minute duration of the self-regulation part. The scan started with a low-resolution anatomical scan (AA-HeadScout) followed by functional runs of self-regulation. The run consisted of 32 regulation blocks (842 volumes). The amount of regulation blocks (16s) towards "smaller" and "larger" were balanced and alternated with "rest" stimulus periods (10s). During the session physiological measures, including heart rate, respiration and skin conductance were collected. After the session, participants answered some questions (see Supplementary Material E).

2.4. Physiological Recordings

Throughout the MRI and the behavioural sessions, several physiological measures were collected. For this, BrainVision Recorder and a BrainAmp ExG MR (Brain Products GmbH; Gliching, Germany) were used. Heart rate was measured by attaching an MR-compatible Pulse Sensor (Brain Products GmbH; Gliching, Germany) to the left ring finger of the participants. For recording of Galvanic Skin Response (Brain Products GmbH; Gliching, Germany), two electrodes were attached to the left middle and index fingers. For the respiration measures, participants wore a respiration belt with an attached pneumatic sensor (Brain Products GmbH; Gliching, Germany).

For the eye recordings during Transfer 1 and Behavioural 1 and 2, an Eyelink-1000 Plus eye-tracker (SR Research, Ottawa, Canada) was used. The samples were acquired with a sampling rate of 1000Hz.

2.5. MRI Data Acquisition

During on-site visits, data was acquired at the Donders Centre for Cognitive Neuroimaging (Nijmegen, The Netherlands). All MR images were acquired with a Siemens Skyra 3T MRI scanner (Siemens, Erlangen, Germany), using a 32-channel receiver head coil. For the high-resolution anatomical scan during the Localizer session, a 3D T1-weighted magnetization-prepared gradient echo (MPRAGE) sequence with a generalized auto calibrating partial parallel acquisition (GRAPPA) acceleration factor of 2 (voxel size = 1 x 1 x 1 mm, repetition time (TR) = 2300 ms, echo time (TE) = 3.03 ms, flip angle (FA) = 8°, field of view (FOV) = 256 × 256 x 192 mm), was used. The initial low-resolution anatomical image acquired in all sessions consisted of a 3D AA-HeadScout scan, with a GRAPPA acceleration factor of 3 (voxel size = 1.6 x 1.6 x 1.6 mm, TR = 3.15 ms, TE = 1.37 ms, FA = 8°, FOV = 260 x 260 x 205 mm, slice thickness = 1.6 mm (no gap), number of slices = 128). This low-resolution anatomical image is part of the Siemens AutoAlign procedure. All functional scans were acquired using an echo planar T2*-weighted BOLD-sensitive multiband sequence with a multiband acceleration factor of 4 (TR = 1000 ms, TE = 33 ms, FA = 60°, FOV = 210 x 210 mm², matrix size = 88 × 88, number of slices = 52, slice thickness = 2.4 mm (no gap), in plane resolution = 2.4 x 2.4 mm²).

2.6. Data Analysis

2.6.1. Pre-Processing

First, all MR images were preprocessed with *fMRIPrep* (version 22.0.0; Esteban, Blair et al., 2018; Esteban, Markiewicz et al., 2018; RRID:SCR_016216), which is a tool based on *Nipype* (Gorgolewski et al., 2011; Gorgolewski et al., 2018; RRID:SCR_002502).

Anatomical T1-weighted (T1w) images were corrected for intensity non-uniformity (INU) with N4BiasFieldCorrection (Tustison et al., 2010), distributed with ANTs 2.3.3. (Avants et al., 2008; RRID:SCR_004757) and then used as T1w-reference throughout the workflow. The resulting T1w-reference was skull-stripped with a *Nipype* implementation of the *antsBrainExtraction.sh* workflow (from ANTs), using OASIS30ANTs as target template. Brain tissue segmentation of cerebrospinal fluid (CSF), white-matter (WM) and gray-matter (GM) was performed on the brain-extracted T1w using *fast* (FSL 6.0.5.1:57b01774, RRID:SCR_002823; Zhang et al., 2001). Volume-based spatial normalization to two standard spaces (MNI152NLin2009cAsym, MNI152NLin6Asym) was performed through nonlinear registration with *antsRegistration* (ANTs 2.3.3), using brain-extracted versions of both T1w reference and the T1w template. The following templates were selected for spatial normalization: *ICBM 152 Nonlinear Asymmetrical template* version 2009c (Fonov et al., 2009; RRID:SCR_008796; TemplateFlow ID: MNI152NLin2009cAsym), *FSL's MNI ICBM 152 non-linear 6th Generation*

Asymmetric Average Brain Stereotaxic Registration Model (Evans et al., 2012; RRID:SCR_002823; TemplateFlow ID: MNI152NLin6Asym).

As a first step of functional data pre-processing, a reference volume and its skull-stripped version were generated by aligning and averaging one single-band references (SBRefs). Head-motion parameters with respect to the BOLD reference (transformation matrices, and six corresponding rotation and translation parameters) were estimated before any spatiotemporal filtering using *mcflirt* (FSL 6.0.5.1:57b01774; Jenkinson et al., 2002). The BOLD time-series were resampled onto their original, native space by applying the transforms to correct for head-motion. These resampled BOLD time-series will be referred to as *preprocessed BOLD in original space*, or just *preprocessed BOLD*. The BOLD reference was then co-registered to the T1w reference using *mri_coreg* (*FreeSurfer*) followed by *flirt* (FSL 6.0.5.1:57b01774; Jenkinson & Smith, 2001) with the boundary-based registration (Greve & Fischl, 2009) cost-function. Co-registration was configured with six degrees of freedom. First, a reference volume and its skull-stripped version were generated using a custom methodology of *fMRIPrep*. Several confounding time-series were calculated based on the preprocessed BOLD: framewise displacement (FD), DVARS and three region-wise global signals. FD was computed using two formulations following Power (absolute sum of relative motions, Power et al., 2014) and Jenkinson (relative root mean square displacement between affines, Jenkinson et al., 2002). FD and DVARS were calculated for each functional run, both using their implementations in *Nipype* (following the definitions by Power et al., 2014). The three global signals were extracted within the CSF, the WM, and the whole-brain masks. Additionally, a set of physiological regressors were extracted to allow for component-based noise correction (CompCor, Behzadi et al., 2007). Principal components were estimated after high-pass filtering the preprocessed BOLD time-series (using a discrete cosine filter with 128s cut-off) for the two CompCor variants: temporal (tCompCor) and anatomical (aCompCor). tCompCor components are then calculated from the top 2% variable voxels within the brain mask. For aCompCor, three probabilistic masks (CSF, WM and combined CSF+WM) were generated in anatomical space. The implementation differs from that of Behzadi et al., (2007), in that instead of eroding the masks by 2 pixels on BOLD space, the aCompCor masks were subtracted a mask of pixels that likely contain a volume fraction of GM. This mask was obtained by thresholding the corresponding partial volume map at 0.05, and it ensures components are not extracted from voxels containing a minimal fraction of GM. Finally, these masks were resampled into BOLD space and binarized by thresholding at 0.99 (as in the original implementation). Components are also calculated separately within the WM and CSF masks. For each CompCor decomposition, the k components with the largest singular values are retained, such that the retained components' time series are sufficient to explain 50 percent of variance across the nuisance mask (CSF, WM, combined, or temporal). The remaining components were dropped from consideration. The head-motion estimates calculated in the correction step were also placed within the corresponding confounds file. The confound time series derived from head motion estimates and global signals were expanded with the inclusion of temporal derivatives and quadratic terms for

each (Satterthwaite et al., 2013). Frames that exceeded a threshold of 0.5 mm FD or 1.5 standardised DVARS were annotated as motion outliers. The BOLD time-series were resampled into standard space, generating a preprocessed BOLD run in MNI152NLin2009cAsym space. First, a reference volume and its skull-stripped version were generated using a custom methodology of *fMRIPrep*. Automatic removal of motion artefacts using independent component analysis (ICA-AROMA, Pruim et al., 2015) was performed on the preprocessed BOLD on MNI space time-series after removal of non-steady state volumes and spatial smoothing with an isotropic, Gaussian kernel of 6mm FWHM (full-width half-maximum). Corresponding “non-aggressively” de-noised runs were produced after such smoothing. Additionally, the “aggressive” noise-regressors were collected and placed in the corresponding confounds file. All resampling can be performed with a single interpolation step by composing all the pertinent transformations (i.e. head-motion transform matrices, susceptibility distortion correction when available, and co-registrations to anatomical and output spaces). Gridded (volumetric) resampling were performed using `antsApplyTransforms` (ANTs), configured with Lanczos interpolation to minimize the smoothing effects of other kernels (Lanczos, 1964). Non-gridded (surface) resampling was performed using `mri_vol2surf` (*FreeSurfer*). Many internal operations of *fMRIPrep* use *Nilearn* (Abraham et al., 2014; RRID:SCR_001362), mostly within the functional processing workflow. For more details of the pipeline see <https://fmripred.org/en/latest/workflows.html>.

As a last pre-processing step on the functional data, spatial smoothing (5 mm FWHM) and temporal high-pass filtering (cut-off = 0.01 Hz/100 s) was applied on the *fMRIPrep* preprocessed data. This was done with a custom-made *Nipype* (version 1.4.2; Gorgolewski et al., 2011; Gorgolewski et al., 2018) pipeline (<https://github.com/can-lab/finish-the-job>).

2.6.2. Whole-Brain Voxel-Wise Analysis

Whole-brain voxel-wise offline fMRI analysis was performed on the data which was collected for the 2-back (cf. Schoofs et al., 2008) and Emotional Faces Oddball (cf. Krebs et al., 2018) tasks during Transfer 1. With the analysis differences in neural activation during the task were explored, after preceding self-regulations towards SN (even participants: “smaller”, uneven participants: “larger”) and towards ECN (even participants: “larger”, uneven participants: “smaller”). Further, brain activation patterns during self-regulation periods were analysed to assess if activation balance shifted towards the targeted brain network. The data for this latter analysis included the volumes acquired during the regulation blocks prior to the task. For the overall analysis, each task was analysed separately since they were conducted during separate runs. Since the analysis procedure was the same for both, the following describes the analysis with respect to one task i.e., one run.

For the subject-/first-level analysis, the run was median-scaled to 10000. Each voxel that exceeded a threshold of 1000 entered a generalized linear model (Smith et al., 2004), which included five regressors that modelled the expected hemodynamic response. These regressors were the different conditions included in the run (two conditions for the regulations before the task block: “larger” and

“smaller” and three conditions for the task block, specified by the preceding regulation or rest stimuli: “rest_task”, “larger_task” and “smaller_task”). Additionally, 49 regressors were included as covariates: 24 motion parameters from the *fMRIPrep* output (3 translational and 3 rotational, each of their temporal derivatives, each of their quadratic terms as well as the quadratic terms of each of the temporal derivatives) and 25 physiological noise components, included from the collected physio data during the respective scans. These consisted of 10 cardiac and 10 respiratory phase regressors (Glover et al., 2000), 3 heart-rate frequency regressors (Shmueli et al., 2007; van Buuren et al., 2009) and 2 respiratory-volume per unit time regressors (Birn et al., 2006; van Buuren et al., 2009).

As mentioned before, the regulation direction (i.e. “larger” and “smaller”) targeted different networks, depending on the participant number (i.e. regulation towards ECN implied by regulation “larger” for even participants and “smaller” for uneven participant; vice versa for SN). Thus, different contrasts were assigned to different participants, based on their participant number. This differentiation is indicated in brackets after the respective contrasts. The following first-level contrasts were included: “regulate to SN” (“larger” for participants 1, 3, 5, 11, 13, 15, 17, 19, 21, 27, 109, 123, 125; “smaller” for participants 2, 4, 8, 10, 12, 14, 16, 18, 22, 26, 106, 120, 124), “regulate to ECN” (“larger” for participants 2, 4, 8, 10, 12, 14, 16, 18, 22, 26, 106, 120, 124; “smaller” for participants 1, 3, 5, 11, 13, 15, 17, 19, 21, 27, 109, 123, 125), “regulate to SN > regulate to ECN” and “Task after regulate to SN > Task after regulate to ECN” (“larger > smaller” for participants 1, 3, 5, 11, 13, 15, 17, 19, 21, 27, 109, 123, 125; “smaller > larger” for participants 2, 4, 8, 10, 12, 14, 16, 18, 22, 26, 106, 120, 124), “Task after regulate to SN > Task after rest” (“larger > rest” for participants 1, 3, 5, 11, 13, 15, 17, 19, 21, 27, 109, 123, 125, “smaller > rest” for participants 2, 4, 8, 10, 12, 14, 16, 18, 22, 26, 106, 120, 124), “Task after regulate to ECN > Task after rest” (“larger > rest” for participants 2, 4, 8, 10, 12, 14, 16, 18, 22, 26, 106, 120, 124, “smaller > rest” for participants 1, 3, 5, 11, 13, 15, 17, 19, 21, 27, 109, 123, 125), and lastly to check for mean activation during the task, a contrast “Task”, including all three conditions prior to the task (i.e. “Task after rest”, “Task after regulate to SN” and “Task after regulate to ECN”). Resulting contrast estimates as well as the variance of the estimates were used as input for a group-/second-level random-effects GLM (FLAME1 from (FLAME1 from FSL version 6.0.5; Smith et al., 2004)). The model had a single-regressor in order to test for main effects of the run within the whole group of subjects. A cluster analysis was performed on the results, using an ingoing cluster-forming threshold of $z = 3.2$ on the voxel-level. Family-wise error (FEW) correction for multiple comparisons was applied on the cluster-level, with a significance threshold for the clusters set at $\alpha = 0.05$. The complete analysis was conducted with a custom-made *Nipype* (Gorgolewski et al., 2011; Gorgolewski et al., 2018) pipeline (FawN version 0.2.1; <https://github.com/can-lab/FawN>).

2.6.3. Post-hoc power analysis and fixed-effects analysis

The results of the second-level random-effects analysis provided little to no neural evidence supporting any effects of the self-regulation on the cognitive performance in both the 2-back and the

Emotional Faces Oddball task. Prior to data collection, a power calculation was conducted which resulted in a power of 80% to find a medium effect size ($d = 0.5$), with a significance level $\alpha = 0.05$. However, the real effects in the data might have been smaller than the expected effect. Therefore, a follow-up analysis was conducted. The GLM model was the same as in the random-effects analysis, but it estimated fixed instead of random-effects (FLAMEO from FSL version 6.0.5; Smith et al., 2004). Results were FWE corrected for multiple comparisons on the voxel-level, with a significance threshold set at $\alpha = 0.05$. The analysis was conducted with a custom-made *Nipype* (Gorgolewski et al., 2011; Gorgolewski et al., 2018) pipeline (FawN version 0.2.1; <https://github.com/can-lab/FawN>).

3. Results

In the following the results for the different tasks will be described, first for the random-effects analysis and then for the fixed-effects analysis. The reported results of the fixed-effects analysis only include the contrasts that were used to analyse a possible effect of the self-regulation on the task performance. An overview of activated brain regions per task and per contrast included in the random-effects analysis can be found in Supplementary Material F and for the fixed-effects analysis in Supplementary Material G.

3.1. Random-effects whole-brain voxel-wise analysis

3.1.1. Self-regulation

Results of the analysis of self-regulation volumes indicated the recruitment of several brain regions of the SN, the ECN but also the DMN. The DMN is described as a network including the posterior cingulate cortex (PCC), the precuneus cortex (PCu), the inferior parietal lobes (IPL), the medial PFC (mPFC) and regions within the temporal lobes, including the hippocampus (HC) (Barrett & Satpute, 2013; van Oort et al., 2017).

During self-regulation periods in the 2-back run, brain activation patterns during regulation towards SN, included positive activations in regions associated to the SN, e.g., the IC, the TH, the ACC and the supplementary motor area (SMA). Other positive activations were seen in the ECN (e.g., the dlPFC). However, negative activations were also observed in regions of the ECN (e.g., the PPC) and the DMN (e.g. the PCC). The balance of activation towards SN was therefore mainly including activation of SN regions and deactivations of the ECN and the DMN. During the regulation to ECN, positive activation patterns were visible in regions of the ECN (e.g., the dlPFC and the dmPFC) and of the SN (e.g., the IC and the ACC). Negative activations were observed in the ECN (e.g. the PPC) and the DMN (e.g., the PCC). The differential contrast, analysing possible activations that were stronger during regulation towards SN compared to regulation towards ECN, showed little overall activation. The activations that were visible included small clusters of positive activations in regions associated to the

SN (e.g. the SMA and the ACC), to the ECN (e.g. the PPC) and the DMN (e.g. the PCC). No negative activations were observed in this contrast. An example overview of the activation patterns for the regulation contrasts during the 2-back task can be seen in Fig. 4A, and all activated brain regions during the different self-regulations are listed in Tables S1-3 (Supplementary Material F).

An example overview of activation results during self-regulation periods in the oddball task can be seen in Fig. 4B. During phases of regulation towards SN, positive activation patterns were observable in the SN (including e.g., the IC, the TH, the ACC and SMA) and the ECN (e.g., the dmPFC) and parts of the mPFC, which is associated with the DMN. Negative activations were seen in the ECN (e.g., the dlPFC and the PPC) and the DMN (e.g., the PCu and the PCC). During regulation towards ECN, positive activations patterns were observed in the ECN (e.g., the dmPFC and small parts of the dlPFC) and in the SN (e.g., the IC and the TH). Negative activations were seen in the ECN (e.g., the PPC) and in the DMN (e.g., the PCC). There were no regions in the SN that activated more during regulation towards SN in comparison to regulation towards ECN. The results only included higher deactivation negative of the right PPC, which is associated with the ECN, after regulation to SN compared to regulation to ECN. An overview of all brain regions included in the self-regulation conditions can be seen in Tables S6-8 (Supplementary Material F).

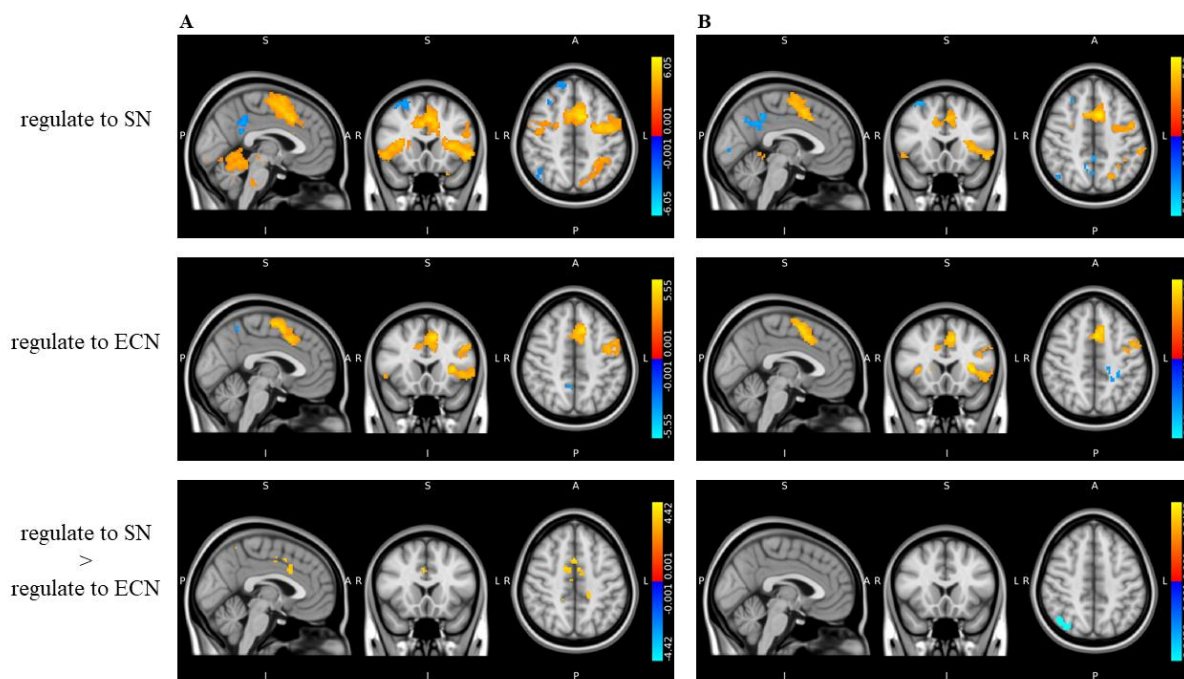


Fig. 4. Full-brain activation during self-regulation periods within (A) the 2-back and (B) the Emotional Faces Oddball task. In both tasks regulation to SN resulted in SN activation as well as minor ECN and DMN deactivations. Regulations to ECN included activations in ECN, SN and DMN. Clusters were formed including voxels exceeding a threshold of $z = 3.2$, and only significant clusters ($p_{FWE} = 0.05$) are visible in the results. MNI- coordinates: $x = -2, y = 18, z = 47$.

3.1.2. Task-related fMRI signal

The results for the mean brain activation patterns during the 2-back task after all pre-task block conditions (i.e. “Task after rest”, “Task after regulate to SN” and “Task after regulate to ECN”) showed activations in several brain regions that have been found in previous fMRI studies implementing the N-back task with numeric stimuli (Mencarelli et al., 2019). An example of the average activation patterns, as well as activations only during the task after “rest”, can be seen in Fig. 5A. Regions that showed positive activations during task blocks and which have been previously observed to be activated during the N-back task included brain regions in the SN (e.g. the ACC), the ECN (e.g. the PPC), the DMN (e.g. the IPL) as well as the cerebellum. Negative activations were observable in the AMG (SN), as well as the HC and parahippocampal gyrus, which are both brain regions in the DMN. Further positive activation was observed in the anterior part of the cerebellum. An overview of all involved brain regions is provided in Table S5 (Supplementary Material F).

The results for the mean brain activation during the Emotional Faces Oddball task blocks (i.e. “Task after rest”, “Task after regulate to SN” and “Task after regulate to ECN”) included multiple brain regions that were also associated to the oddball paradigm in previous fMRI studies (Ardekani et al., 2002; Rusiniak et al., 2013). Positive activation patterns included task-related regions in the SN (e.g. the ACC and the TH), the ECN (e.g. dmPFC) and the anterior cerebellum. Further, positive activation in the AMG (SN), as well as negative activation in the PPC (ECN) was observed. An example overview can be seen in Fig. 5B and a summary of all brain regions included can be seen in Table S9 (Supplementary Material F).

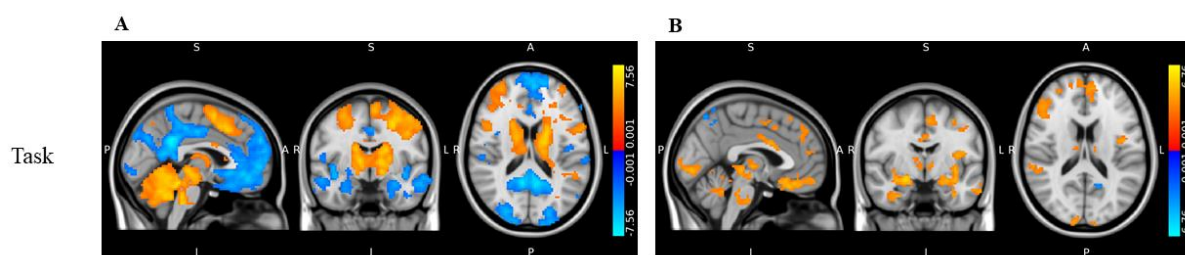


Fig. 5. Full-brain activation during task periods within (A) the 2-back and (B) the Emotional Faces Oddball task. The images show the mean task activations across all three conditions before the task (i.e. both regulation directions and resting). Task-related activations were visible for both tasks, with overall less activation during the Emotional Faces Oddball task. Clusters were formed including voxels exceeding a threshold of $z = 3.2$, and only significant clusters ($p_{FWE} = 0.05$) are visible in the results. MNI- coordinates: $x = -2$, $y = -6$, $z = 17$.

3.1.3. Self-regulation dependent changes in activation during tasks blocks

To examine if the regulation to SN or ECN resulted in stronger brain activation patterns during task blocks, in comparison to each other or to rest, multiple differential contrasts were included in the analysis of both tasks (i.e. “Task after regulate SN”/ “Task after regulate to ECN” vs. “rest”, “Task after regulate to SN” vs. “Task after regulate to ECN”).

During the 2-back task, the only activations were found in results for the contrast “Task after regulate to SN vs. rest”. Here, positive activation was found in the anterior part of the left IC (SN). However, the activation cluster was at the border of the anterior IC. An overview of all brain regions involved in the results of this contrast can be seen in Table S5 (Supplementary Material F).

For the Emotional Faces Oddball task (see Fig. 6A), only the “Task after regulate to SN vs Task after rest” yielded some minor positive activation pattern in the left cerebral white matter region. An example overview of the activation patterns for the task-specific contrasts during the Emotional Faces Oddball task can be seen in Fig. 6B, and all an overview of involved brain regions is listed in Table S10 (Supplementary Material F).

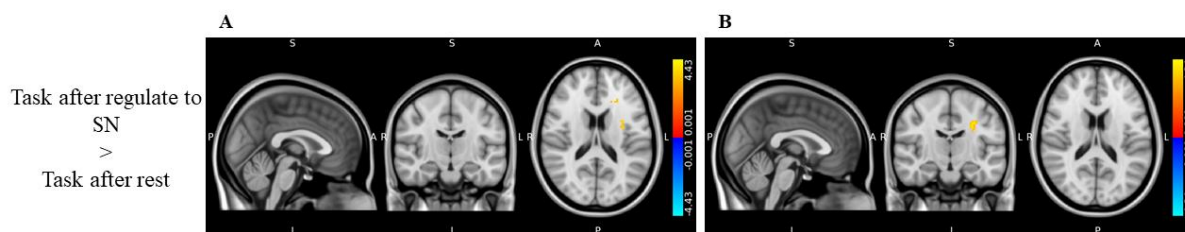


Fig. 6. Full-brain activation during task periods within (A) the 2-back and (B) the Emotional Faces Oddball task. The activation patterns are shown for the differential contrast, showing higher activations during the task after regulation to SN in comparison to activation during the task after regulation to ECN. For both tasks, this contrast yielded almost no activation. Clusters were formed including voxels exceeding a threshold of $z = 3.2$, and only significant clusters ($p_{\text{FWE}} = 0.05$) are visible in the results. MNI- coordinates: $x = 0$, $y = -15$, $z = 17$.

3.2. Fixed-effects whole-brain voxel-wise analysis

3.2.1. Self-regulation dependent changes in activation during tasks blocks

Activations during the task blocks, found within the differential contrasts (i.e. “Task after regulate SN”/ “Task after regulate to ECN” vs. “rest”, “Task after regulate to SN” vs. “Task after regulate to ECN”) will be reported with a focus on brain regions that have been reported in previous fMRI studies of the n-back task (Mencarelli et al., 2019) regarding the 2-back task results, and of the oddball task (Ardekani et al., 2002; Rusiniak et al., 2013) for results obtained from the Emotional Faces Oddball task.

Positive activation during the 2-back task blocks after regulation towards SN, compared to task after rest included e.g., the TH, the ACC, the cerebellum, the dmPFC, the bilateral parietal cortex (PC) and the IC. Small clusters of negative activations were visible in the lateral parts of the occipital cortex (OC). These results suggest that regulation towards SN prior to the task, resulted in higher activations within these areas compared to brain activations during the task after rest. Comparing task activations after regulation to ECN to activations during the task after rest periods, yielded positive activation in the bilateral PC, the dmPFC, the dlPFC, the IC, the caudate, the anterior cerebellum, the TH and the PCu. A small cluster of negative activation was apparent in the left OC. The last differential contrast, which

compared task activations after regulation to SN vs. regulation to ECN, presented minor activation patterns in task-related brain regions. A few voxels of negative activation were visible in the dlPFC, indicating that after regulation to SN stronger deactivation of dlPFC (ECN region) was apparent during the task. An example overview of the activation patterns is given in Fig. 7A. A summary of all activations can be seen in Tables S1-3 (Supplementary Material G).

Brain regions showing higher positive activation during the Emotional Faces Oddball task period after regulation to SN compared to after rest, included the cerebellum, the TH, the inferior occipitotemporal cortex, the primary motor cortex as well as the SMA, the IC, the PCu and the right middle frontal gyrus. No negative activation pattern was visible. For the differential contrast comparing task activations after regulation to ECN compared to after rest, positive activations were visible in the IC, the supramarginal gyrus and the SMA. A few voxels of negative activations were visible in the ACC as well as the OC. Lastly, small voxels of activation were visible in results of the differential contrast comparing activations during the task, after regulation to SN vs. after regulation to ECN. These included the ACC and the dmPFC. Higher activations during the task in task-related brain regions after regulation to SN vs. regulation to ECN were also observed in the last differential contrast including e.g., positive activation in the ACC. An example overview of the activation patterns reported here can be seen in Fig. 7B. A summary of all activations can be seen in Tables S4-6 (Supplementary Material G).

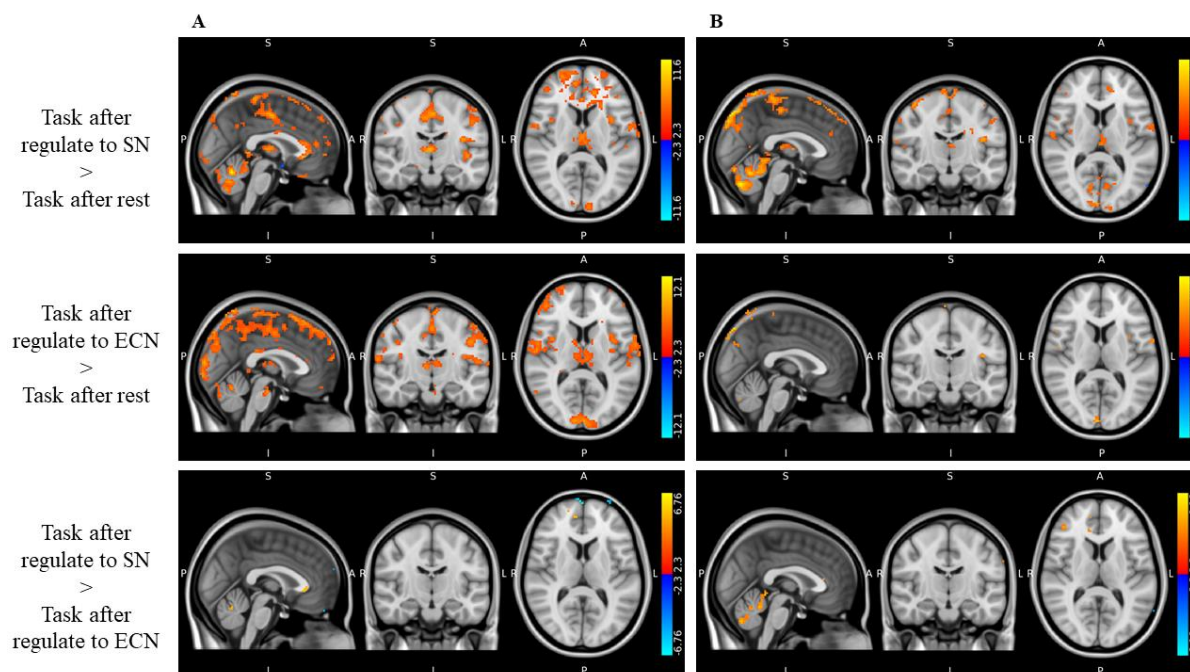


Fig. 7. Full-brain activation during task periods within (A) the 2-back and (B) the Emotional Faces Oddball task. A) Overall activation was highest for the contrast showing results during task periods after regulation to ECN in vs. after rest. Generally, task-related brain activation was visible in all contrasts. Only a small difference in activation was visible comparing activations during the task after regulation to SN vs. regulation to ECN. B) Overall activation was highest during task periods for the contrast results of comparing task activations after regulation to SN vs. after rest. Low patterns of activation were visible for the other two differential contrasts. Overall brain activation during the oddball task was lower compared to the 2-back task. Only significant voxels are visible here ($p_{FWE} = 0.05$). MNI- coordinates: $x = 0$, $y = -15$, $z = 10$.

4. Discussion

The current study implemented a promising rtfMRI-based neurofeedback paradigm to teach participants to self-regulate the activation balance of two stress-related large-scale brain networks, which was shown to be successful before (Krause et al., 2021). The target of the self-regulation, in comparison to other neurofeedback-based studies, included whole large-scale brain networks and not only single brain regions. As suggested in previous literature it is more advisable to target whole brain networks, since they are more representative of the underlying neural changes in cognitive functions, compared to single brain regions (Barrett & Satpute, 2013; Lanius et al., 2015). Especially the SN and the ECN are two of the three large-scale brain networks that have been, together with the DMN, associated with dysfunctions of cognitive processes as seen in various stress-related psychopathologies, such as PTSD (Lanius et al., 2015; Menon, 2011). The aim of the study was to analyse if the self-regulation had any modulatory effects on cognitive performance on the neural or behavioural level, for cognitive functions that change in response to stress (Hermans et al., 2014; van Marle et al., 2009). In order to observe if there were any increased task-related neural changes due to the self-regulation, the

included analyses focused on two cognitive tasks, an n-back task to target higher executive functions like WM (Schoofs et al., 2013; Soveri et al., 2017) and a visual oddball task to target vigilance (Linden et al., 1999; Rusiniak et al., 2013).

4.1. Self-regulation

The participants performed in regular intervals of self-regulation or rest intermixed with task blocks. Overall, the self-regulation results during the 2-back task run indicated that participants regulated towards SN when asked to regulate towards SN. Furthermore, regulation towards SN included deactivations in ECN and DMN regions, adding to the balance towards SN. However, some brain areas of the opposing networks were also active, indicating that effect of the self-regulation was not as strong as I expected. Similar observations were made during regulation towards ECN. During regulation towards SN stronger activation was found in clusters of all three networks, compared to the activation during regulation to ECN. The self-regulation results during the Emotional Faces Oddball task, showed similar patterns. Generally, the self-regulations in both directions was mainly achieved by the activation of SN regions and deactivation of regions of the ECN and DMN. Similar neural activation patterns during self-regulation were observed in the previous study by Krause et al. (2021). Referring to the argumentation made by the researchers of that study, reasons for the dominant activation of the SN in both regulation directions can have multiple reasons. Firstly, this could have been a result of the participants feeling pressure after being instructed to apply their self-regulation on command. This could have resulted in a stressful situation, leading to activation in the SN (Hermans et al., 2014; Krause et al., 2021; Young et al., 2017). Another explanation could have been the previously made connection between neural activations during reward anticipation and increases in cognitive effort and SN brain regions (Krause et al., 2021; Vassena et al., 2014). Building on this, self-regulation via neurofeedback has generally been associated with network activations connected to the perception and processing of rewards. Furthermore, the executive component of the self-regulation was also connected to activations in regions of the ECN, which would explain why ECN activation was observable during regulation to SN (Krause et al., 2021; Sitaram et al., 2017). Overall, the results of the self-regulation I observed in this study were comparable to the ones observed in the proof-of-concept study (Krause et al., 2021). It is important to mention that the analysis of the current results were obtained from a random-effects analysis, in comparison to the fixed-effects analysis used by Krause et al. (2021). Importantly, the inferences based on the current random-effects analysis can be generalized to the population, in contrast to inferences of a fixed-effects analysis (Monti, 2011). The resulting effects of the self-regulations were therefore expected to be lower than in a fixed-effects analysis, however they are generalizable to the population and not restricted to the used sample of participants (Krause et al., 2021; Monti, 2011). Lastly it should also be mentioned that the transfer of the self-regulation strategies after the neurofeedback training was mainly addressed with Transfer 2. The self-regulations during Transfer 1 were mainly included to observe if the self-regulation might have any effects on the neural activations during the task, therefore a prior analyses if this was applied successful was necessary for the overall aim of the

analyses. Thus, the results of Transfer 2 would give more insight on the lasting effects of the learned self-regulation strategies.

4.2. Task-related activation

The mean activation during task periods overlapped with previous fMRI studies that reported on brain activation patterns for both numeric n-back tasks (Mencarelli et al., 2019) and visual oddball tasks (Ardekani et al., 2002; Rusiniak et al., 2013). Interestingly, the 2-back task included deactivations of the AMG which is associated with the SN (Hermans et al., 2014) and the HC and parahippocampal gyrus which are associated with the DMN (Barrett & Satpute, 2013; van Oort et al., 2017). The deactivation of regions in the DMN seem to support the notion that the DMN generally decreases in response during tasks of higher cognitive functions, while the ECN's activation response is increasing (Hermans et al., 2014; Voogd, Hermans, & Phelps, 2018). In addition, the deactivation of the AMG during a two-back WM task, has also been observed in a previous study, supporting the validity of the current findings (Voogd, Kanen et al., 2018). In this previous study, this finding led the researchers to the notion that the implementation of cognitively demanding tasks might be useful for decreasing effects of stress via deactivated regions that are associated to stress (Voogd, Hermans, & Phelps, 2018; Voogd, Kanen et al., 2018). Hence, the current results might support this idea, by showing that the solving of the n-back task resulted in a decreased activation in the AMG. As mentioned, activations that were observable during task blocks of the Emotional Faces Oddball task, were also reported previously (Ardekani et al., 2002; Rusiniak et al., 2013). An additional region that was positively activated in this oddball task, was the AMG. Previously, positive activation of the AMG was observed in a study that used an oddball paradigm, specifically during emotional stimuli presentation (Fichtenholtz et al., 2004). Since we implemented emotional faces in the used oddball task, the observed activation in the AMG is in line with those previous results.

4.3. Self-regulation dependent changes in activation during tasks blocks

The most interesting part of the current analysis, focused on the differences in activation during the task blocks after different self-regulation conditions before the task. Based on the different pre-task conditions, the aim was to find differences in modulation of neural activation during the tasks as a result of the direction of the self-regulation.

4.3.1. 2-back task

Within the 2-back task, I expected an enhancing effect on the task-related neural activation after regulation to ECN, due to the ECN's connection to WM performance (Schoofs et al., 2013; Soveri et al., 2017; van Oort et al., 2017). However, the results of the initial analysis did not support this hypothesis. The only stronger positive activation during the task was observed after regulation to SN compared to prior rest periods. The activated region included the left anterior IC. This finding might be connected to the notion that specifically the anterior IC, may be involved in processes of higher executive control, by integrating networks that are required in higher executive functions (i.e. the ECN)

(Molnar-Szakacs & Uddin, 2022). However, the activation observed in the anterior IC was quite peripheral, and therefore this interpretation should be considered carefully.

Because of the lack of clear findings from the random-effects analysis, I conducted a follow-up analysis using a fixed-effects approach. Importantly, no results of this analysis are transferrable to the general population (Krause et al., 2021), and are therefore restricted to the current sample. Nevertheless, the results of a fixed-effects analysis are still valid, even if it only produces sample-specific results i.e., the effects that were discovered in the current fixed-effects analysis were still valid for the participants included in the analysis (Monti, 2011). For both differential contrasts the results indicated that prior self-regulation towards both directions resulted in higher activation patterns during the task within task-related brain regions. However, prior regulation towards ECN included additional task-related brain region activation vs. rest, compared to the activated task-related brain regions seen in the differential contrast of prior regulation to SN vs. rest. This might support the hypothesis that prior regulation to ECN might increase task-related neural performance during the 2-back task. In addition, these findings were in line with results of a previous study by Sherwood et al. (2016), showing that previous training in self-regulation of activation towards the dlPFC (ECN), increased performance in an n-back task (Sherwood et al., 2016). To infer if the regulation towards ECN resulted in higher performance during the n-back, the behavioural data should be analysed. The current results only indicate a possible enhancing effect on task-related neural activation. Some higher deactivation during the task in task-associated brain regions was observable after regulation to SN compared to regulation to ECN. The deactivation was for example, observable in the dlPFC. This pattern of deactivation was seen previously in a study observing the effects of stress on a working memory task. Within this study the induction of stress resulted in reduced dlPFC activation (Qin et al., 2009). Finding the same deactivation in the current study, indicates that the regulation towards SN also modulates neural responses specific to the n-back tasks (Young et al., 2017). Investigating if the higher deactivation in task-related regions also results in decreased performance on the behavioural level, should be investigated by a future analysis of the behavioural response data during Transfer 1.

4.3.2. Emotional Faces Oddball task

With respect to the Emotional Faces Oddball paradigm, I expected that prior regulation to SN might increase neural oddball task-related activation, in comparison to the regulation to ECN or rest before the task blocks. I assumed this due to increases in vigilance after regulation to SN, which might result in higher performance levels during an oddball task that relies on the detection of salient stimuli (Hermans et al., 2014; Linden et al., 1999). The random-effects analysis did not yield any task-related activation patterns for any of the used contrasts, and thus did not provide any supportive results for the hypothesis. Therefore, I also applied a post-hoc fixed-effects analysis on the Emotional Faces Oddball task run. Overall, the results of the differential contrasts, yielded activations in multiple task-related brain regions. Supportive of the current hypothesis, more overall activation patterns in more task-related

brain regions were visible during the task periods after regulation to SN vs. rest, compared to overall activation patterns during the task periods following regulation to ECN vs. rest. Furthermore, there were small clusters of activation in task-related brain regions that showed stronger activation during task blocks after regulation to SN compared to regulation to ECN. This finding additionally supports the hypothesis, that prior regulation to SN might increase task-related activation during the oddball task. In addition, small amounts of voxels within the OC were observed to be stronger deactivated, in both differential contrasts comparing activation during the task after regulation to SN vs. rest and regulation to ECN vs. rest. A previous study investigating regions of brain activation during the oddball task in sleep-deprived participants, also found deactivation in the occipital cortex (Martínez-Cancino et al., 2015). Thus the deactivation of the OC might be due to tiredness in participants, since the Emotional Faces Oddball task started after participants had already spent about an hour in the scanner.

4.4. Limitations

Overall, the lack of results supporting the main hypotheses after a random-effects analyses indicate that the effects the study was looking for seemed to be smaller than expected. Therefore, the study might have required a larger sample size in order to observe a possible effect. Nevertheless, the fixed-effects analysis yielded some results in line with both hypotheses. However, it is important to mention again that the inferences drawn from this only apply to the specific group of participants (Monti, 2011). Furthermore, more follow-up analyses could have been conducted that were not included for the current thesis. Starting with the pre-processing the acquired EPI data was not corrected for susceptibility distortion, which is usually recommended for EPI data that suffers from B0 field inhomogeneities (Boegle et al., 2010). Further, analyses could be repeated on the ICA Aroma preprocessed data which resulted in motion corrected fMRI data (Pruim et al., 2015). Concerning the group-level analyses, ROI analyses with masks specific for the large-scale brain networks and for task-related activation regions could be conducted. This way signal extraction for the self-regulation analyses could be restricted to the large-scale brain networks. The same could be done for the data collected during the task blocks by using a mask that is specific to the average activation patterns observed during each task. A ROI analysis would be especially helpful to in reducing the amounts of statistical tests and therefore minimizes the amount of multiple comparisons correction necessary (Poldrack, 2007). A possible improvement of the study design might target the long duration of the session. This might have exhausted the participants too much, leading to a possible decrease in motivation but also increase in tiredness throughout the session. A possible solution might be to decrease the duration of the single tasks or to split them on two consecutive days.

4.5. Conclusion and Outlook

In the current study, the implementation of the neurofeedback training was used to find possible effects of the learned self-regulation on cognition. Self-regulation via neurofeedback could be a potential method for building resilience against negative and possibly lasting effects of stress (Krause et al., 2021).

In a prolonged or maladapted stress reaction, this skill might be useful to counteract the lasting downregulation of executive functions (Qin et al., 2009) and by regular implementation might increase resilience in stress by balancing the shift in stress-related brain networks (Hermans et al., 2014). Another implementation of this neurofeedback-based paradigm could be in individuals that are already affected by a stress-related disorder, and see if the self-regulation improves cognitive dysfunctions in such disorders. Gaining insight in these effects might help in the implementation of neurofeedback training in the clinical setting as e.g., a supplementary intervention to already existing therapies for PTSD (Gapen et al., 2016). Existing therapies for PTSD include interventions that e.g., aim to extinct the memory of patient's traumatic event by means of exposure therapy, but overall do not result in successful and lasting effects in many individuals (Bradley et al., 2005; van der Kolk et al., 2016). However, in recent years it became apparent that one of the main dysfunction that PTSD patients have includes the control of intrusive memories, which generally infers a dysfunction of higher cognitive processes (Lanius et al., 2015; van der Kolk et al., 2016). Therefore, the currently used neurofeedback training might be used to target these dysfunctions in cognitive processes by learning to voluntarily balance the activation patterns towards the ECN, which is involved in such higher cognitive functions (Hermans et al., 2014; Lanius et al., 2015). If this is shown to be successful, neurofeedback-based self-regulation could be implemented as a supplement in currently existing therapies (van der Kolk et al., 2016). Further, this would provide patients with a method they can voluntarily apply anywhere and anytime, with personally developed strategies.

To conclude, the observations of the current study, although not transferrable to the general population, already indicate that voluntarily balancing activation of the SN and ECN (as well as the DMN) via mental strategies, seems to affect cognitive performance. Showing that this method does not only modulate neural activation during self-regulation periods but also the neural activation during subsequent cognitive processes used in various cognitive tasks, adds to the validation process of this method and brings us a step further to implement it as a potential preventive as well as a treatment strategy.

5. References

- Abraham, A., Pedregosa, F., Eickenberg, M., Gervais, P., Mueller, A., Kossaifi, J., Gramfort, A., Thirion, B., & Varoquaux, G. (2014). Machine learning for neuroimaging with scikit-learn. *Frontiers in Neuroinformatics*, 8. <https://doi.org/10.3389/fninf.2014.00014>
- Ardekani, B. A., Choi, S. J., Hossein-Zadeh, G.-A., Porjesz, B., Tanabe, J. L., Lim, K. O., Bilder, R., Helpner, J. A., & Begleiter, H. (2002). Functional magnetic resonance imaging of brain activity in the visual oddball task. *Cognitive Brain Research*, 14(3), 347–356. [https://doi.org/10.1016/S0926-6410\(02\)00137-4](https://doi.org/10.1016/S0926-6410(02)00137-4)
- Avants, B. B., Epstein, C. L., Grossman, M., & Gee, J. C. (2008). Symmetric diffeomorphic image registration with cross-correlation: Evaluating automated labeling of elderly and neurodegenerative brain. *Medical Image Analysis*, 12(1), 26–41. <https://doi.org/10.1016/j.media.2007.06.004>
- Barrett, L. F., & Satpute, A. B. (2013). Large-scale brain networks in affective and social neuroscience: Towards an integrative functional architecture of the brain. *Current Opinion in Neurobiology*, 23(3), 361–372. <https://doi.org/10.1016/j.conb.2012.12.012>
- Beck, A. T., Steer, R. A., & Brown, G. (1996). *PsycTESTS Dataset*. American Psychological Association (APA). <https://doi.org/10.1037/t00742-000>
- Behzadi, Y., Restom, K., Liau, J., & Liu, T. T. (2007). A component based noise correction method (CompCor) for BOLD and perfusion based fMRI. *NeuroImage*, 37(1), 90–101. <https://doi.org/10.1016/j.neuroimage.2007.04.042>
- Birn, R. M., Diamond, J. B., Smith, M. A., & Bandettini, P. A. (2006). Separating respiratory-variation-related fluctuations from neuronal-activity-related fluctuations in fMRI. *NeuroImage*, 31(4), 1536–1548. <https://doi.org/10.1016/j.neuroimage.2006.02.048>
- Boegle, R., Maclaren, J., & Zaitsev, M. (2010). Combining prospective motion correction and distortion correction for EPI: Towards a comprehensive correction of motion and susceptibility-induced artifacts. *Magnetic Resonance Materials in Physics, Biology and Medicine*, 23(4), 263–273. <https://doi.org/10.1007/s10334-010-0225-8>
- Bradley, R., Greene, J., Russ, E., Dutra, L., & Westen, D. (2005). A multidimensional meta-analysis of psychotherapy for PTSD. *The American Journal of Psychiatry*, 162(2), 214–227. <https://doi.org/10.1176/appi.ajp.162.2.214>
- Carver, C. S., & White, T. L. (1994). Behavioral inhibition, behavioral activation, and affective responses to impending reward and punishment: The BIS/BAS Scales. *Journal of Personality and Social Psychology*, 67(2), 319–333. <https://doi.org/10.1037/0022-3514.67.2.319>
- Corr, R., Glier, S., Bizzell, J., Pelletier-Baldelli, A., Campbell, A., Killian-Farrell, C., & Belger, A. (2022). Triple Network Functional Connectivity During Acute Stress in Adolescents and the Influence of Polyvictimization. *Biological Psychiatry. Cognitive Neuroscience and Neuroimaging*. Advance online publication. <https://doi.org/10.1016/j.bpsc.2022.03.003>
- Daniel, T. A., Katz, J. S., & Robinson, J. L. (2016). Delayed match-to-sample in working memory: A BrainMap meta-analysis. *Biological Psychology*, 120, 10–20. <https://doi.org/10.1016/j.biopsycho.2016.07.015>
- Esteban, O., Blair, R., Markiewicz, C. J., Berleant, S. L., Moodie, C., Ma, F., Isik, A. I., Erramuzpe, A., Kent, James D. andGoncalves, Mathias, DuPre, E., Sitek, K. R., Gomez, D. E. P., Lurie, D. J., Ye, Z., Poldrack, R. A., & Gorgolewski, K. J. (2018). fMRIPrep. *Software*. Advance online publication. <https://doi.org/10.5281/zenodo.852659>
- Esteban, O., Markiewicz, C., Blair, R. W., Moodie, C., Isik, A. I., Erramuzpe Aliaga, A., Kent, J., Goncalves, M., DuPre, E., Snyder, M., Oya, H., Ghosh, S., Wright, J., Durnez, J., Poldrack, R., & Gorgolewski, K. J. (2018). fMRIPrep: a robust preprocessing pipeline for functional MRI. *Nature Methods*. Advance online publication. <https://doi.org/10.1038/s41592-018-0235-4>

- Etkin, A., Egner, T., Peraza, D. M., Kandel, E. R., & Hirsch, J. (2006). Resolving emotional conflict: A role for the rostral anterior cingulate cortex in modulating activity in the amygdala. *Neuron*, *51*(6), 871–882. <https://doi.org/10.1016/j.neuron.2006.07.029>
- Evans, A. C., Janke, A. L., Collins, D. L., & Baillet, S. (2012). Brain templates and atlases. *NeuroImage*, *62*(2), 911–922. <https://doi.org/10.1016/j.neuroimage.2012.01.024>
- Fichtenholtz, H. M., Dean, H. L., Dillon, D. G., Yamasaki, H., McCarthy, G., & LaBar, K. S. (2004). Emotion-attention network interactions during a visual oddball task. *Cognitive Brain Research*, *20*(1), 67–80. <https://doi.org/10.1016/j.cogbrainres.2004.01.006>
- Fonov, V. S., Evans, A. C., McKinstry, R. C., Almlí, C. R., & Collins, D. L. (2009). Unbiased nonlinear average age-appropriate brain templates from birth to adulthood. *NeuroImage*, *47*, Supplement 1, S102. [https://doi.org/10.1016/S1053-8119\(09\)70884-5](https://doi.org/10.1016/S1053-8119(09)70884-5)
- Gapen, M., van der Kolk, B. A., Hamlin, E., Hirshberg, L., Suvak, M., & Spinazzola, J. (2016). A Pilot Study of Neurofeedback for Chronic PTSD. *Applied Psychophysiology and Biofeedback*, *41*(3), 251–261. <https://doi.org/10.1007/s10484-015-9326-5>
- Glover, G. H., Li, T.-Q., & Ress, D. (2000). Image-based method for retrospective correction of physiological motion effects in fMRI: Retroicor. *Magnetic Resonance in Medicine*, *44*(1), 162–167. [https://doi.org/10.1002/1522-2594\(200007\)44:1<162::AID-MRM23>3.0.CO;2-E](https://doi.org/10.1002/1522-2594(200007)44:1<162::AID-MRM23>3.0.CO;2-E)
- Gorgolewski, K., Burns, C. D., Madison, C., Clark, D., Halchenko, Y. O., Waskom, M. L., & Ghosh, S. (2011). Nipype: a flexible, lightweight and extensible neuroimaging data processing framework in Python. *Frontiers in Neuroinformatics*, *5*, 13. <https://doi.org/10.3389/fninf.2011.00013>
- Gorgolewski, K. J., Esteban, O., Markiewicz, C. J., Ziegler, E., Ellis, D. G., Notter, M. P., Jarecka, D., Johnson, H., Burns, C., Manhães-Savio, A., Hamalainen, C., Yvernault, B., Salo, T., Jordan, K., Goncalves, M., Waskom, M., Clark, D., Wong, J., Loney, F., . . . Ghosh, S. (2018). Nipype. *Software*. Advance online publication. <https://doi.org/10.5281/zenodo.596855>
- Greve, D. N., & Fischl, B. (2009). Accurate and robust brain image alignment using boundary-based registration. *NeuroImage*, *48*(1), 63–72. <https://doi.org/10.1016/j.neuroimage.2009.06.060>
- Hariri, A. R., Mattay, V. S., Tessitore, A., Kolachana, B., Fera, F., Goldman, D., Egan, M. F., & Weinberger, D. R. (2002). Serotonin transporter genetic variation and the response of the human amygdala. *Science (New York, N.Y.)*, *297*(5580), 400–403. <https://doi.org/10.1126/science.1071829>
- Hermans, E. J., Henckens, M. J. A. G., Joëls, M., & Fernández, G. (2014). Dynamic adaptation of large-scale brain networks in response to acute stressors. *Trends in Neurosciences*, *37*(6), 304–314. <https://doi.org/10.1016/j.tins.2014.03.006>
- Herrman, H., Stewart, D. E., Diaz-Granados, N., Berger, E. L., Jackson, B., & Yuen, T. (2011). What is resilience? *Canadian Journal of Psychiatry. Revue Canadienne De Psychiatrie*, *56*(5), 258–265. <https://doi.org/10.1177/0706743711105600504>
- Jenkinson, M., Bannister, P., Brady, M., & Smith, S. (2002). Improved Optimization for the Robust and Accurate Linear Registration and Motion Correction of Brain Images. *NeuroImage*, *17*(2), 825–841. <https://doi.org/10.1006/nimg.2002.1132>
- Jenkinson, M., & Smith, S. (2001). A global optimisation method for robust affine registration of brain images. *Medical Image Analysis*, *5*(2), 143–156. [https://doi.org/10.1016/S1361-8415\(01\)00036-6](https://doi.org/10.1016/S1361-8415(01)00036-6)
- Joëls, M., & Baram, T. Z. (2009). The neuro-symphony of stress. *Nature Reviews Neuroscience*, *10*(6), 459–466. <https://doi.org/10.1038/nrn2632>
- Kalisch, R., Baker, D. G., Basten, U., Boks, M. P., Bonanno, G. A., Brummelman, E., Chmitorz, A., Fernández, G., Fiebach, C. J., Galatzer-Levy, I., Geuze, E., Groppa, S., Helmreich, I., Hendlér, T., Hermans, E. J., Jovanovic, T., Kubiak, T., Lieb, K., Lutz, B., . . . Kleim, B. (2017). The resilience framework as a strategy to combat stress-related disorders. *Nature Human Behaviour*, *1*(11), 784–790. <https://doi.org/10.1038/s41562-017-0200-8>

- Kalisch, R., Müller, M. B., & Tüscher, O. (2015). A conceptual framework for the neurobiological study of resilience. *Behavioral and Brain Sciences*, 38, e92. <https://doi.org/10.1017/S0140525X1400082X>
- Kanske, P., & Kotz, S. A. (2011). Emotion speeds up conflict resolution: A new role for the ventral anterior cingulate cortex? *Cerebral Cortex*, 21(4), 911–919. <https://doi.org/10.1093/cercor/bhq157>
- Kloet, E. R. de, Joëls, M., & Holsboer, F. (2005). Stress and the brain: From adaptation to disease. *Nature Reviews Neuroscience*, 6(6), 463–475. <https://doi.org/10.1038/nrn1683>
- Krause, F., Kogias, N., Krentz, M., Lührs, M., Goebel, R., & Hermans, E. J. (2021). Self-regulation of stress-related large-scale brain network balance using real-time fMRI Neurofeedback. *BioRxiv*, 2021.04.12.439440. <https://doi.org/10.1101/2021.04.12.439440>
- Krause, F., & Lindemann, O. (2014). Expyriment: A Python library for cognitive and neuroscientific experiments. *Behavior Research Methods*, 46(2), 416–428. <https://doi.org/10.3758/s13428-013-0390-6>
- Krebs, R. M., Park, H. R. P., Bombeck, K., & Boehler, C. N. (2018). Modulation of locus coeruleus activity by novel oddball stimuli. *Brain Imaging and Behavior*, 12(2), 577–584. <https://doi.org/10.1007/s11682-017-9700-4>
- Lanczos, C. (1964). Evaluation of Noisy Data. *Journal of the Society for Industrial and Applied Mathematics Series B Numerical Analysis*, 1(1), 76–85. <https://doi.org/10.1137/0701007>
- Lanius, R. A., Frewen, P. A., Tursich, M., Jetly, R., & McKinnon, M. C. (2015). Restoring large-scale brain networks in PTSD and related disorders: A proposal for neuroscientifically-informed treatment interventions. *European Journal of Psychotraumatology*, 6(1), 27313. <https://doi.org/10.3402/ejpt.v6.27313>
- Linden, D. E., Prvulovic, D., Formisano, E., Völlinger, M., Zanella, F. E., Goebel, R., & Dierks, T. (1999). The functional neuroanatomy of target detection: An fMRI study of visual and auditory oddball tasks. *Cerebral Cortex*, 9(8), 815–823. <https://doi.org/10.1093/cercor/9.8.815>
- Maples-Keller, J. L., Williamson, R. L., Sleep, C. E., Carter, N. T., Campbell, W. K., & Miller, J. D. (2019). Using Item Response Theory to Develop a 60-Item Representation of the NEO PI-R Using the International Personality Item Pool: Development of the IPIP-NEO-60. *Journal of Personality Assessment*, 101(1), 4–15. <https://doi.org/10.1080/00223891.2017.1381968>
- Martínez-Cancino, D. P., Azpiroz-Leehan, J., & Jiménez-Angeles, L. (2015). The Effects of Sleep Deprivation in Working Memory Using the N-back Task. In *VI Latin American Congress on Biomedical Engineering CLAIB 2014, Paraná, Argentina 29, 30 & 31 October 2014* (pp. 421–424). Springer, Cham. https://doi.org/10.1007/978-3-319-13117-7_108
- Mary, A., Dayan, J., Leone, G., Postel, C., Fraisse, F., Malle, C., Vallée, T., Klein-Peschanski, C., Viader, F., La Sayette, V. de, Peschanski, D., Eustache, F., & Gagnepain, P. (2020). Resilience after trauma: The role of memory suppression. *Science*, 367(6479). <https://doi.org/10.1126/science.aay8477>
- McEwen, B. S., & Akil, H. (2020). Revisiting the Stress Concept: Implications for Affective Disorders. *Journal of Neuroscience*, 40(1), 12–21. <https://doi.org/10.1523/JNEUROSCI.0733-19.2019>
- Mencarelli, L., Neri, F., Momi, D., Menardi, A., Rossi, S., Rossi, A., & Santarnecchi, E. (2019). Stimuli, presentation modality, and load-specific brain activity patterns during n-back task. *Human Brain Mapping*, 40(13), 3810–3831. <https://doi.org/10.1002/hbm.24633>
- Menon, V. (2011). Large-scale brain networks and psychopathology: A unifying triple network model. *Trends in Cognitive Sciences*, 15(10), 483–506. <https://doi.org/10.1016/j.tics.2011.08.003>
- Molnar-Szakacs, I., & Uddin, L. Q. (2022). Anterior insula as a gatekeeper of executive control. *Neuroscience and Biobehavioral Reviews*, 139, 104736. <https://doi.org/10.1016/j.neubiorev.2022.104736>
- Monti, M. M. (2011). Statistical Analysis of fMRI Time-Series: A Critical Review of the GLM Approach. *Frontiers in Human Neuroscience*, 5, 28. <https://doi.org/10.3389/fnhum.2011.00028>

- Notter, M., Gale, D., Herholz, P., Markello, R., Notter-Bieler, M.-L., & Whitaker, K. (2019). AtlasReader: A Python package to generate coordinate tables, region labels, and informative figures from statistical MRI images. *Journal of Open Source Software*, *4*(34), 1257. <https://doi.org/10.21105/joss.01257>
- Poldrack, R. A. (2007). Region of interest analysis for fMRI. *Social Cognitive and Affective Neuroscience*, *2*(1), 67–70. <https://doi.org/10.1093/scan/nsm006>
- Power, J. D., Mitra, A., Laumann, T. O., Snyder, A. Z., Schlaggar, B. L., & Petersen, S. E. (2014). Methods to detect, characterize, and remove motion artifact in resting state fMRI. *NeuroImage*, *84*(Supplement C), 320–341. <https://doi.org/10.1016/j.neuroimage.2013.08.048>
- Pruim, R. H. R., Mennes, M., van Rooij, D., Llera, A., Buitelaar, J. K., & Beckmann, C. F. (2015). ICA-AROMA: A robust ICA-based strategy for removing motion artifacts from fMRI data. *NeuroImage*, *112*(Supplement C), 267–277. <https://doi.org/10.1016/j.neuroimage.2015.02.064>
- Qin, S., Hermans, E. J., van Marle, H. J. F., Luo, J., & Fernández, G. (2009). Acute psychological stress reduces working memory-related activity in the dorsolateral prefrontal cortex. *Biological Psychiatry*, *66*(1), 25–32. <https://doi.org/10.1016/j.biopsych.2009.03.006>
- Rehm, J., & Shield, K. D. (2019). Global Burden of Disease and the Impact of Mental and Addictive Disorders. *Current Psychiatry Reports*, *21*(2), 10. <https://doi.org/10.1007/s11920-019-0997-0>
- Rohleder, N., Wolf, J. M., Piel, M., & Kirschbaum, C. (2003). Impact of oral contraceptive use on glucocorticoid sensitivity of pro-inflammatory cytokine production after psychosocial stress. *Psychoneuroendocrinology*, *28*(3), 261–273. [https://doi.org/10.1016/S0306-4530\(02\)00019-7](https://doi.org/10.1016/S0306-4530(02)00019-7)
- Rusiniak, M., Lewandowska, M., Wolak, T., Pluta, A., Milner, R., Ganc, M., Włodarczyk, A., Senderski, A., Sliwa, L., & Skarżyński, H. (2013). A modified oddball paradigm for investigation of neural correlates of attention: A simultaneous ERP-fMRI study. *Magnetic Resonance Materials in Physics, Biology and Medicine*, *26*(6), 511–526. <https://doi.org/10.1007/s10334-013-0374-7>
- Russell, G., & Lightman, S. (2019). The human stress response. *Nature Reviews Endocrinology*, *15*(9), 525–534. <https://doi.org/10.1038/s41574-019-0228-0>
- Satterthwaite, T. D., Elliott, M. A., Gerraty, R. T., Ruparel, K., Loughhead, J., Calkins, M. E., Eickhoff, S. B., Hakonarson, H., Gur, R. C., Gur, R. E., & Wolf, D. H. (2013). An improved framework for confound regression and filtering for control of motion artifact in the preprocessing of resting-state functional connectivity data. *NeuroImage*, *64*(1), 240–256. <https://doi.org/10.1016/j.neuroimage.2012.08.052>
- Schoofs, D., Pabst, S., Brand, M., & Wolf, O. T. (2013). Working memory is differentially affected by stress in men and women. *Behavioural Brain Research*, *241*, 144–153. <https://doi.org/10.1016/j.bbr.2012.12.004>
- Schoofs, D., Preuss, D., & Wolf, O. T. (2008). Psychosocial stress induces working memory impairments in an n-back paradigm. *Psychoneuroendocrinology*, *33*(5), 643–653. <https://doi.org/10.1016/j.psyneuen.2008.02.004>
- Sherwood, M. S., Kane, J. H., Weisend, M. P., & Parker, J. G. (2016). Enhanced control of dorsolateral prefrontal cortex neurophysiology with real-time functional magnetic resonance imaging (rt-fMRI) neurofeedback training and working memory practice. *NeuroImage*, *124*(Pt A), 214–223. <https://doi.org/10.1016/j.neuroimage.2015.08.074>
- Shmueli, K., van Gelderen, P., Zwart, J. A. de, Horowitz, S. G., Fukunaga, M., Jansma, J. M., & Duyn, J. H. (2007). Low-frequency fluctuations in the cardiac rate as a source of variance in the resting-state fMRI BOLD signal. *NeuroImage*, *38*(2), 306–320. <https://doi.org/10.1016/j.neuroimage.2007.07.037>
- Sitaram, R., Ros, T., Stoeckel, L., Haller, S., Scharnowski, F., Lewis-Peacock, J., Weiskopf, N., Blefari, M. L., Rana, M., Oblak, E., Birbaumer, N., & Sulzer, J. (2017). Closed-loop brain training: The science of neurofeedback. *Nature Reviews Neuroscience*, *18*(2), 86–100. <https://doi.org/10.1038/nrn.2016.164>
- Smith, S. M., Jenkinson, M., Woolrich, M. W., Beckmann, C. F., Behrens, T. E. J., Johansen-Berg, H., Bannister, P. R., Luca, M. de, Drobnjak, I., Flitney, D. E., Niazy, R. K., Saunders, J., Vickers,

- J., Zhang, Y., Stefano, N. de, Brady, J. M., & Matthews, P. M. (2004). Advances in functional and structural MR image analysis and implementation as FSL. *NeuroImage*, *23 Suppl 1*, S208-19. <https://doi.org/10.1016/j.neuroimage.2004.07.051>
- Soveri, A., Antfolk, J., Karlsson, L., Salo, B., & Laine, M. (2017). Working memory training revisited: A multi-level meta-analysis of n-back training studies. *Psychonomic Bulletin & Review*, *24*(4), 1077–1096. <https://doi.org/10.3758/s13423-016-1217-0>
- Spielberger, C. D., Gorsuch, R. L., Lushene, R. D. (1970). Manual for the State-Trait Anxiety Inventory. *Palo Alto, CA: Consulting Psychologists Press.*
- Sulzer, J., Haller, S., Scharnowski, F., Weiskopf, N., Birbaumer, N., Blefari, M. L., Bruehl, A. B., Cohen, L. G., deCharms, R. C., Gassert, R., Goebel, R., Herwig, U., LaConte, S., Linden, D., Luft, A., Seifritz, E., & Sitaram, R. (2013). Real-time fMRI neurofeedback: Progress and challenges. *NeuroImage*, *76*, 386–399. <https://doi.org/10.1016/j.neuroimage.2013.03.033>
- Thibault, R. T., MacPherson, A., Lifshitz, M., Roth, R. R., & Raz, A. (2018). Neurofeedback with fMRI: A critical systematic review. *NeuroImage*, *172*, 786–807. <https://doi.org/10.1016/j.neuroimage.2017.12.071>
- Tian, F., Shen, Q., Hu, Y., Ye, W., Valdimarsdóttir, U. A., Song, H., & Fang, F. (2022). Association of stress-related disorders with subsequent risk of all-cause and cause-specific mortality: A population-based and sibling-controlled cohort study. *The Lancet Regional Health - Europe*, *18*, 100402. <https://doi.org/10.1016/j.lanep.2022.100402>
- Tursic, A., Eck, J., Lührs, M., Linden, D. E. J., & Goebel, R. (2020). A systematic review of fMRI neurofeedback reporting and effects in clinical populations. *NeuroImage: Clinical*, *28*, 102496. <https://doi.org/10.1016/j.nicl.2020.102496>
- Tustison, N. J., Avants, B. B., Cook, P. A., Zheng, Y., Egan, A., Yushkevich, P. A., & Gee, J. C. (2010). N4ITK: Improved N3 Bias Correction. *IEEE Transactions on Medical Imaging*, *29*(6), 1310–1320. <https://doi.org/10.1109/TMI.2010.2046908>
- Tutunji, R., Kogias, N., Kapteijns, B., Krentz, M., Krause, F., Vassena, E., & Hermans, E. J. (2021). Using wearable biosensors and ecological momentary assessments for the detection of prolonged stress in real life. *BioRxiv*, 2021.06.29.450360. <https://doi.org/10.1101/2021.06.29.450360>
- Vaessen, T. J. A., Overeem, S., & Sitskoorn, M. M. (2015). Cognitive complaints in obstructive sleep apnea. *Sleep Medicine Reviews*, *19*, 51–58. <https://doi.org/10.1016/j.smrv.2014.03.008>
- van Buuren, M., Gladwin, T. E., Zandbelt, B. B., van den Heuvel, M., Ramsey, N. F., Kahn, R. S., & Vink, M. (2009). Cardiorespiratory effects on default-mode network activity as measured with fMRI. *Human Brain Mapping*, *30*(9), 3031–3042. <https://doi.org/10.1002/hbm.20729>
- van der Kolk, B. A., Hodgdon, H., Gapen, M., Musicaro, R., Suvak, M. K., Hamlin, E., & Spinazzola, J. (2016). A Randomized Controlled Study of Neurofeedback for Chronic PTSD. *PLOS ONE*, *11*(12), e0166752. <https://doi.org/10.1371/journal.pone.0166752>
- van Marle, H. J. F., Hermans, E. J., Qin, S., & Fernández, G. (2009). From specificity to sensitivity: How acute stress affects amygdala processing of biologically salient stimuli. *Biological Psychiatry*, *66*(7), 649–655. <https://doi.org/10.1016/j.biopsych.2009.05.014>
- van Oort, J., Tendolkar, I., Hermans, E. J., Mulders, P. C., Beckmann, C. F., Schene, A. H., Fernández, G., & van Eijndhoven, P. F. (2017). How the brain connects in response to acute stress: A review at the human brain systems level. *Neuroscience and Biobehavioral Reviews*, *83*, 281–297. <https://doi.org/10.1016/j.neubiorev.2017.10.015>
- van Rossum, G., & Drake, F. L. (2009). *Python 3 Reference Manual*. Scotts Valley, CA: CreateSpace.
- Vassena, E., Deraeve, J., & Alexander, W. H. (2019). Task-specific prioritization of reward and effort information: Novel insights from behavior and computational modeling. *Cognitive, Affective, & Behavioral Neuroscience*, *19*(3), 619–636. <https://doi.org/10.3758/s13415-018-00685-w>
- Vassena, E., Silvetti, M., Boehler, C. N., Achten, E., Fias, W., & Verguts, T. (2014). Overlapping neural systems represent cognitive effort and reward anticipation. *PLOS ONE*, *9*(3), e91008. <https://doi.org/10.1371/journal.pone.0091008>

- Voogd, L. D. de, Fernández, G., & Hermans, E. J. (2016). Awake reactivation of emotional memory traces through hippocampal-neocortical interactions. *NeuroImage*, *134*, 563–572. <https://doi.org/10.1016/j.neuroimage.2016.04.026>
- Voogd, L. D. de, Hermans, E. J., & Phelps, E. A. (2018). Regulating defensive survival circuits through cognitive demand via large-scale network reorganization. *Current Opinion in Behavioral Sciences*, *24*, 124–129. <https://doi.org/10.1016/j.cobeha.2018.08.009>
- Voogd, L. D. de, Kanen, J. W., Neville, D. A., Roelofs, K., Fernández, G., & Hermans, E. J. (2018). Eye-Movement Intervention Enhances Extinction via Amygdala Deactivation. *Journal of Neuroscience*, *38*(40), 8694–8706. <https://doi.org/10.1523/JNEUROSCI.0703-18.2018>
- Wells, A., & Davies, M. I. (1994). The thought control questionnaire: A measure of individual differences in the control of unwanted thoughts. *Behaviour Research and Therapy*, *32*(8), 871–878. [https://doi.org/10.1016/0005-7967\(94\)90168-6](https://doi.org/10.1016/0005-7967(94)90168-6)
- Young, C. B., Raz, G., Everaerd, D., Beckmann, C. F., Tendolkar, I., Hendler, T., Fernández, G., & Hermans, E. J. (2017). Dynamic Shifts in Large-Scale Brain Network Balance As a Function of Arousal. *Journal of Neuroscience*, *37*(2), 281–290. <https://doi.org/10.1523/JNEUROSCI.1759-16.2016>
- Zhang, Y., Brady, M., & Smith, S. (2001). Segmentation of brain MR images through a hidden Markov random field model and the expectation-maximization algorithm. *IEEE Transactions on Medical Imaging*, *20*(1), 45–57. <https://doi.org/10.1109/42.906424>

7. Supplementary Material

A. Real-time fMRI Neurofeedback Paradigm

For the Neurofeedback Training a real-time fMRI neurofeedback paradigm was used (see Fig. X). A custom functor was implemented in the MR image reconstruction pipeline, for real-time functional imaging. This enabled the export of the pixel data to an additional computer as soon as it was available. For every volume, TurboExport (version 0.261, Brain Innovation, Maastricht, The Netherlands) transformed the incoming pixel data into an image, on the additional computer. Real-time pre-processing of the resulting images was done by Turbo-BrainVoyager software (TBV; version 4.2, Brain Innovation, Maastricht, The Netherlands). These pre-processing steps included motion correction and spatial smoothing (5 mm FWHM). Motion correction included the realignment of each image to the first image of the first neurofeedback run. After pre-processing, the resulting images were co-registered to the acquired AA-HeadScout of the respective session. Afterwards, the stimulation computer requested the real-time data on Turbo-BrainVoyager, in order to generate and display the “feedback” stimulus. The communication between the stimulation computer and Turbo-BrainVoyager was established with a network connection, using the Transmission Control Protocol (TCP).

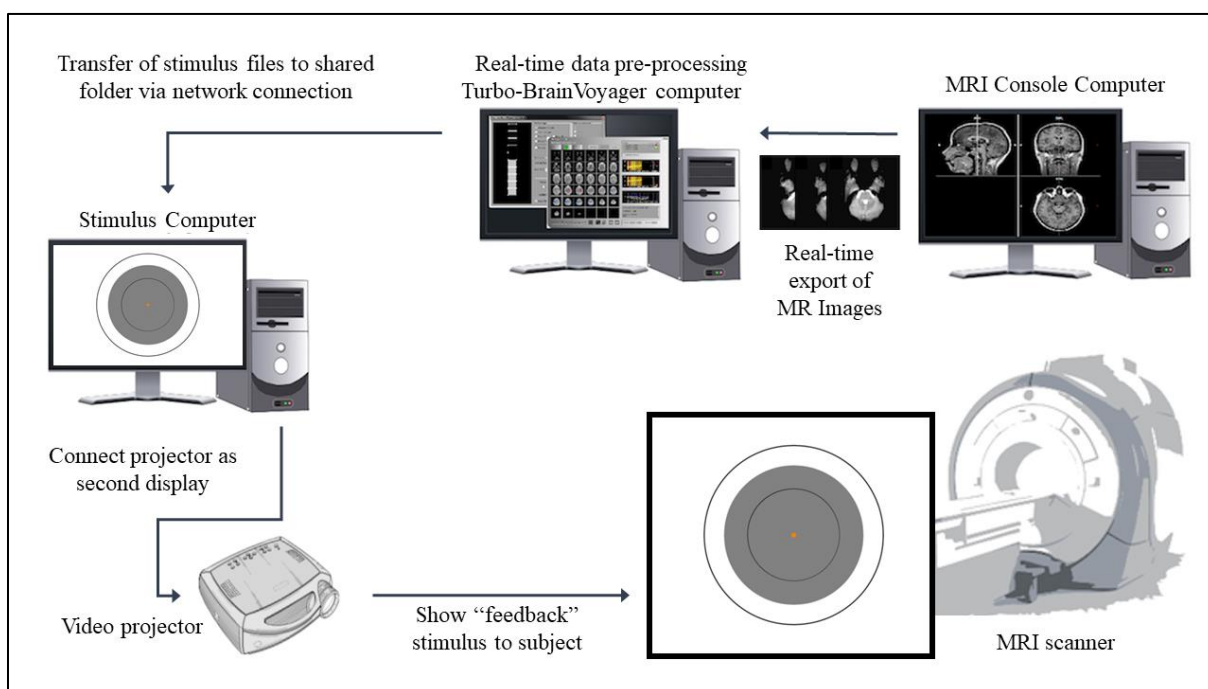


Fig. X. Simplified overview of the rtfMRI neurofeedback paradigm used in this study. (Adapted from <https://download.brainvoyager.com/tbv/doc/TBVUsersGuide/Setup/SetupForNeurofeedback.html>)

B. Neurofeedback Signal Calculation

The calculation of the neurofeedback signal relied on different aspects within each run and were presented to the participants with the “feedback stimulus” after each self-regulation application. First, the initial “rest” period (34s) of each run was used to set the baseline difference and initial display boundaries for the feedback signal, i.e. the smallest and largest possible size of the grey disc. The

feedback signal itself relied on the difference signal between mean average voxel activation in the SN and ECN ROIs. The difference in signal acquisition depended on the participant number. For uneven participants, the signal was calculated by subtracting the mean average voxel activation in the ECN from the SN (SN-ECN) and vice versa for even participants (ECN-SN). This difference value was calculated based on voxel activations in the self-regulation period and the baseline period. Then the median average difference of the whole self-regulation period in one run is compared to the median average difference during the baseline period. This difference signal during the self-regulation period during one run was then compared to the difference signal during the baseline period. The initially lower and upper boundaries of the feedback stimulus were changed to two standard deviations from the obtained baseline. Then, the actual calculation of the feedback was computed via a custom feedback presentation Python script using *Experiment* (Krause & Lindemann, 2014). The “feedback” stimulus was presented on the participant’s screen and showed the resulting circle size of the disc.

To keep it difficult to achieve the maximum or minimum of the circle size during the improved performance, the lower and upper limits of the grey disc were updated before each new regulation block. For this, the average (median) of the five lowest or highest difference values in that specific run were used and the limits were set according to these difference values. Within each regulation block, positive and negative changes in the difference signal resulted in a feedback value between -1 and 1. These values are -1 for the minimum circle size and 1 for the maximum circle size. The feedback values for each regulation direction were based on the following calculations:

$$(1) \quad feedback_{smaller} = \frac{regulation - baseline}{limit_{lower} - baseline}$$

$$(2) \quad feedback_{larger} = \frac{regulation - baseline}{limit_{upper} - baseline}$$

Further, the points which the participants received after each self-regulation run were proportional to the calculated feedback values. Scores could range from 0 to 100. A score of 0 was obtained when the difference signal for one regulation did not change towards the instructed direction or when it changed into the opposite direction. Therefore, a score of 100 was obtained when participants reached the specified limit with their mental self-regulation strategy. For each self-regulation, the sum of the scores was presented to the participant at the end of each run. The points served the purpose of motivating the participants since they knew from the start of the experiment that the best performers would gain an additional €25.

C. EMA Questionnaires

For all items, unless otherwise indicated, the answer options range from ‘1. Not at all’ to ‘7. Very much’

Morning questions (on sleep quality)

- at what time did you fall asleep?

- at what time did you wake up?
- I slept well (slider)
- I feel rested (slider)
- how long did it take you to fall asleep?
 - < 30 minutes
 - 30 – 60 minutes
 - > 60 minutes
- for female participants:
 - what phase of your menstrual cycle are you currently in?
 - Not applicable/Hormonal birth control
 - Menstruation
 - No menstruation, and 1 to 7 day(s) until next menstruation
 - No menstruation, and 8 to 14 days until next menstruation
 - No menstruation, and > 14 days until next menstruation
 - I don't know

Momentary assessment questions

Mood items

- To what extent are the following statements true (1 Not at all; 7 Very much)
 - I feel cheerful
 - I feel irritated
 - I feel anxious
 - I feel satisfied
 - I feel insecure
 - I feel relaxed
 - I feel sad
 - I feel stressed
 - I feel restless
 - I feel tired
 - My mind is at ease
 - I cannot get these thoughts out of my mind
 - I can concentrate well

Social items

- I am in virtual contact with others (yes/no)
 - If answered **yes**:
 - Who am I with?
 - Partner
 - Parents
 - Other family
 - Friend(s)
 - Other peer(s)
 - Other (familiar) people
 - Unfamiliar people
 - I am doing something together with these people (yes/no)
 - I feel at ease with these people (slider)
 - I would rather be alone (slider)

- If answered **No**:
 - I would like to be in virtual contact with others (slider)
 - I choose not to be in virtual contact with others myself (slider)
 - I feel, from a virtual perspective, excluded
- I am in contact with others who are physically present:
 - If answered **yes**:
 - Who am I with?
 - Partner
 - Parents
 - Other family
 - Friend(s)
 - Other peer(s)
 - Other (familiar) people
 - Unfamiliar people
 - We are doing something together (e.g. talking, learning, gaming etc.) (yes/no)
 - I feel at ease in this company (slider)
 - I would rather be alone (slider)
 - I like to be alone
 - If answered **No**:
 - I like to be alone (slider)
 - I feel excluded (slider)
 - I would rather be with other people (slider)

Physical context/activity items

- What were you doing right before you started this questionnaire?
 - Leisure – active (e.g. playing games, going out)
 - Leisure – passive (e.g. watching TV, reading)
 - School or work
 - Chores
 - Travel
 - Personal care (e.g. washing, getting dressed)
 - Physical exercise (sports)
 - Eating/drinking
 - Social contact
 - Something else
 - Nothing
- I like doing this
- I would rather be doing something else
- I can do this well (if answer was != ‘Nothing’)

Event appraisal items

‘Now think about the most important event for you since the last questionnaire you answered’

- How pleasant was this event? (slider)
- This was a stressful event

Substance use items

- Since the last questionnaire, I have used one (or more) of the following: medication, caffeine, alcohol, cigarettes, cannabis, other drugs
- If yes:
 - o What did you use?
 - Caffeine
 - Medication
 - Alcohol
 - Cigarettes
 - Cannabis/Hash
 - Hallucinogenic drugs (e.g. ketamine, LSD, magic mushrooms)
 - Stimulants (e.g. Cocaine, ecstasy, Ritalin)
 - Narcotics (e.g. sedatives, heroine, morphine)

Anticipation of pleasure items

‘Now think about the most important situation for you in the next two hours’

- I am looking forward to this situation (slider)
- I am dreading this situation (slider)

Evening questions (self-reflection)

- This was a normal day for me (slider)
- This was a nice day (slider)
- Today I spent about ... minutes exercising:
 - o 0
 - o 1 – 15
 - o 16 – 30
 - o 31 – 60
 - o 61 – 120
 - o 121 – 180
 - o > 180

‘Think back at the most negative event of the day’

- When was this?
 - o Morning
 - o Midday
 - o Afternoon
 - o Evening
- Where was I?
 - o At school/work
 - o At home
 - o At my partner’s home
 - o At a friend’s home
 - o At the home of other family members
 - o On a bike/in a car/on the train
 - o Somewhere else (inside)
 - o Somewhere else (outside)
- With whom was I
 - o Partner
 - o Father

- Mother
- Other family (from nuclear family)
- Other family (outside of nuclear family)
- Friend(s)
- Other peer(s)
- Colleagues; teacher
- Other (familiar) people
- Unfamiliar people
- No one
- How unpleasant was this event (slider)
- I talked to someone about it (yes/no)
 - If yes:
 - These person(s) responded with understanding (slider)
 - If no:
 - I would have liked to talk to someone about it
- I have since thought about it often (slider)
- I have put it into perspective (slider)
- I just let it happen (slider)
- I expressed my emotions about it (slider)
- I tried to quickly forget about it (slider)
- I tried to change the situation (slider)
- Today, I avoided attending social activities (slider)
- Today, I failed to follow through with achievement-related goals (slider)
- Today, I avoided trying new activities in which I might have failed (slider)
- Today, I waited out tension in my relationship, hoping it would go away (slider)

‘Think back of the most positive event of the day’

- When was this?
 - Morning
 - Midday
 - Afternoon
 - Evening
- Where was I?
 - At school/work
 - At home
 - At my partner’s home
 - At a friend’s home
 - At the home of other family members
 - On a bike/in a car/on the train
 - Somewhere else (inside)
 - Somewhere else (outside)
- With whom was I
 - Partner
 - Father
 - Mother
 - Other family (from nuclear family)
 - Other family (outside of nuclear family)

- Friend(s)
- Other peer(s)
- Colleagues; teacher
- Other (familiar) people
- Unfamiliar people
- No one
- How pleasant was this event (slider)
- I talked to someone about it (yes/no)
 - If yes:
 - These person(s) responded with understanding (slider)
 - If no:
 - I would have liked to talk to someone about it (slider)
- I have since thought about it often (slider)
- I have put it into perspective (slider)
- I just let it happen (slider)
- I expressed my emotions about it (slider)
- I expect tomorrow to be a stressful experience (slider)
- I am confident I can cope with tomorrow's challenges (slider)
- I am worried about how tomorrow will turn out (slider)
- Filling out the questionnaires influenced my mood today (slider)

D. Questionnaires

The set of questionnaires that the participants had to complete before their first Neurofeedback Training session, included the 60 item International Personality Item Pool NEO (IPIP-NEO-60) to assess individual personality traits (Maples-Keller et al., 2019), the behavioural inhibition system (BIS) and behavioural activation system (BAS) questionnaires, used to model two of the main motivational systems involved in behaviour and affect (Carver & White, 1994), the trait component of the state-trait anxiety inventory (STAI-trait), used to assess trait-anxiety severity or existence (Spielberger, C. D., Gorsuch, R. L., Lushene, R. D., 1970), the thought control questionnaire (TCQ) which is used to self-assess individual use of strategies to cope with experiencing negative events in life (Wells & Davies, 1994), and lastly the Beck's depression inventory II (BDI-II), used to measure indications of depression (Beck et al., 1996).

E. Neurofeedback Training and Transfer Questionnaires

Participants had to answer several open answered questions after each neurofeedback training session, Transfer 1 and Transfer 2. The questions for each session are listed below in the order in which the participants also received them.

Post-Neurofeedback Training Questions

1. Did you have an explicit strategy to increase the size of the circle? If so, what was your best strategy?
2. Did you have an explicit strategy to decrease the size of the circle? If so, what was your best strategy?

3. Do you think you would change your strategy for the next session?

For female participants only: What was the first day of your current menstrual cycle?

Post-Transfer 1 & 2 Questions

1. How well do you think you learned to gain control over the size of the circle across all training sessions?
2. How confident were you to apply the strategies you learned during the training sessions, without receiving feedback?
3. Which strategy did you use to increase the size of the circle?
4. Which strategy did you use to decrease the size of the circle?
5. How do you think you performed during this session?
6. Do you have any thoughts that you would like to share?

For female participants only: What was the first day of your current menstrual cycle?

F. Whole-brain fMRI random-effects analysis - Result tables

The clusters which are reported in the result tables, consist of a minimum of five thresholded voxels. Further, the sub-peaks of the clusters are included, which have a minimal distance of 10 voxels (i.e. 24mm). This was not done for the statistical inference as part of the analysis, but only to reduce the number of peaks reported in the tables, by only including peaks that are more different in location. First the result tables for the 2-back task analysis, and then the results tables for the Emotional-Faces Oddball task will be listed below. Result tables were created using *AtlasReader* (version 0.1.2; Notter et al., 2019).

2-back

Table S1. Brain regions whose activation change was positive (red) or negative (blue) over time for the contrast “regulate to SN”. The X-, Y- and Z-coordinates are in MNI space and volume is in mm.

NR	X	Y	Z	Z-VALUE	VOLUME	AAL	HARVARD_OXFORD
1	-46	13	3	5.94	162127	Frontal_Inf_Oper_L	35.0% Left_Frontal_Operculum_Cortex; 27.0% Left_Inferior_Frontal_Gyrus_pars_opercularis; 8.0% Left_Central_Opercular_Cortex
1	-10	3	48	5.86	162127	Supp_Motor_Area_L	30.0% Left_Juxtapositional_Lobule_Cortex_(formerly_Supplementary_Motor_Cortex)
1	46	10	5	5.81	162127	Frontal_Inf_Oper_R	30.0% Right_Frontal_Operculum_Cortex; 14.0% Right_Inferior_Frontal_Gyrus_pars_opercularis; 11.0% Right_Central_Opercular_Cortex; 10.0% Right_Precentral_Gyrus
1	15	-3	-8	5.57	162127	no_label	20.0% Right_Pallidum
1	6	15	34	5.54	162127	Cingulate_Mid_R	73.0% Right_Cingulate_Gyrus_anterior_division; 10.0% Right_Paracingulate_Gyrus

1	-39	41	19	5.52	162127	Frontal_Mid_2_L	78.0% Left_Frontal_Pole; 6.0% Left_Middle_Frontal_Gyrus
1	-22	3	7	5.16	162127	Putamen_L	99.0% Left_Putamen
1	-36	-6	41	5.13	162127	Precentral_L	16.0% Left_Precentral_Gyrus
1	-29	51	-13	5.11	162127	OFCant_L	84.0% Left_Frontal_Pole
1	-12	-17	-16	5.11	162127	no_label	0% no_label
1	6	1	70	4.98	162127	Supp_Motor_Area_R	44.0% Right_Juxtapositional_Lobule_Cortex_(formerly_Supplementary_Motor_Cortex); 28.0% Right_Superior_Frontal_Gyrus
1	22	-20	17	4.95	162127	no_label	0% no_label
1	-55	10	29	4.95	162127	Precentral_L	36.0% Left_Precentral_Gyrus; 25.0% Left_Inferior_Frontal_Gyrus_pars_opercularis
1	29	27	-13	4.87	162127	OFCpost_R	40.0% Right_Frontal_Orbital_Cortex
1	-29	-25	3	4.81	162127	no_label	15.0% Left_Putamen
1	49	-1	39	4.49	162127	Precentral_R	32.0% Right_Precentral_Gyrus
1	27	-8	53	4.39	162127	Precentral_R	29.0% Right_Precentral_Gyrus; 14.0% Right_Superior_Frontal_Gyrus; 10.0% Right_Middle_Frontal_Gyrus
1	-12	-25	72	4.29	162127	Paracentral_Lobule_L	46.0% Left_Precentral_Gyrus
1	-32	24	-16	4.19	162127	OFCpost_L	36.0% Left_Frontal_Orbital_Cortex
1	53	36	-1	3.96	162127	Frontal_Inf_Tri_R	58.0% Right_Frontal_Pole; 22.0% Right_Inferior_Frontal_Gyrus_pars_triangularis
1	6	-22	53	3.33	162127	Supp_Motor_Area_R	63.0% Right_Precentral_Gyrus
2	46	-53	-30	5.44	47862	Cerebelum_Crus1_R	0% no_label
2	22	-84	-11	5.34	47862	Lingual_R	41.0% Right_Occipital_Fusiform_Gyrus; 10.0% Right_Occipital_Pole; 5.0% Right_Lateral_Occipital_Cortex_inferior_division
2	-34	-63	-23	5.32	47862	Cerebelum_6_L	0% no_label
2	-22	-87	-13	4.82	47862	Lingual_L	47.0% Left_Occipital_Fusiform_Gyrus; 10.0% Left_Lateral_Occipital_Cortex_inferior_division; 7.0% Left_Occipital_Pole
2	-8	-46	-28	4.7	47862	no_label	0% no_label
2	-3	-56	-4	4.4	47862	Cerebelum_4_5_L	0% no_label
2	49	-75	-4	4.05	47862	Occipital_Inf_R	81.0% Right_Lateral_Occipital_Cortex_inferior_division
2	18	-37	-20	3.82	47862	Cerebelum_4_5_R	0% no_label
3	-34	-46	51	4.65	7227	Parietal_Inf_L	40.0% Left_Superior_Parietal_Lobule; 10.0% Left_Supramarginal_Gyrus_posterior_division
3	-15	-70	43	3.97	7227	Parietal_Sup_L	25.0% Left_Lateral_Occipital_Cortex_superior_division; 13.0% Left_Precuneous_Cortex
4	58	-53	27	-5.08	4085	Angular_R	72.0% Right_Angular_Gyrus; 7.0% Right_Lateral_Occipital_Cortex_superior_division

4	44	-68	41	-3.98	4085	Angular_R	86.0% Right_Lateral_Occipital_Cortex_superior_division
5	1	-46	24	-4.61	3374	Cingulate_Post_R	65.0% Right_Cingulate_Gyrus_posterior_division; 17.0% Left_Cingulate_Gyrus_posterior_division
6	13	-75	-40	5.02	2418	Cerebelum_Crus2_R	0% no_label
6	32	-56	-47	4.48	2418	Cerebelum_8_R	0% no_label
7	25	17	58	-3.98	2158	Frontal_Sup_2_R	53.0% Right_Superior_Frontal_Gyrus; 14.0% Right_Middle_Frontal_Gyrus
8	13	36	53	-4.74	1858	Frontal_Sup_2_R	41.0% Right_Frontal_Pole; 37.0% Right_Superior_Frontal_Gyrus
9	34	46	7	4	1625	Frontal_Mid_2_R	39.0% Right_Frontal_Pole
9	34	41	31	3.83	1625	Frontal_Mid_2_R	70.0% Right_Frontal_Pole; 9.0% Right_Middle_Frontal_Gyrus
10	-60	-37	27	4.81	1420	SupraMarginal_L	43.0% Left_Supramarginal_Gyrus_anterior_division; 16.0% Left_Parietal_Operculum_Cortex; 15.0% Left_Planum_Temporale; 8.0% Left_Supramarginal_Gyrus_posterior_division
11	53	-8	-28	-5.2	1216	Temporal_Inf_R	27.0% Right_Middle_Temporal_Gyrus_posterior_division; 20.0% Right_Middle_Temporal_Gyrus_anterior_division; 9.0% Right_Inferior_Temporal_Gyrus_anterior_division; 7.0% Right_Inferior_Temporal_Gyrus_posterior_division
12	65	-34	-8	-3.96	1038	Temporal_Mid_R	60.0% Right_Middle_Temporal_Gyrus_posterior_division; 15.0% Right_Middle_Temporal_Gyrus_temporooccipital_part
13	-48	-75	0	4.37	983	Occipital_Mid_L	86.0% Left_Lateral_Occipital_Cortex_inferior_division
14	15	-53	-44	4.16	915	Cerebelum_9_R	0% no_label
15	44	-34	7	4.07	724	Temporal_Sup_R	6.0% Right_Supramarginal_Gyrus_posterior_division; 6.0% Right_Superior_Temporal_Gyrus_posterior_division
16	6	-34	-42	4.37	696	no_label	100.0% Brain-Stem
17	-46	-65	7	3.51	218	Temporal_Mid_L	44.0% Left_Lateral_Occipital_Cortex_inferior_division; 14.0% Left_Middle_Temporal_Gyrus_temporooccipital_part
18	-39	-60	7	4.07	204	no_label	8.0% Left_Middle_Temporal_Gyrus_temporooccipital_part; 6.0% Left_Lateral_Occipital_Cortex_inferior_division
19	15	-22	72	3.74	163	Precentral_R	58.0% Right_Precentral_Gyrus; 11.0% Right_Postcentral_Gyrus
20	32	-34	-37	3.77	163	Cerebelum_6_R	0% no_label
21	-27	15	-28	4.25	109	Temporal_Pole_Sup_L	40.0% Left_Frontal_Orbital_Cortex;

							20.0% Left_Temporal_Pole
22	10	-8	39	3.66	95	Cingulate_Mid_R	27.0% Right_Cingulate_Gyrus_anterior_division
23	22	-48	-42	3.81	81	no_label	0% no_label
24	39	-41	-11	3.52	81	Fusiform_R	0% no_label
25	-10	-6	36	3.54	68	Cingulate_Mid_L	11.0% Left_Cingulate_Gyrus_anterior_division; 6.0% Left_Juxtapositional_Lobule_Cortex_(formerly_Supplementary_Motor_Cortex)

Table S2. Brain regions whose activation change was positive (red) or negative (blue) over time for the contrast “regulate to ECN”. The X-, Y- and Z-coordinates are in MNI space and volume is in mm.

NR	X	Y	Z	Z-VALUE	VOLUME	AAL	HARVARD_OXFORD
1	-41	53	19	5.13	19073	Frontal_Mid_2_L	14.0% Left_Frontal_Pole
1	-36	27	24	4.63	19073	Frontal_Inf_Tri_L	35.0% Left_Middle_Frontal_Gyrus
1	-48	1	43	4.43	19073	Precentral_L	58.0% Left_Precentral_Gyrus; 7.0% Left_Middle_Frontal_Gyrus
1	-36	41	-1	4.03	19073	Frontal_Mid_2_L	15.0% Left_Frontal_Pole
1	-29	-1	67	3.69	19073	Frontal_Sup_2_L	14.0% Left_Superior_Frontal_Gyrus; 9.0% Left_Middle_Frontal_Gyrus
2	-5	-6	63	5.11	13704	Supp_Motor_Area_L	50.0% Left_Juxtapositional_Lobule_Cortex_(formerly_Supplementary_Motor_Cortex)
2	-10	17	46	5.06	13704	Supp_Motor_Area_L	11.0% Left_Paracingulate_Gyrus
3	-46	8	3	5.15	7637	Frontal_Inf_Oper_L	30.0% Left_Central_Opercular_Cortex; 29.0% Left_Frontal_Operculum_Cortex; 6.0% Left_Precentral_Gyrus; 5.0% Left_Inferior_Frontal_Gyrus_pars_opercularis
3	-22	27	3	3.62	7637	no_label	0% no_label
4	22	-84	-11	4.89	7104	Lingual_R	41.0% Right_Occipital_Fusiform_Gyrus; 10.0% Right_Occipital_Pole; 5.0% Right_Lateral_Occipital_Cortex_inferior_division
5	44	-58	-28	5.46	5547	Cerebelum_Crus1_R	0% no_label
6	-17	-1	0	5.23	5355	Pallidum_L	98.0% Left_Pallidum
6	-29	-22	3	4	5355	no_label	39.0% Left_Putamen
7	20	1	10	4.86	3607	no_label	13.0% Right_Putamen
8	-34	-65	-20	4.96	3320	Cerebelum_6_L	16.0% Left_Occipital_Fusiform_Gyrus; 14.0% Left_Temporal_Occipital_Fusiform_Cortex
8	-22	-84	-8	4.7	3320	Fusiform_L	46.0% Left_Occipital_Fusiform_Gyrus; 9.0% Left_Lateral_Occipital_Cortex_inferior_division
9	3	-51	53	-4.05	1981	Precuneus_R	87.0% Right_Precuneus_Cortex
10	-27	-84	-37	-4.17	1434	Cerebelum_Crus2_L	0% no_label
11	-27	-80	10	3.94	1243	Occipital_Mid_L	9.0% Left_Lateral_Occipital_Cortex_superior_division

12	46	10	3	4.78	1079	Frontal_Inf_Oper_R	38.0% Right_Frontal_Operculum_Cortex; 14.0% Right_Inferior_Frontal_Gyrus_pars_opercularis; 13.0% Right_Central_Opercular_Cortex; 6.0% Right_Precentral_Gyrus
13	13	-53	72	-3.65	204	Postcentral_R	38.0% Right_Superior_Parietal_Lobule; 19.0% Right_Lateral_Occipital_Cortex_superior_division
14	-46	48	-4	3.59	191	Frontal_Mid_2_L	87.0% Left_Frontal_Pole
15	-20	-17	22	3.64	68	Caudate_L	7.0% Left_Caudate

Table S3. Brain regions whose activation change was positive (red) or negative (blue) over time for the differential contrast “regulate to SN > regulate to ECN”. The X-, Y- and Z-coordinates are in MNI space and volume is in mm.

NR	X	Y	Z	Z-VALUE	VOLUME	AAL	HARVARD_OXFORD
1	13	-51	58	4.25	3333	Precuneus_R	34.0% Right_Precuneous_Cortex; 20.0% Right_Superior_Parietal_Lobule; 6.0% Right_Postcentral_Gyrus
2	6	-8	55	4.38	3087	Supp_Motor_Area_R	60.0% Right_Juxtapositional_Lobule_Cortex_(formerly_Supplementary_Motor_Cortex); 13.0% Right_Precentral_Gyrus
2	6	8	36	3.83	3087	Cingulate_Mid_R	66.0% Right_Cingulate_Gyrus_anterior_division; 5.0% Right_Paracingulate_Gyrus
3	-15	-29	41	4.27	3046	Cingulate_Mid_L	38.0% Left_Precentral_Gyrus; 13.0% Left_Cingulate_Gyrus_posterior_division; 5.0% Left_Precuneous_Cortex
3	-17	-48	67	3.62	3046	Parietal_Sup_L	42.0% Left_Superior_Parietal_Lobule; 24.0% Left_Postcentral_Gyrus
4	18	-15	70	4.02	1653	Frontal_Sup_2_R	43.0% Right_Precentral_Gyrus; 7.0% Right_Superior_Frontal_Gyrus
5	-63	-27	22	4.1	1557	Temporal_Sup_L	51.0% Left_Supramarginal_Gyrus_anterior_division; 17.0% Left_Parietal_Operculum_Cortex; 12.0% Left_Postcentral_Gyrus
6	-12	5	41	3.84	929	Cingulate_Mid_L	12.0% Left_Juxtapositional_Lobule_Cortex_(formerly_Supplementary_Motor_Cortex)
7	27	-44	-37	4.21	874	no_label	0% no_label
8	3	-15	41	3.59	300	Cingulate_Mid_R	56.0% Right_Cingulate_Gyrus_posterior_division; 26.0% Right_Cingulate_Gyrus_anterior_division

Table S4. Brain regions whose activation change was positive (red) or negative (blue) over time for the mean activation contrast during the 2-back task, including all three conditions (“Task after rest”, “Task after regulate to SN” and “Task after regulate to ECN”). The X-, Y- and Z-coordinates are in MNI space and volume is in mm.

NR	X	Y	Z	Z-VALUE	VOLUME	AAL	HARVARD_OXFORD
----	---	---	---	---------	--------	-----	----------------

1	8	-20	-13	7.41	260653	no_label	0% no_label
1	27	-60	-28	7.18	260653	Cerebelum_6_R	0% no_label
1	-12	-10	3	7.11	260653	Thalamus_L	82.0% Left_Thalamus
1	29	24	0	7.03	260653	no_label	49.0% Right_Insular_Cortex; 7.0% Right_Frontal_Orbital_Cortex
1	-34	22	0	6.83	260653	Insula_L	53.0% Left_Insular_Cortex; 14.0% Left_Frontal_Operculum_Cortex; 12.0% Left_Frontal_Orbital_Cortex
1	-27	-60	-30	6.73	260653	Cerebelum_6_L	0% no_label
1	-27	-3	48	6.73	260653	Precentral_L	31.0% Left_Middle_Frontal_Gyrus; 13.0% Left_Precentral_Gyrus; 8.0% Left_Superior_Frontal_Gyrus
1	32	5	53	6.54	260653	Frontal_Mid_2_R	35.0% Right_Middle_Frontal_Gyrus; 11.0% Right_Superior_Frontal_Gyrus
1	-1	-41	-23	6.53	260653	Vermis_1_2	14.0% Brain-Stem
1	-3	3	58	6.42	260653	Supp_Motor_Area_L	77.0% Left_Juxtapositional_Lobule_Cortex_(formerly_Supple mentary_Motor_Cortex); 8.0% Left_Superior_Frontal_Gyrus
1	10	-6	5	6.27	260653	Thalamus_R	98.0% Right_Thalamus
1	-8	-75	-23	6.18	260653	Cerebelum_Crus1_L	0% no_label
1	-44	-65	-1	6.02	260653	Occipital_Mid_L	48.0% Left_Lateral_Occipital_Cortex_inferior_division; 13.0% Left_Middle_Temporal_Gyrus_temporooccipital_part
1	-46	5	31	5.91	260653	Precentral_L	30.0% Left_Precentral_Gyrus; 28.0% Left_Middle_Frontal_Gyrus; 15.0% Left_Inferior_Frontal_Gyrus_pars_opercularis
1	6	24	41	5.9	260653	Frontal_Sup_Medial_R	77.0% Right_Paracingulate_Gyrus
1	44	39	29	5.9	260653	Frontal_Mid_2_R	64.0% Right_Frontal_Pole; 27.0% Right_Middle_Frontal_Gyrus
1	49	10	27	5.82	260653	Frontal_Inf_Oper_R	34.0% Right_Precentral_Gyrus; 32.0% Right_Inferior_Frontal_Gyrus_pars_opercularis; 6.0% Right_Middle_Frontal_Gyrus
1	18	41	-16	5.7	260653	OFCmed_R	46.0% Right_Frontal_Pole
1	-44	-44	-35	5.36	260653	Cerebelum_Crus1_L	0% no_label
1	-34	-15	-8	5.31	260653	Putamen_L	16.0% Left_Putamen
1	18	-34	-42	5.23	260653	no_label	27.0% Brain-Stem
1	-48	29	29	5.18	260653	Frontal_Mid_2_L	60.0% Left_Middle_Frontal_Gyrus
1	3	17	7	5.15	260653	no_label	90.0% Right_Lateral_Ventricle
1	46	-60	5	5.07	260653	Temporal_Mid_R	38.0% Right_Lateral_Occipital_Cortex_inferior_division; 18.0% Right_Middle_Temporal_Gyrus_temporooccipital_part
1	32	55	15	4.96	260653	Frontal_Sup_2_R	88.0% Right_Frontal_Pole
1	-17	-39	-42	4.89	260653	Cerebelum_10_L	0% no_label

1	-24	-39	10	4.89	260653	no_label	65.0% Left_Lateral_Ventricular
1	20	-17	24	4.29	260653	Caudate_R	17.0% Right_Caudate
1	-17	20	19	4	260653	no_label	0% no_label
1	1	-48	3	3.91	260653	Vermis_4_5	0% no_label
2	-1	-44	31	-7.33	144557	Cingulate_Post_L	92.0% Left_Cingulate_Gyrus_posterior_division
2	-39	36	-16	-6.44	144557	OFClat_L	44.0% Left_Frontal_Pole; 38.0% Left_Frontal_Orbital_Cortex
2	-32	-37	-13	-6.28	144557	Fusiform_L	41.0% Left_Parahippocampal_Gyrus_posterior_division; 38.0% Left_Temporal_Fusiform_Cortex_posterior_division
2	22	-89	27	-6.03	144557	Occipital_Sup_R	52.0% Right_Occipital_Pole; 19.0% Right_Lateral_Occipital_Cortex_superior_division
2	-36	-15	-1	-6.01	144557	Insula_L	81.0% Left_Insular_Cortex
2	39	-3	-8	-5.98	144557	Insula_R	95.0% Right_Insular_Cortex
2	-5	-91	-8	-5.89	144557	Calcarine_L	30.0% Left_Occipital_Pole; 22.0% Left_Lingual_Gyrus; 7.0% Left_Intracalcarine_Cortex
2	-17	-63	22	-5.82	144557	Cuneus_L	53.0% Left_Precuneous_Cortex; 15.0% Left_Supracalcarine_Cortex; 5.0% Left_Cuneal_Cortex
2	18	-87	-6	-5.79	144557	Lingual_R	22.0% Right_Lingual_Gyrus; 21.0% Right_Occipital_Fusiform_Gyrus; 20.0% Right_Occipital_Pole
2	-1	-15	39	-5.71	144557	Cingulate_Mid_L	57.0% Left_Cingulate_Gyrus_posterior_division; 38.0% Left_Cingulate_Gyrus_anterior_division
2	29	-34	-11	-5.62	144557	ParaHippocampal_R	26.0% Right_Parahippocampal_Gyrus_posterior_division; 18.0% Right_Hippocampus; 8.0% Right_Lingual_Gyrus
2	-15	-101	15	-5.61	144557	Occipital_Sup_L	71.0% Left_Occipital_Pole
2	-55	-8	-18	-5.43	144557	Temporal_Mid_L	32.0% Left_Middle_Temporal_Gyrus_anterior_division; 16.0% Left_Middle_Temporal_Gyrus_posterior_division; 7.0% Left_Superior_Temporal_Gyrus_posterior_division; 7.0% Left_Superior_Temporal_Gyrus_anterior_division
2	-27	-3	-23	-5.36	144557	Amygdala_L	85.0% Left_Amygdala; 12.0% Left_Hippocampus
2	37	34	-16	-5.34	144557	OFCpost_R	58.0% Right_Frontal_Pole; 31.0% Right_Frontal_Orbital_Cortex
2	-15	-37	5	-5.27	144557	Hippocampus_L	21.0% Left_Thalamus; 20.0% Left_Hippocampus
2	-1	-46	63	-5.24	144557	Precuneus_L	26.0% Left_Precuneous_Cortex; 13.0% Left_Postcentral_Gyrus
2	-3	-84	36	-5.18	144557	Cuneus_L	52.0% Left_Cuneal_Cortex; 13.0% Left_Precuneous_Cortex
2	-55	29	15	-5.18	144557	Frontal_Inf_Tri_L	26.0% Left_Inferior_Frontal_Gyrus_pars_triangularis; 6.0% Left_Middle_Frontal_Gyrus
2	22	-53	22	-5.12	144557	Precuneus_R	24.0% Right_Precuneous_Cortex

2	13	-32	48	-5.1	144557	Paracentral_Lobule_R	33.0% Right_Precentral_Gyrus; 21.0% Right_Postcentral_Gyrus; 6.0% Right_Precuneous_Cortex; 5.0% Right_Cingulate_Gyrus_posterior_division
2	25	-58	-11	-4.56	144557	Fusiform_R	36.0% Right_Temporal_Occipital_Fusiform_Cortex; 27.0% Right_Lingual_Gyrus; 19.0% Right_Occipital_Fusiform_Gyrus
2	10	-32	7	-4.56	144557	Thalamus_R	77.0% Right_Thalamus
2	-48	13	-35	-4.31	144557	Temporal_Pole_Mid_L	73.0% Left_Temporal_Pole
2	-41	8	-4	-4.2	144557	Insula_L	68.0% Left_Insular_Cortex; 12.0% Left_Central_Opercular_Cortex
3	1	58	29	-6.29	72032	Frontal_Sup_Medial_L	15.0% Right_Frontal_Pole; 8.0% Right_Superior_Frontal_Gyrus; 5.0% Left_Frontal_Pole
3	-1	41	-13	-6.12	72032	Frontal_Med_Orb_L	57.0% Left_Frontal_Medial_Cortex; 18.0% Left_Paracingulate_Gyrus; 14.0% Right_Frontal_Medial_Cortex
3	-10	36	51	-6.05	72032	Frontal_Sup_Medial_L	41.0% Left_Superior_Frontal_Gyrus; 22.0% Left_Frontal_Pole
3	-17	63	10	-6.04	72032	Frontal_Sup_2_L	65.0% Left_Frontal_Pole
3	-3	17	-8	-5.54	72032	Olfactory_L	92.0% Left_Subcallosal_Cortex
3	8	63	3	-5.36	72032	Frontal_Sup_Medial_R	55.0% Right_Frontal_Pole
3	13	44	48	-5.32	72032	Frontal_Sup_2_R	75.0% Right_Frontal_Pole
3	1	32	17	-4.4	72032	Cingulate_Ant_R	51.0% Right_Cingulate_Gyrus_anterior_division; 36.0% Left_Cingulate_Gyrus_anterior_division
3	-36	22	48	-4.19	72032	Frontal_Mid_2_L	79.0% Left_Middle_Frontal_Gyrus
4	39	-44	41	7.15	31971	Parietal_Inf_R	36.0% Right_Supramarginal_Gyrus_posterior_division; 19.0% Right_Angular_Gyrus; 13.0% Right_Superior_Parietal_Lobule
4	29	-65	53	5.84	31971	Parietal_Sup_R	61.0% Right_Lateral_Occipital_Cortex_superior_division
5	-34	-46	43	7.14	29198	Parietal_Inf_L	36.0% Left_Superior_Parietal_Lobule; 17.0% Left_Supramarginal_Gyrus_posterior_division; 6.0% Left_Angular_Gyrus
5	-8	-68	53	5.14	29198	Precuneus_L	37.0% Left_Precuneous_Cortex; 26.0% Left_Lateral_Occipital_Cortex_superior_division
5	-27	-72	36	4.84	29198	Occipital_Mid_L	79.0% Left_Lateral_Occipital_Cortex_superior_division
6	39	-75	-37	-6.12	7104	Cerebelum_Crus2_R	0% no_label
6	8	-91	-30	-3.87	7104	Cerebelum_Crus2_R	0% no_label
7	-53	-65	27	-5.45	5793	Angular_L	84.0% Left_Lateral_Occipital_Cortex_superior_division; 6.0% Left_Angular_Gyrus
8	51	5	-25	-6.14	5560	Temporal_Mid_R	39.0% Right_Temporal_Pole; 15.0% Right_Middle_Temporal_Gyrus_anterior_division

9	37	5	12	-6.07	3702	Insula_R	62.0% Right_Central_Opercular_Cortex; 7.0% Right_Insular_Cortex; 5.0% Right_Frontal_Operculum_Cortex
10	18	-27	60	-5.02	3251	no_label	38.0% Right_Precentral_Gyrus; 18.0% Right_Postcentral_Gyrus
11	-29	-84	-37	-5.85	3197	Cerebelum_Crus2_L	0% no_label
12	32	-91	-8	5.85	2855	Occipital_Inf_R	50.0% Right_Occipital_Pole; 19.0% Right_Lateral_Occipital_Cortex_inferior_division
13	46	39	5	-5.42	2705	Frontal_Inf_Tri_R	55.0% Right_Frontal_Pole; 14.0% Right_Inferior_Frontal_Gyrus_pars_triangularis
14	60	-22	24	-5.52	2445	SupraMarginal_R	50.0% Right_Supramarginal_Gyrus_anterior_division; 15.0% Right_Parietal_Operculum_Cortex; 14.0% Right_Postcentral_Gyrus; 6.0% Right_Planum_Temporale
15	-48	-44	19	4.52	2213	Temporal_Sup_L	17.0% Left_Planum_Temporale; 12.0% Left_Supramarginal_Gyrus_posterior_division
16	-15	-51	60	-4.72	2145	no_label	27.0% Left_Superior_Parietal_Lobule; 18.0% Left_Postcentral_Gyrus; 6.0% Left_Precuneus_Cortex; 5.0% Left_Lateral_Occipital_Cortex_superior_division
17	-36	51	12	5.61	2049	Frontal_Mid_2_L	86.0% Left_Frontal_Pole
18	-32	-91	-8	4.99	1926	Occipital_Inf_L	43.0% Left_Occipital_Pole; 29.0% Left_Lateral_Occipital_Cortex_inferior_division
19	37	-15	41	-5.53	1516	Precentral_R	59.0% Right_Precentral_Gyrus; 16.0% Right_Postcentral_Gyrus
20	49	-25	-1	4.46	1352	Temporal_Sup_R	38.0% Right_Superior_Temporal_Gyrus_posterior_division; 14.0% Right_Middle_Temporal_Gyrus_posterior_division
21	-3	3	24	4.84	1093	no_label	12.0% Left_Cingulate_Gyrus_anterior_division
22	-58	-29	22	-4.83	874	Temporal_Sup_L	44.0% Left_Parietal_Operculum_Cortex; 18.0% Left_Supramarginal_Gyrus_anterior_division; 7.0% Left_Planum_Temporale
23	-36	-17	41	-5.21	819	Postcentral_L	43.0% Left_Postcentral_Gyrus; 30.0% Left_Precentral_Gyrus
24	-24	48	-8	4.67	806	Frontal_Sup_2_L	37.0% Left_Frontal_Pole
25	-65	-46	0	-4.13	628	Temporal_Mid_L	64.0% Left_Middle_Temporal_Gyrus_temporooccipital_part; 12.0% Left_Middle_Temporal_Gyrus_posterior_division; 8.0% Left_Angular_Gyrus
26	-41	-15	22	-4.35	601	Rolandic_Oper_L	31.0% Left_Central_Opercular_Cortex
27	-27	34	17	4.12	245	no_label	0% no_label
28	63	-8	-25	-3.85	245	Temporal_Mid_R	48.0% Right_Middle_Temporal_Gyrus_posterior_division;

							35.0% Right_Middle_Temporal_Gyrus_anterior_division
29	-51	-41	31	3.55	136	SupraMarginal_L	27.0% Left_Supramarginal_Gyrus_posterior_division; 10.0% Left_Supramarginal_Gyrus_anterior_division; 5.0% Left_Parietal_Operculum_Cortex
30	-27	46	34	-3.56	95	Frontal_Mid_2_L	85.0% Left_Frontal_Pole
31	1	13	31	-3.54	81	Cingulate_Mid_R	70.0% Right_Cingulate_Gyrus_anterior_division; 22.0% Left_Cingulate_Gyrus_anterior_division
32	-29	27	19	3.47	68	no_label	5.0% Left_Middle_Frontal_Gyrus
33	-15	3	-23	-4.56	68	ParaHippocampal_L	7.0% Left_Parahippocampal_Gyrus_anterior_division

Table S5. Brain regions whose activation change was positive (red) or negative (blue) over time for the differential contrast “Task after regulate to SN > Task after rest”. The X-, Y- and Z-coordinates are in MNI space and volume is in mm.

NR	X	Y	Z	Z-VALUE	VOLUME	AAL	HARVARD_OXFORD
1	-29	-10	27	4.39	819	no_label	0% no_label
2	-10	27	10	4.34	765	no_label	15.0% Left_Lateral_Ventrical

Emotional Faces Oddball task

Table S6. Brain regions whose activation change was positive (red) or negative (blue) over time for the contrast “regulate to SN”. The X-, Y- and Z-coordinates are in MNI space and volume is in mm.

NR	X	Y	Z	Z-VALUE	VOLUME	AAL	HARVARD_OXFORD
1	-8	8	43	5.42	40771	Supp_Motor_Area_L	30.0% Left_Paracingulate_Gyrus; 20.0% Left_Cingulate_Gyrus_anterior_division; 15.0% Left_Juxtapositional_Lobule_Cortex_(formerly_Supple- mentary_Motor_Cortex)
1	-17	-1	10	4.98	40771	no_label	0% no_label
1	10	1	63	4.95	40771	Supp_Motor_Area_R	23.0% Right_Superior_Frontal_Gyrus; 12.0% Right_Juxtapositional_Lobule_Cortex_(formerly_Suppl- ementary_Motor_Cortex)
1	-46	3	34	4.9	40771	Precentral_L	42.0% Left_Precentral_Gyrus; 27.0% Left_Middle_Frontal_Gyrus; 7.0% Left_Inferior_Frontal_Gyrus_pars_opercularis
1	-48	13	3	4.83	40771	Frontal_Inf_Oper_L	53.0% Left_Inferior_Frontal_Gyrus_pars_opercularis; 11.0% Left_Frontal_Operculum_Cortex; 9.0% Left_Precentral_Gyrus
1	-34	-6	53	4.82	40771	Precentral_L	45.0% Left_Precentral_Gyrus; 25.0% Left_Middle_Frontal_Gyrus
1	15	20	34	4.32	40771	Cingulate_Mid_R	0% no_label
1	-27	29	5	4.24	40771	Insula_L	5.0% Left_Frontal_Orbital_Cortex; 5.0% Left_Inferior_Frontal_Gyrus_pars_triangularis; 5.0% Left_Insular_Cortex
2	-34	46	17	4.89	6612	Frontal_Mid_2_L	79.0% Left_Frontal_Pole
3	13	-48	39	-4.68	6093	Precuneus_R	32.0% Right_Precuneous_Cortex; 10.0% Right_Cingulate_Gyrus_posterior_division
4	41	-68	-25	5.18	5834	Cerebelum_Crus1_R	0% no_label
4	32	-41	-35	3.75	5834	Cerebelum_6_R	0% no_label
5	56	-53	22	-5.23	5642	Temporal_Sup_R	76.0% Right_Angular_Gyrus; 6.0% Right_Lateral_Occipital_Cortex_superior_division
5	44	-65	51	-3.81	5642	Angular_R	61.0% Right_Lateral_Occipital_Cortex_superior_division
6	20	-3	12	4.86	3962	no_label	0% no_label
7	-44	-58	-32	4.78	2951	Cerebelum_Crus1_L	0% no_label

8	51	13	-4	4.44	1953	no_label	30.0% Right_Temporal_Pole; Right_Frontal_Operculum_Cortex; Right_Inferior_Frontal_Gyrus_pars_opercularis; Right_Precentral_Gyrus; Right_Central_Opercular_Cortex	12.0% 12.0% 6.0% 5.0%
9	32	22	58	-4.19	1803	Frontal_Mid_2_R	43.0% Right_Middle_Frontal_Gyrus; Right_Superior_Frontal_Gyrus	17.0%
10	10	-48	-13	4.19	1694	Cerebelum_4_5_R	0% no_label	
11	3	-89	5	-4.27	1461	Calcarine_L	34.0% Right_Occipital_Pole; Right_Intracalcarine_Cortex; Right_Supracalcarine_Cortex; Left_Occipital_Pole; 5.0% Right_Cuneal_Cortex	12.0% 10.0% 6.0%
12	-20	-65	46	3.91	1420	Parietal_Sup_L	52.0% Left_Lateral_Occipital_Cortex_superior_division	
13	-55	-37	46	4.01	888	Parietal_Inf_L	59.0% Left_Supramarginal_Gyrus_anterior_division; 12.0% Left_Supramarginal_Gyrus_posterior_division	
14	60	-34	-8	-4.95	874	Temporal_Mid_R	25.0% Right_Middle_Temporal_Gyrus_posterior_division; 10.0% Right_Middle_Temporal_Gyrus_temporooccipital_part	
15	27	-6	53	4.02	847	Precentral_R	19.0% Right_Precentral_Gyrus; Right_Superior_Frontal_Gyrus; Right_Middle_Frontal_Gyrus	18.0% 16.0%
16	-29	-44	36	3.7	833	no_label	15.0% Left_Supramarginal_Gyrus_posterior_division; 10.0% Left_Superior_Parietal_Lobule; Left_Supramarginal_Gyrus_anterior_division	5.0%
17	10	-82	36	-4.06	724	Cuneus_R	48.0% Right_Cuneal_Cortex; Right_Lateral_Occipital_Cortex_superior_division; 5.0% Right_Precuneus_Cortex	16.0%
18	-17	44	-16	3.99	601	OFCmed_L	45.0% Left_Frontal_Pole	
19	-32	-17	-4	4.48	519	Putamen_L	55.0% Left_Putamen	
20	68	-15	-13	-3.73	177	Temporal_Mid_R	80.0% Right_Middle_Temporal_Gyrus_posterior_division; 8.0% Right_Middle_Temporal_Gyrus_anterior_division	
21	-65	-37	27	3.84	163	no_label	60.0% Left_Supramarginal_Gyrus_anterior_division; 11.0% Left_Planum_Temporale; Left_Supramarginal_Gyrus_posterior_division	8.0%
22	20	-87	27	-3.46	150	Occipital_Sup_R	43.0% Right_Lateral_Occipital_Cortex_superior_division; 25.0% Right_Occipital_Pole	
23	15	-77	0	-3.7	136	Lingual_R	13.0% Right_Lingual_Gyrus; Right_Intracalcarine_Cortex	13.0%
24	-24	53	-16	3.72	95	OFCant_L	73.0% Left_Frontal_Pole	
25	-8	-91	3	-3.47	81	Calcarine_L	46.0% Left_Occipital_Pole; Left_Intracalcarine_Cortex	16.0%
26	-10	-20	0	3.48	68	Thalamus_L	99.0% Left_Thalamus	
27	60	-22	-13	-3.55	68	Temporal_Mid_R	44.0% Right_Middle_Temporal_Gyrus_posterior_division	

Table S7. Brain regions whose activation change was positive (red) or negative (blue) over time for the contrast “regulate to ECN”. The X-, Y- and Z-coordinates are in MNI space and volume is in mm.

NR	X	Y	Z	Z-VALUE	VOLUME	AAL	HARVARD_oxford	
1	-44	29	19	5.16	14496	Frontal_Inf_Tri_L	41.0% Left_Inferior_Frontal_Gyrus_pars_triangularis; 33.0% Left_Middle_Frontal_Gyrus	
1	-36	55	17	4.58	14496	Frontal_Mid_2_L	55.0% Left_Frontal_Pole	
1	-46	1	43	4.46	14496	Precentral_L	50.0% Left_Precentral_Gyrus; Left_Middle_Frontal_Gyrus	17.0%
1	-58	-1	17	3.73	14496	Postcentral_L	58.0% Left_Precentral_Gyrus; Left_Postcentral_Gyrus	8.0%
2	-3	5	51	5.12	9878	Supp_Motor_Area_L	62.0% Left_Juxtapositional_Lobule_Cortex_(formerly_Supplementary_Motor_Cortex); Left_Paracingulate_Gyrus	22.0%
2	8	22	29	3.82	9878	Cingulate_Mid_R	43.0% Right_Cingulate_Gyrus_anterior_division; Right_Paracingulate_Gyrus	22.0%

3	-46	8	0	4.94	5697	Insula_L	36.0% Left_Central_Opercular_Cortex; Left_Frontal_Operculum_Cortex; Left_Precentral_Gyrus	32.0% 5.0%
3	-27	17	12	4.7	5697	Insula_L	14.0% Left_Insular_Cortex	
4	-17	-1	15	4.49	4139	no_label	0% no_label	
5	18	8	3	4.4	3128	Pallidum_R	37.0% Right_Putamen; 16.0% Right_Pallidum	
5	18	-8	22	3.48	3128	Caudate_R	50.0% Right_Caudate	
6	44	-58	-28	4.52	2664	Cerebellum_Crus1_R	0% no_label	
7	-24	-80	-37	-4.5	2131	Cerebellum_Crus2_L	0% no_label	
8	22	-84	-11	4.85	2076	Lingual_R	41.0% Right_Occipital_Fusiform_Gyrus; Right_Occipital_Pole; Right_Lateral_Occipital_Cortex_inferior_division	10.0% 5.0%
9	49	13	-1	4.62	1817	Frontal_Inf_Oper_R	29.0% Right_Frontal_Operculum_Cortex; Right_Inferior_Frontal_Gyrus_pars_opercularis; Right_Temporal_Pole; Right_Central_Opercular_Cortex	13.0% 7.0% 6.0%
10	6	-89	24	-5.26	1817	Cuneus_R	53.0% Right_Occipital_Pole; Right_Cuneal_Cortex	19.0%
11	32	-84	10	4.63	1776	Occipital_Mid_R	25.0% Right_Lateral_Occipital_Cortex_inferior_division; 18.0% Right_Lateral_Occipital_Cortex_superior_division; 8.0% Right_Occipital_Pole	
12	18	-48	75	-4.26	1243	Postcentral_R	27.0% Right_Superior_Parietal_Lobule; Right_Postcentral_Gyrus	17.0%
13	-15	-51	67	-4.41	1188	Precuneus_L	34.0% Left_Superior_Parietal_Lobule; Left_Postcentral_Gyrus; Left_Lateral_Occipital_Cortex_superior_division	25.0% 6.0%
14	13	-48	39	-4.11	1038	Precuneus_R	32.0% Right_Precuneus_Cortex; Right_Cingulate_Gyrus_posterior_division	10.0%
15	-22	-84	-13	5.12	1038	Lingual_L	53.0% Left_Occipital_Fusiform_Gyrus; Left_Lateral_Occipital_Cortex_inferior_division	8.0%
16	-20	-75	53	3.77	737	Parietal_Sup_L	59.0% Left_Lateral_Occipital_Cortex_superior_division	
17	-8	-20	-4	4.35	710	no_label	22.0% Left_Thalamus	
18	-17	-29	43	-4.1	560	no_label	5.0% Left_Precentral_Gyrus	
19	-32	-29	43	-3.91	273	Postcentral_L	9.0% Left_Postcentral_Gyrus	
20	-20	-27	31	-4.09	81	no_label	0% no_label	
21	3	-44	39	-3.62	68	Precuneus_R	48.0% Right_Cingulate_Gyrus_posterior_division; 43.0% Right_Precuneous_Cortex	

Table S8. Brain regions whose activation change was positive (red) or negative (blue) over time for the differential contrast “regulate to SN > regulate to ECN”. The X-, Y- and Z-coordinates are in MNI space and volume is in mm.

NR	X	Y	Z	Z-VALUE	VOLUME	AAL	HARVARD_OXFORD
1	27	-70	41	-4.53	2637	Occipital_Sup_R	65.0% Right_Lateral_Occipital_Cortex_superior_division
1	44	-56	27	-3.58	2637	Angular_R	30.0% Right_Angular_Gyrus; 6.0% Right_Lateral_Occipital_Cortex_superior_division

Table S9. Brain regions whose activation change was positive (red) or negative (blue) over time for the mean activation contrast during the Emotional Faces Oddball task, including all three conditions (“Task after rest”, “Task after regulate to SN” and “Task after regulate to ECN”). The X-, Y- and Z-coordinates are in MNI space and volume is in mm.

NR	X	Y	Z	Z-VALUE	VOLUME	AAL	HARVARD_OXFORD	
1	25	-91	-8	6.64	121192	Lingual_R	35.0% Right_Occipital_Pole; Right_Lateral_Occipital_Cortex_inferior_division; 11.0% Right_Occipital_Fusiform_Gyrus	12.0%
1	37	-56	-16	6.46	121192	Fusiform_R	59.0% Right_Temporal_Occipital_Fusiform_Cortex; 6.0% Right_Occipital_Fusiform_Gyrus	
1	-39	-44	-20	6.39	121192	Fusiform_L	34.0% Left_Temporal_Fusiform_Cortex_posterior_division; 30.0% Left_Temporal_Occipital_Fusiform_Cortex; 7.0%	

							Left_Inferior_Temporal_Gyrus_temporooccipital_part; 6.0% Left_Inferior_Temporal_Gyrus_posterior_division
1	-32	-91	-11	6.18	121192	Occipital_Inf_L	38.0% Left_Occipital_Pole; 28.0% Left_Lateral_Occipital_Cortex_inferior_division; 6.0% Left_Occipital_Fusiform_Gyrus
1	34	1	-18	5.92	121192	no_label	11.0% Right_Amygdala
1	49	-75	-6	5.86	121192	Occipital_Inf_R	84.0% Right_Lateral_Occipital_Cortex_inferior_division
1	-5	-99	-1	5.84	121192	Calcarine_L	72.0% Left_Occipital_Pole
1	18	-32	0	5.59	121192	no_label	96.0% Right_Thalamus
1	-5	-29	-4	5.46	121192	no_label	70.0% Brain-Stem
1	8	-56	-8	4.97	121192	Cerebelum_4_5_R	0% no_label
1	37	20	-4	4.89	121192	Insula_R	69.0% Right_Insular_Cortex; 12.0% Right_Frontal_Orbital_Cortex
1	-48	-68	-16	4.88	121192	Occipital_Inf_L	53.0% Left_Lateral_Occipital_Cortex_inferior_division; 14.0% Left_Occipital_Fusiform_Gyrus; 11.0% Left_Inferior_Temporal_Gyrus_temporooccipital_part
1	39	5	29	4.54	121192	Frontal_Inf_Oper_R	31.0% Right_Precentral_Gyrus; 14.0% Right_Inferior_Frontal_Gyrus_pars_opercularis; 14.0% Right_Middle_Frontal_Gyrus
1	51	29	19	4.43	121192	Frontal_Inf_Tri_R	35.0% Right_Inferior_Frontal_Gyrus_pars_triangularis; 23.0% Right_Middle_Frontal_Gyrus; 5.0% Right_Frontal_Pole
1	-10	-25	-28	4.42	121192	no_label	100.0% Brain-Stem
1	37	48	-8	4.37	121192	Frontal_Mid_2_R	49.0% Right_Frontal_Pole
1	49	-41	-32	4.28	121192	Cerebelum_Crus1_R	0% no_label
1	-8	-6	3	3.91	121192	Thalamus_L	98.0% Left_Thalamus
1	13	-58	-32	3.65	121192	no_label	0% no_label
1	29	-29	-23	3.63	121192	Fusiform_R	57.0% Right_Temporal_Fusiform_Cortex_posterior_division; 27.0% Right_Parahippocampal_Gyrus_posterior_division; 7.0% Right_Temporal_Occipital_Fusiform_Cortex
1	-48	-68	7	3.61	121192	Temporal_Mid_L	69.0% Left_Lateral_Occipital_Cortex_inferior_division; 5.0% Left_Middle_Temporal_Gyrus_temporooccipital_part
2	-5	-8	53	5.06	19565	Supp_Motor_Area_L	67.0% Left_Juxtapositional_Lobule_Cortex_(formerly_Supple mentary_Motor_Cortex)
2	-5	13	41	4.71	19565	Cingulate_Mid_L	55.0% Left_Paracingulate_Gyrus; 21.0% Left_Cingulate_Gyrus_anterior_division
2	8	51	41	4.67	19565	Frontal_Sup_Medial_R	68.0% Right_Frontal_Pole; 13.0% Right_Superior_Frontal_Gyrus
2	-8	53	17	4.34	19565	Frontal_Sup_Medial_L	25.0% Left_Superior_Frontal_Gyrus; 16.0% Left_Paracingulate_Gyrus; 11.0% Left_Frontal_Pole
2	-12	32	27	3.92	19565	Cingulate_Ant_L	22.0% Left_Paracingulate_Gyrus; 6.0% Left_Cingulate_Gyrus_anterior_division
2	-17	36	51	3.82	19565	Frontal_Sup_2_L	49.0% Left_Superior_Frontal_Gyrus; 29.0% Left_Frontal_Pole
2	13	29	55	3.77	19565	Frontal_Sup_2_R	74.0% Right_Superior_Frontal_Gyrus
2	18	58	17	3.35	19565	Frontal_Sup_2_R	51.0% Right_Frontal_Pole
3	-22	-8	-13	5.32	13567	Amygdala_L	98.0% Left_Amygdala
3	-27	27	5	4.83	13567	Insula_L	14.0% Left_Insular_Cortex; 5.0% Left_Inferior_Frontal_Gyrus_pars_triangularis
3	-36	-6	12	4.46	13567	Insula_L	76.0% Left_Insular_Cortex; 12.0% Left_Central_Opercular_Cortex
3	-44	32	-11	4.1	13567	Frontal_Inf_Orb_2_L	45.0% Left_Frontal_Orbital_Cortex; 11.0% Left_Frontal_Pole

3	-29	3	-35	3.64	13567	no_label	35.0% Left_Temporal_Pole
4	1	27	-23	5.26	6394	Rectus_L	61.0% Right_Subcallosal_Cortex; 11.0% Left_Subcallosal_Cortex; 9.0% Right_Frontal_Medial_Cortex
4	-8	51	-13	4.8	6394	Frontal_Med_Orb_L	33.0% Left_Frontal_Medial_Cortex; 7.0% Left_Frontal_Pole
5	-5	-70	58	-4.82	5260	Precuneus_L	38.0% Left_Precuneous_Cortex; 33.0% Left_Lateral_Occipital_Cortex_superior_division
5	20	-56	60	-4.34	5260	Parietal_Sup_R	30.0% Right_Superior_Parietal_Lobule; 23.0% Right_Lateral_Occipital_Cortex_superior_division
6	-41	-1	34	4.72	2992	Precentral_L	56.0% Left_Precentral_Gyrus; 10.0% Left_Middle_Frontal_Gyrus
7	-39	-20	53	4.13	2869	Precentral_L	44.0% Left_Precentral_Gyrus; 16.0% Left_Postcentral_Gyrus
8	-5	-75	-40	5.18	2841	Cerebelum_7b_L	0% no_label
9	6	1	29	5.4	2677	Cingulate_Mid_R	42.0% Right_Cingulate_Gyrus_anterior_division
10	-63	-13	-28	5	2049	Temporal_Inf_L	38.0% Left_Middle_Temporal_Gyrus_posterior_division; 15.0% Left_Middle_Temporal_Gyrus_anterior_division; 8.0% Left_Inferior_Temporal_Gyrus_anterior_division; 7.0% Left_Inferior_Temporal_Gyrus_posterior_division
11	29	-6	-32	4.48	1858	ParaHippocampal_R	41.0% Right_Parahippocampal_Gyrus_anterior_division; 28.0% Right_Temporal_Fusiform_Cortex_anterior_division; 7.0% Right_Temporal_Fusiform_Cortex_posterior_division
12	29	-56	48	4.21	1694	Parietal_Sup_R	39.0% Right_Superior_Parietal_Lobule; 26.0% Right_Lateral_Occipital_Cortex_superior_division; 9.0% Right_Angular_Gyrus
13	-12	-65	24	-4.4	1461	Cuneus_L	47.0% Left_Precuneous_Cortex; 9.0% Left_Supracalcarine_Cortex; 9.0% Left_Cuneal_Cortex
14	-55	-51	41	4.08	1393	Parietal_Inf_L	49.0% Left_Supramarginal_Gyrus_posterior_division; 37.0% Left_Angular_Gyrus
15	58	-34	17	4.15	942	Temporal_Sup_R	36.0% Right_Planum_Temporale; 15.0% Right_Supramarginal_Gyrus_posterior_division; 6.0% Right_Parietal_Operculum_Cortex; 5.0% Right_Superior_Temporal_Gyrus_posterior_division
16	-34	-82	34	-4.23	683	Occipital_Mid_L	62.0% Left_Lateral_Occipital_Cortex_superior_division
17	56	-51	7	4.21	546	Temporal_Mid_R	53.0% Right_Middle_Temporal_Gyrus_temporooccipital_part; 12.0% Right_Angular_Gyrus
18	34	46	12	4.1	478	Frontal_Mid_2_R	45.0% Right_Frontal_Pole
19	63	-37	0	4.09	464	Temporal_Mid_R	40.0% Right_Middle_Temporal_Gyrus_posterior_division; 27.0% Right_Middle_Temporal_Gyrus_temporooccipital_part; 8.0% Right_Supramarginal_Gyrus_posterior_division; 6.0% Right_Superior_Temporal_Gyrus_posterior_division
20	-39	-65	-30	3.64	136	Cerebelum_Crus1_L	0% no_label
21	-63	-37	-18	4.09	109	Temporal_Inf_L	46.0% Left_Middle_Temporal_Gyrus_posterior_division; 27.0% Left_Inferior_Temporal_Gyrus_posterior_division
22	-15	-39	3	4.1	95	Hippocampus_L	70.0% Left_Hippocampus; 13.0% Left_Thalamus
23	-29	5	10	3.57	68	Insula_L	16.0% Left_Insular_Cortex

24	-41	-15	-25	3.46	68	Temporal_Inf_L	30.0% Left_Inferior_Temporal_Gyrus_posterior_division; 27.0% Left_Temporal_Fusiform_Cortex_posterior_division; 10.0% Left_Temporal_Fusiform_Cortex_anterior_division; 8.0% Left_Inferior_Temporal_Gyrus_anterior_division
25	-58	-20	51	3.48	68	no_label	54.0% Left_Postcentral_Gyrus

Table S10. Brain regions whose activation change was positive (red) or negative (blue) over time for the differential contrast “Task after regulate to SN > Task after rest”. The X-, Y- and Z-coordinates are in MNI space and volume is in mm.

NR	X	Y	Z	Z-VALUE	VOLUME	AAL	HARVARD_OXFORD
1	-29	-13	36	4.3	901	no_label	0% no_label

G. Offline whole-brain fMRI fixed-effects analysis - Result tables

The clusters which are reported in the result tables, consist of a minimum of five thresholded voxels. Further, the sub-peaks of the clusters are included, which have a minimal distance of 10 voxels (i.e. 24mm). This was not done for the statistical inference as part of the analysis, but only to reduce the number of peaks reported in the tables, by only including peaks that are more different in location. First the result tables for the 2-back task analysis, and then the results tables for the Emotional-Faces Oddball task will be listed below. Result tables were created using *AtlasReader* (version 0.1.2; Notter et al., 2019).

2-back

Table S1. Brain regions whose activation change was positive (red) or negative (blue) over time for the differential contrast “Task after regulate to SN > Task after rest”. The X-, Y- and Z-coordinates are in MNI space and volume is in mm.

NR	X	Y	Z	Z-VALUE	VOLUME	AAL	HARVARD_OXFORD
1	22	58	7	8.32	11176	Frontal_Sup_2_R	54.0% Right_Frontal_Pole
1	13	53	34	8.29	11176	Frontal_Sup_2_R	76.0% Right_Frontal_Pole
1	3	27	63	7.04	11176	no_label	33.0% Right_Superior_Frontal_Gyrus
1	-3	58	12	6.78	11176	Frontal_Sup_Medial_L	57.0% Left_Frontal_Pole; 13.0% Left_Paracingulate_Gyrus; 10.0% Left_Superior_Frontal_Gyrus
1	-3	36	41	6.41	11176	Frontal_Sup_Medial_L	68.0% Left_Superior_Frontal_Gyrus; 14.0% Left_Paracingulate_Gyrus
2	6	-13	46	8.68	7419	Cingulate_Mid_R	29.0% Right_Cingulate_Gyrus_anterior_division; 26.0% Right_Juxtapositional_Lobule_Cortex_(formerly_Suppl ementary_Motor_Cortex); 20.0% Right_Cingulate_Gyrus_posterior_division; 16.0% Right_Precentral_Gyrus
2	3	-20	79	8.55	7419	Paracentral_Lobule_R	14.0% Right_Precentral_Gyrus
3	53	17	-1	8.61	4249	Frontal_Inf_Oper_R	28.0% Right_Inferior_Frontal_Gyrus_pars_opercularis; 16.0% Right_Inferior_Frontal_Gyrus_pars_triangularis
3	56	-6	7	6.48	4249	Rolandic_Oper_R	61.0% Right_Central_Opercular_Cortex; 17.0% Right_Planum_Polare; 7.0% Right_Heschl's_Gyrus_(includes_H1_and_H2)
4	-27	51	-4	8.05	3292	Frontal_Sup_2_L	20.0% Left_Frontal_Pole
5	-1	-65	-32	7.94	2814	Vermis_8	0% no_label
5	3	-82	-16	6.81	2814	no_label	24.0% Right_Lingual_Gyrus

6	-1	24	-1	9.59	2677	Olfactory_L	35.0% Left_Subcallosal_Cortex; Right_Subcallosal_Cortex	6.0%
6	-22	24	10	6.59	2677	no_label	0% no_label	
7	1	-15	7	8.91	2500	Thalamus_R	55.0% Right_Thalamus; 35.0% Left_Thalamus	
8	-60	3	5	8.48	2158	Rolandic_Oper_L	54.0% Left_Precentral_Gyrus	
8	-51	20	-13	6.84	2158	Temporal_Pole_Sup_L	31.0% Left_Temporal_Pole; Left_Frontal_Orbital_Cortex	6.0%
9	-15	44	43	8.06	2049	Frontal_Sup_2_L	75.0% Left_Frontal_Pole; Left_Superior_Frontal_Gyrus	10.0%
10	39	44	3	8.26	1543	Frontal_Mid_2_R	62.0% Right_Frontal_Pole	
11	53	-56	39	7.19	1502	Parietal_Inf_R	64.0% Right_Angular_Gyrus; Right_Lateral_Occipital_Cortex_superior_division	19.0%
12	-12	-44	34	6.59	1352	Cingulate_Mid_L	33.0% Left_Cingulate_Gyrus_posterior_division; 13.0% Left_Precuneus_Cortex	
13	-12	39	12	7.57	1325	no_label	18.0% Left_Paracingulate_Gyrus; Left_Cingulate_Gyrus_anterior_division	13.0%
14	10	39	3	7.19	1311	Cingulate_Ant_R	23.0% Right_Cingulate_Gyrus_anterior_division; 10.0% Right_Paracingulate_Gyrus	
15	-53	-15	55	7.34	1216	Postcentral_L	38.0% Left_Postcentral_Gyrus	
15	-32	-25	67	6.83	1216	Precentral_L	36.0% Left_Postcentral_Gyrus; Left_Precentral_Gyrus	30.0%
16	27	53	-4	8.71	1175	Frontal_Sup_2_R	61.0% Right_Frontal_Pole	
17	-5	-99	12	6.89	1147	Cuneus_L	63.0% Left_Occipital_Pole	
18	1	-96	3	7.38	1106	Calcarine_L	38.0% Left_Occipital_Pole; 16.0% Right_Occipital_Pole	
18	3	-94	27	6.67	1106	no_label	20.0% Right_Occipital_Pole	
19	-46	-17	43	6.72	1093	Postcentral_L	55.0% Left_Postcentral_Gyrus; Left_Precentral_Gyrus	25.0%
20	-44	-58	27	7.76	1011	Angular_L	46.0% Left_Angular_Gyrus; Left_Lateral_Occipital_Cortex_superior_division	22.0%
21	-12	-80	-18	7.27	929	Cerebelum_6_L	19.0% Left_Occipital_Fusiform_Gyrus; Left_Lingual_Gyrus	18.0%
22	-36	-15	19	7.94	929	Insula_L	56.0% Left_Central_Opercular_Cortex; Left_Insular_Cortex	14.0%
23	-44	-13	-1	7.58	806	Temporal_Sup_L	31.0% Left_Planum_Polare; Left_Heschl's_Gyrus_(includes_H1_and_H2); Left_Insular_Cortex	19.0% 13.0%
24	-1	-60	-20	11.44	792	Vermis_6	0% no_label	
25	-1	-82	48	7.07	765	Precuneus_L	12.0% Left_Precuneus_Cortex	
26	-39	-82	-28	7.85	710	Cerebelum_Crus1_L	0% no_label	
27	25	-37	-25	6.35	669	Cerebelum_4_5_R	0% no_label	
28	34	27	36	6.31	601	Frontal_Mid_2_R	36.0% Right_Middle_Frontal_Gyrus	
29	1	-44	-18	6.83	573	Vermis_3	0% no_label	
30	10	-46	36	7.18	560	Cingulate_Mid_R	37.0% Right_Cingulate_Gyrus_posterior_division; 34.0% Right_Precuneus_Cortex	
31	-12	-25	-11	7.69	532	no_label	20.0% Brain-Stem	
32	51	-53	-32	7.44	519	Cerebelum_Crus1_R	0% no_label	
33	-41	1	-6	6.86	491	Insula_L	69.0% Left_Insular_Cortex	
34	68	-3	17	6.39	491	Postcentral_R	18.0% Right_Postcentral_Gyrus	
35	29	-82	-25	7.05	491	Cerebelum_Crus1_R	0% no_label	
36	-1	-39	3	7.84	423	no_label	0% no_label	
37	-10	65	17	6.32	423	Frontal_Sup_Medial_L	91.0% Left_Frontal_Pole	
38	10	-82	5	6.37	409	Calcarine_R	52.0% Right_Intracalcarine_Cortex; Right_Lingual_Gyrus	8.0%
39	39	-10	19	7.17	382	Rolandic_Oper_R	70.0% Right_Central_Opercular_Cortex	
40	-1	53	0	6.39	355	Frontal_Sup_Medial_L	36.0% Left_Paracingulate_Gyrus; Left_Frontal_Pole; 9.0% Right_Paracingulate_Gyrus; 6.0% Left_Frontal_Medial_Cortex	12.0%

41	-34	8	10	7.18	355	Insula_L	46.0% Left_Insular_Cortex; Left_Central_Opercular_Cortex; Left_Frontal_Operculum_Cortex	20.0% 9.0%
42	-41	22	46	6.66	355	Frontal_Mid_2_L	68.0% Left_Middle_Frontal_Gyrus	
43	22	-37	70	7.71	341	Postcentral_R	56.0% Right_Postcentral_Gyrus; Right_Superior_Parietal_Lobule	6.0%
44	34	-89	5	-6.2	327	Occipital_Mid_R	38.0% Right_Occipital_Pole; Right_Lateral_Occipital_Cortex_superior_division; 15.0% Right_Lateral_Occipital_Cortex_inferior_division	17.0%
45	20	-84	22	6.77	300	Occipital_Sup_R	38.0% Right_Lateral_Occipital_Cortex_superior_division; 8.0% Right_Occipital_Pole	
46	-53	-25	12	7.7	286	Temporal_Sup_L	36.0% Left_Parietal_Operculum_Cortex; Left_Central_Opercular_Cortex; Left_Planum_Temporale; Left_Heschl's_Gyrus_(includes_H1_and_H2)	20.0% 17.0% 12.0%
47	8	-44	75	6.92	273	Paracentral_Lobule_R	53.0% Right_Postcentral_Gyrus; Right_Precuneous_Cortex	10.0%
48	-34	20	-37	-6.82	273	Temporal_Pole_Mid_L	72.0% Left_Temporal_Pole	
49	-58	-3	31	6.14	259	Precentral_L	69.0% Left_Precentral_Gyrus; Left_Postcentral_Gyrus	14.0%
50	37	39	-13	6.87	245	OFCant_R	73.0% Right_Frontal_Pole; Right_Frontal_Orbital_Cortex	14.0%
51	-5	1	-11	-6.54	232	no_label	0% no_label	
52	-17	10	-16	-7.14	232	Olfactory_L	50.0% Left_Frontal_Orbital_Cortex	
53	-24	34	7	5.84	232	no_label	0% no_label	
54	-1	-58	75	7.82	232	no_label	0% no_label	
55	25	-17	72	6.24	218	Precentral_R	51.0% Right_Precentral_Gyrus	
56	15	10	-13	-6.58	204	Olfactory_R	31.0% Right_Frontal_Orbital_Cortex; Right_Putamen	6.0%
57	27	39	22	6.63	204	Frontal_Sup_2_R	36.0% Right_Frontal_Pole; Right_Middle_Frontal_Gyrus	14.0%
58	60	-17	46	7.5	204	Postcentral_R	39.0% Right_Postcentral_Gyrus; Right_Supramarginal_Gyrus_anterior_division	19.0%
59	-44	-68	-23	7.35	204	Cerebelum_Crus1_L	6.0% Left_Occipital_Fusiform_Gyrus	
60	-8	-39	53	5.72	204	Cingulate_Mid_L	36.0% Left_Postcentral_Gyrus; Left_Precuneous_Cortex; 9.0% Left_Precentral_Gyrus	18.0%
61	46	22	-18	7.25	204	Temporal_Pole_Sup_R	31.0% Right_Temporal_Pole; Right_Frontal_Orbital_Cortex	13.0%
62	-12	-44	63	6.1	204	Precuneus_L	41.0% Left_Postcentral_Gyrus; Left_Precuneous_Cortex	9.0%
63	39	-22	65	6.46	204	Precentral_R	37.0% Right_Postcentral_Gyrus; Right_Precentral_Gyrus	36.0%
64	10	-37	53	5.87	191	Precuneus_R	35.0% Right_Postcentral_Gyrus; Right_Precuneous_Cortex; Right_Precentral_Gyrus	16.0% 10.0%
65	56	-70	3	-7.21	191	Temporal_Mid_R	70.0% Right_Lateral_Occipital_Cortex_inferior_division	
66	8	-63	22	6.17	177	Precuneus_R	54.0% Right_Precuneous_Cortex; Right_Supracalcarine_Cortex; Right_Cuneal_Cortex	8.0% 8.0%
67	41	-41	-28	7.1	177	Fusiform_R	16.0% Right_Temporal_Occipital_Fusiform_Cortex; 7.0% Right_Temporal_Fusiform_Cortex_posterior_division	
68	68	-34	3	5.67	163	Temporal_Mid_R	26.0% Right_Superior_Temporal_Gyrus_posterior_division; 25.0%	

							Right_Middle_Temporal_Gyrus_posterior_division; 11.0% Right_Middle_Temporal_Gyrus_temporooccipital_part; 10.0% Right_Supramarginal_Gyrus_posterior_division
69	32	-27	60	5.39	163	Postcentral_R	43.0% Right_Postcentral_Gyrus; 28.0% Right_Precentral_Gyrus
70	41	3	-8	6.63	163	Insula_R	71.0% Right_Insular_Cortex
71	-44	-65	48	5.91	163	Angular_L	78.0% Left_Lateral_Occipital_Cortex_superior_division
72	46	41	-6	5.61	150	Frontal_Inf_Orb_2_R	77.0% Right_Frontal_Pole
73	68	-8	3	6.61	136	Temporal_Sup_R	9.0% Right_Planum_Temporale; 9.0% Right_Superior_Temporal_Gyrus_posterior_division; 6.0% Right_Superior_Temporal_Gyrus_anterior_division
74	63	-10	31	5.9	136	Postcentral_R	76.0% Right_Postcentral_Gyrus
75	-20	15	19	6.35	136	no_label	0% no_label
76	-20	-41	75	5.87	136	Postcentral_L	43.0% Left_Postcentral_Gyrus; 14.0% Left_Superior_Parietal_Lobule
77	-3	24	-28	6.17	136	no_label	18.0% Left_Subcallosal_Cortex
78	-22	-10	31	5.87	136	no_label	0% no_label
79	-22	-87	-8	-5.92	122	Occipital_Inf_L	37.0% Left_Occipital_Fusiform_Gyrus; 14.0% Left_Lateral_Occipital_Cortex_inferior_division
80	-41	-3	-11	6.85	122	Temporal_Sup_L	33.0% Left_Insular_Cortex; 19.0% Left_Planum_Polare
81	1	13	34	6.23	122	Cingulate_Mid_R	60.0% Right_Cingulate_Gyrus_anterior_division; 22.0% Left_Cingulate_Gyrus_anterior_division
82	-39	48	-11	6.45	122	OFClat_L	65.0% Left_Frontal_Pole
83	37	-37	-35	5.6	122	Cerebelum_6_R	0% no_label
84	63	-20	17	6.11	109	SupraMarginal_R	22.0% Right_Parietal_Operculum_Cortex; 21.0% Right_Central_Opercular_Cortex; 18.0% Right_Postcentral_Gyrus; 13.0% Right_Planum_Temporale; 10.0% Right_Supramarginal_Gyrus_anterior_division
85	60	3	-16	7.12	109	Temporal_Pole_Mid_R	31.0% Right_Middle_Temporal_Gyrus_anterior_division; 20.0% Right_Superior_Temporal_Gyrus_anterior_division; 14.0% Right_Temporal_Pole
86	41	-70	-25	6.81	109	Cerebelum_Crus1_R	0% no_label
87	39	-13	-4	6.33	109	Insula_R	69.0% Right_Insular_Cortex; 16.0% Right_Planum_Polare
88	-70	15	10	5.46	109	no_label	0% no_label
89	27	-1	-16	6.61	109	Amygdala_R	85.0% Right_Amygdala
90	-1	-94	-6	5.99	95	Calcarine_L	42.0% Left_Occipital_Pole; 8.0% Left_Lingual_Gyrus; 5.0% Right_Occipital_Pole
91	68	-17	-6	5.96	95	Temporal_Sup_R	46.0% Right_Middle_Temporal_Gyrus_posterior_division; 16.0% Right_Superior_Temporal_Gyrus_posterior_division
92	8	51	-20	5.79	95	Rectus_R	33.0% Right_Frontal_Pole; 29.0% Right_Frontal_Medial_Cortex
93	29	-34	-42	6.18	95	Cerebelum_10_R	0% no_label
94	-22	-77	-23	5.62	95	Cerebelum_Crus1_L	6.0% Left_Occipital_Fusiform_Gyrus
95	1	-3	29	5.84	95	Cingulate_Mid_R	36.0% Right_Cingulate_Gyrus_anterior_division; 24.0% Left_Cingulate_Gyrus_anterior_division
96	3	53	-16	5.9	81	Rectus_R	48.0% Right_Frontal_Medial_Cortex; 37.0% Right_Frontal_Pole
97	22	-25	-28	6.47	81	Cerebelum_3_R	26.0% Right_Parahippocampal_Gyrus_posterior_division; 14.0% Right_Parahippocampal_Gyrus_anterior_division

98	6	22	12	5.94	81	no_label	0% no_label
99	27	27	53	5.53	81	Frontal_Sup_2_R	36.0% Right_Superior_Frontal_Gyrus; 25.0% Right_Middle_Frontal_Gyrus
100	10	-32	-4	6.09	81	no_label	21.0% Brain-Stem; 5.0% Right_Thalamus
101	51	-25	55	5.55	81	Postcentral_R	62.0% Right_Postcentral_Gyrus; 11.0% Right_Supramarginal_Gyrus_anterior_division
102	-5	-70	65	7.43	81	no_label	8.0% Left_Lateral_Occipital_Cortex_superior_division; 6.0% Left_Precuneous_Cortex
103	27	-29	-28	5.79	81	Cerebelum_4_5_R	29.0% Right_Temporal_Fusiform_Cortex_posterior_division; 13.0% Right_Parahippocampal_Gyrus_posterior_division; 5.0% Right_Temporal_Occipital_Fusiform_Cortex
104	8	-27	7	5.46	81	Thalamus_R	93.0% Right_Thalamus
105	6	55	46	-6.8	68	no_label	6.0% Right_Frontal_Pole
106	-65	1	0	5.35	68	no_label	0% no_label
107	-60	-41	0	5.76	68	Temporal_Mid_L	35.0% Left_Middle_Temporal_Gyrus_posterior_division; 21.0% Left_Middle_Temporal_Gyrus_temporooccipital_part; 12.0% Left_Supramarginal_Gyrus_posterior_division; 8.0% Left_Superior_Temporal_Gyrus_posterior_division
108	-60	34	-30	6.41	68	no_label	0% no_label
109	37	13	-13	5.64	68	Insula_R	77.0% Right_Insular_Cortex
110	-5	-56	-4	5.6	68	Cerebelum_4_5_L	12.0% Left_Lingual_Gyrus
111	46	-72	-30	5.48	68	Cerebelum_Crus1_R	0% no_label
112	22	46	19	5.52	68	no_label	39.0% Right_Frontal_Pole
113	-41	34	10	5.82	68	Frontal_Inf_Tri_L	34.0% Left_Inferior_Frontal_Gyrus_pars_triangularis; 24.0% Left_Frontal_Pole
114	39	-17	39	5.27	68	Precentral_R	47.0% Right_Postcentral_Gyrus; 21.0% Right_Precentral_Gyrus
115	-29	10	-13	5.75	68	Insula_L	56.0% Left_Insular_Cortex; 9.0% Left_Frontal_Orbital_Cortex
116	39	-37	63	6.76	68	Postcentral_R	53.0% Right_Postcentral_Gyrus; 23.0% Right_Superior_Parietal_Lobule
117	18	-37	-20	5.72	68	Cerebelum_4_5_R	0% no_label

Table S2. Brain regions whose activation change was positive (red) or negative (blue) over time for the differential contrast “Task after regulate to ECN > Task after rest”. The X-, Y- and Z-coordinates are in MNI space and volume is in mm.

NR	X	Y	Z	Z-VALUE	VOLUME	AAL	HARVARD_oxford
1	6	-22	79	11.88	34499	Paracentral_Lobule_R	31.0% Right_Precentral_Gyrus
1	3	-56	75	9.42	34499	no_label	0% no_label
1	1	-82	53	9.35	34499	no_label	0% no_label
1	15	-94	15	8.88	34499	Occipital_Sup_R	32.0% Right_Occipital_Pole
1	-1	-96	-4	7.96	34499	Calcarine_L	41.0% Left_Occipital_Pole; 8.0% Right_Occipital_Pole
1	-24	-53	70	7.86	34499	Parietal_Sup_L	42.0% Left_Superior_Parietal_Lobule; 12.0% Left_Lateral_Occipital_Cortex_superior_division
1	-8	-41	53	7.55	34499	Cingulate_Mid_L	33.0% Left_Precuneous_Cortex; 29.0% Left_Postcentral_Gyrus; 6.0% Left_Precentral_Gyrus
1	-10	-77	31	7.52	34499	Cuneus_L	36.0% Left_Cuneal_Cortex; 26.0% Left_Precuneous_Cortex; 5.0% Left_Lateral_Occipital_Cortex_superior_division
1	1	-15	53	7.39	34499	Supp_Motor_Area_R	32.0% Right_Precentral_Gyrus; 15.0% Right_Juxtapositional_Lobule_Cortex_(formerly_Supplementary_Motor_Cortex); 14.0%

							Left_Precentral_Gyrus; 6.0% Left_Juxtapositional_Lobule_Cortex_(formerly_Supplementary_Motor_Cortex)
1	18	-70	29	6.96	34499	Cuneus_R	32.0% Right_Precuneous_Cortex; 25.0% Right_Cuneal_Cortex
1	10	-48	39	5.91	34499	Precuneus_R	44.0% Right_Precuneous_Cortex; 25.0% Right_Cingulate_Gyrus_posterior_division
1	6	-70	5	5.41	34499	Lingual_R	39.0% Right_Intracalcarine_Cortex; 32.0% Right_Lingual_Gyrus
2	-55	15	-4	9.58	12283	no_label	9.0% Left_Temporal_Pole; 9.0% Left_Inferior_Frontal_Gyrus_pars_opercularis
2	-55	-13	12	8.04	12283	Temporal_Sup_L	67.0% Left_Central_Opercular_Cortex; 5.0% Left_Heschl's_Gyrus_(includes_H1_and_H2)
2	-46	-15	36	7.45	12283	Postcentral_L	36.0% Left_Postcentral_Gyrus; 35.0% Left_Precentral_Gyrus
3	56	15	0	9.5	11709	Frontal_Inf_Oper_R	43.0% Right_Inferior_Frontal_Gyrus_pars_opercularis; 7.0% Right_Precentral_Gyrus; 5.0% Right_Inferior_Frontal_Gyrus_pars_triangularis
3	39	-10	19	8.5	11709	Rolandic_Oper_R	70.0% Right_Central_Opercular_Cortex
3	41	29	-16	6.7	11709	OFCpost_R	72.0% Right_Frontal_Orbital_Cortex; 22.0% Right_Frontal_Pole
3	39	-1	-4	6.6	11709	Insula_R	95.0% Right_Insular_Cortex
3	58	-3	39	6.41	11709	Precentral_R	53.0% Right_Precentral_Gyrus; 21.0% Right_Postcentral_Gyrus
4	32	58	22	8.48	8389	Frontal_Mid_2_R	70.0% Right_Frontal_Pole
4	49	41	5	7	8389	Frontal_Inf_Tri_R	79.0% Right_Frontal_Pole; 8.0% Right_Inferior_Frontal_Gyrus_pars_triangularis
4	27	55	-4	6.13	8389	Frontal_Sup_2_R	70.0% Right_Frontal_Pole
4	13	46	41	6.04	8389	Frontal_Sup_2_R	60.0% Right_Frontal_Pole
5	-3	24	63	9.53	6954	Supp_Motor_Area_L	47.0% Left_Superior_Frontal_Gyrus
5	-1	58	36	8.29	6954	Frontal_Sup_Medial_L	0% no_label
5	13	39	51	6.59	6954	Frontal_Sup_2_R	54.0% Right_Frontal_Pole; 33.0% Right_Superior_Frontal_Gyrus
6	63	-25	22	8.51	5560	SupraMarginal_R	40.0% Right_Supramarginal_Gyrus_anterior_division; 27.0% Right_Parietal_Operculum_Cortex; 14.0% Right_Planum_Temporale; 5.0% Right_Postcentral_Gyrus
6	60	-20	46	8.13	5560	Postcentral_R	33.0% Right_Postcentral_Gyrus; 32.0% Right_Supramarginal_Gyrus_anterior_division
7	20	-75	-18	8.31	3730	Cerebelum_6_R	17.0% Right_Occipital_Fusiform_Gyrus; 8.0% Right_Lingual_Gyrus
7	-5	-77	-13	7.94	3730	Cerebelum_6_L	40.0% Left_Lingual_Gyrus; 12.0% Left_Occipital_Fusiform_Gyrus
8	-41	22	48	7.81	3620	Frontal_Mid_2_L	52.0% Left_Middle_Frontal_Gyrus
8	-36	44	34	6.92	3620	Frontal_Mid_2_L	50.0% Left_Frontal_Pole
9	8	-17	7	7.4	2322	Thalamus_R	100.0% Right_Thalamus
10	-29	51	0	7.49	2090	Frontal_Sup_2_L	57.0% Left_Frontal_Pole
11	-44	-70	-23	7.36	2090	Cerebelum_Crus1_L	6.0% Left_Occipital_Fusiform_Gyrus
12	51	-65	-30	7.7	1789	Cerebelum_Crus1_R	0% no_label
13	44	22	46	6.88	1325	Frontal_Mid_2_R	81.0% Right_Middle_Frontal_Gyrus
14	51	-46	27	6.57	1120	SupraMarginal_R	43.0% Right_Angular_Gyrus; 13.0% Right_Supramarginal_Gyrus_posterior_division
15	-44	-51	60	8.29	1011	Parietal_Inf_L	18.0% Left_Superior_Parietal_Lobule; 7.0% Left_Angular_Gyrus; 7.0% Left_Supramarginal_Gyrus_posterior_division
16	-29	3	63	6.82	942	Frontal_Mid_2_L	37.0% Left_Middle_Frontal_Gyrus; 18.0% Left_Superior_Frontal_Gyrus

17	-44	-58	27	6.68	888	Angular_L	46.0% Left_Angular_Gyrus; 22.0% Left_Lateral_Occipital_Cortex_superior_division
18	46	-34	60	7.66	874	Postcentral_R	24.0% Right_Postcentral_Gyrus; 11.0% Right_Supramarginal_Gyrus_posterior_division
19	-65	-41	41	7.59	806	no_label	10.0% Left_Supramarginal_Gyrus_posterior_division
20	25	-25	72	8.35	751	Precentral_R	38.0% Right_Precentral_Gyrus; 15.0% Right_Postcentral_Gyrus
21	32	-82	-23	7.48	724	Cerebelum_Crus1_R	0% no_label
22	49	-10	55	7.64	642	Precentral_R	41.0% Right_Precentral_Gyrus; 27.0% Right_Postcentral_Gyrus
23	41	3	55	6.62	601	Frontal_Mid_2_R	54.0% Right_Middle_Frontal_Gyrus; 16.0% Right_Precentral_Gyrus
24	-36	1	12	7.1	560	Insula_L	60.0% Left_Central_Opercular_Cortex; 17.0% Left_Insular_Cortex
25	20	-41	72	6.44	505	Postcentral_R	39.0% Right_Postcentral_Gyrus; 15.0% Right_Superior_Parietal_Lobule
26	-24	55	15	6.4	491	Frontal_Sup_2_L	71.0% Left_Frontal_Pole
27	-39	-25	65	6.67	491	Precentral_L	50.0% Left_Postcentral_Gyrus; 27.0% Left_Precentral_Gyrus
28	-1	-17	-23	7.81	478	no_label	96.0% Brain-Stem
29	-10	-65	0	6.88	450	Lingual_L	37.0% Left_Lingual_Gyrus; 15.0% Left_Intracalcarine_Cortex
30	-24	-41	75	7.17	437	Postcentral_L	18.0% Left_Postcentral_Gyrus; 5.0% Left_Superior_Parietal_Lobule
31	53	-58	-23	7.51	437	Temporal_Inf_R	17.0% Right_Inferior_Temporal_Gyrus_temporooccipital_part
32	-29	53	29	5.97	409	Frontal_Mid_2_L	45.0% Left_Frontal_Pole
33	-3	63	17	7.19	409	Frontal_Sup_Medial_L	69.0% Left_Frontal_Pole
34	1	-63	-18	7.64	396	Vermis_6	0% no_label
35	-22	-65	-16	6.51	382	Cerebelum_6_L	26.0% Left_Occipital_Fusiform_Gyrus; 16.0% Left_Temporal_Occipital_Fusiform_Cortex; 13.0% Left_Lingual_Gyrus
36	-1	-29	27	6.79	368	no_label	71.0% Left_Cingulate_Gyrus_posterior_division
37	65	-29	0	7.31	355	Temporal_Mid_R	33.0% Right_Superior_Temporal_Gyrus_posterior_division; 28.0% Right_Middle_Temporal_Gyrus_posterior_division; 5.0% Right_Supramarginal_Gyrus_posterior_division
38	53	10	17	6.24	355	Frontal_Inf_Oper_R	44.0% Right_Inferior_Frontal_Gyrus_pars_opercularis; 25.0% Right_Precentral_Gyrus
39	-20	-29	67	6.3	341	Postcentral_L	35.0% Left_Postcentral_Gyrus; 25.0% Left_Precentral_Gyrus
40	-44	44	27	6.68	300	Frontal_Mid_2_L	28.0% Left_Frontal_Pole
41	20	-56	70	7.2	300	Parietal_Sup_R	35.0% Right_Superior_Parietal_Lobule; 28.0% Right_Lateral_Occipital_Cortex_superior_division
42	-34	-8	7	6.05	286	Insula_L	32.0% Left_Insular_Cortex
43	29	-27	60	6.47	286	Postcentral_R	43.0% Right_Postcentral_Gyrus; 29.0% Right_Precentral_Gyrus
44	20	-27	17	7.49	286	no_label	37.0% Right_Lateral_Ventricle; 5.0% Right_Caudate
45	-1	3	55	6.67	273	Supp_Motor_Area_L	52.0% Left_Juxtapositional_Lobule_Cortex_(formerly_Supplementary_Motor_Cortex)
46	-29	34	27	6.16	273	Frontal_Mid_2_L	33.0% Left_Middle_Frontal_Gyrus; 19.0% Left_Frontal_Pole
47	-55	-27	53	6.97	218	no_label	23.0% Left_Postcentral_Gyrus; 8.0% Left_Supramarginal_Gyrus_anterior_division
48	-29	-68	-25	6.14	218	Cerebelum_6_L	0% no_label

49	18	-53	-8	6.06	204	Lingual_R	76.0% Right_Lingual_Gyrus; Right_Temporal_Occipital_Fusiform_Cortex	7.0%
50	10	1	10	6.6	204	Caudate_R	25.0% Right_Caudate; 21.0% Right_Thalamus	
51	-15	46	41	6.41	191	Frontal_Sup_2_L	75.0% Left_Frontal_Pole	
52	-39	-41	65	6.23	177	Postcentral_L	26.0% Left_Superior_Parietal_Lobule; Left_Postcentral_Gyrus	24.0%
53	15	-84	-25	5.77	177	Cerebellum_Crus1_R	0% no_label	
54	-12	-6	17	6.27	163	Caudate_L	71.0% Left_Caudate; 5.0% Left_Lateral_Ventrical	
55	53	-48	0	5.9	163	Temporal_Mid_R	43.0% Right_Middle_Temporal_Gyrus_temporooccipital_part	
56	34	-89	0	-5.66	163	Occipital_Mid_R	40.0% Right_Occipital_Pole; Right_Lateral_Occipital_Cortex_inferior_division	29.0%
57	46	-68	-44	6.87	150	Cerebellum_Crus2_R	0% no_label	
58	-20	13	19	6.55	150	no_label	0% no_label	
59	-20	-6	72	5.85	136	Frontal_Sup_2_L	43.0% Left_Superior_Frontal_Gyrus	
60	-41	-10	-6	5.86	136	Temporal_Sup_L	34.0% Left_Insular_Cortex; 30.0% Left_Planum_Polare	
61	-20	-87	-23	6.46	136	Cerebellum_Crus1_L	20.0% Left_Occipital_Fusiform_Gyrus	
62	13	-87	34	6.11	136	Cuneus_R	33.0% Right_Occipital_Pole; Right_Lateral_Occipital_Cortex_superior_division; 12.0% Right_Cuneal_Cortex	16.0%
63	-1	-39	3	5.95	136	no_label	0% no_label	
64	65	-20	-4	6.67	122	Temporal_Sup_R	38.0% Right_Middle_Temporal_Gyrus_posterior_division; 25.0% Right_Superior_Temporal_Gyrus_posterior_division	
65	10	-34	-28	5.91	122	no_label	84.0% Brain-Stem	
66	56	-15	27	5.57	122	SupraMarginal_R	34.0% Right_Postcentral_Gyrus; Right_Supramarginal_Gyrus_anterior_division	8.0%
67	-10	-87	39	5.41	122	Occipital_Sup_L	43.0% Left_Lateral_Occipital_Cortex_superior_division; 16.0% Left_Occipital_Pole; 7.0% Left_Cuneal_Cortex	
68	22	-1	70	6.23	109	Frontal_Sup_2_R	48.0% Right_Superior_Frontal_Gyrus; Right_Precentral_Gyrus	11.0%
69	-51	-29	-6	6.06	109	Temporal_Mid_L	51.0% Left_Middle_Temporal_Gyrus_posterior_division; 12.0% Left_Superior_Temporal_Gyrus_posterior_division	
70	10	-60	0	6.16	109	Lingual_R	58.0% Right_Lingual_Gyrus; Right_Intracalcarine_Cortex	5.0%
71	22	27	-18	5.85	95	OFCmed_R	85.0% Right_Frontal_Orbital_Cortex	
72	-15	-1	75	5.7	95	Frontal_Sup_2_L	42.0% Left_Superior_Frontal_Gyrus	
73	-12	-27	-4	6.23	95	no_label	39.0% Left_Thalamus	
74	49	39	22	6.1	81	Frontal_Mid_2_R	59.0% Right_Frontal_Pole; Right_Middle_Frontal_Gyrus	20.0%
75	3	15	39	5.6	81	Cingulate_Mid_R	51.0% Right_Cingulate_Gyrus_anterior_division; 45.0% Right_Paracingulate_Gyrus	
76	56	-60	10	6	81	Temporal_Mid_R	41.0% Right_Lateral_Occipital_Cortex_inferior_division; 27.0% Right_Middle_Temporal_Gyrus_temporooccipital_part; 5.0% Right_Lateral_Occipital_Cortex_superior_division	
77	53	-53	22	5.51	81	Temporal_Sup_R	72.0% Right_Angular_Gyrus; Right_Lateral_Occipital_Cortex_superior_division	6.0%
78	-41	-34	15	5.71	81	Temporal_Sup_L	50.0% Left_Planum_Temporale; Left_Parietal_Operculum_Cortex	37.0%
79	15	-94	-16	6.9	81	Lingual_R	32.0% Right_Occipital_Pole; Right_Lateral_Occipital_Cortex_inferior_division	6.0%
80	-41	-3	-13	6.21	81	Temporal_Sup_L	60.0% Left_Planum_Polare; 8.0% Left_Insular_Cortex	

81	13	-22	-6	5.99	81	no_label	6.0% Right_Thalamus
82	-3	60	29	6.05	81	Frontal_Sup_Medial_L	43.0% Left_Frontal_Pole; 6.0% Left_Superior_Frontal_Gyrus
83	-27	-1	70	6.77	81	Frontal_Sup_2_L	27.0% Left_Superior_Frontal_Gyrus
84	-20	-20	22	5.78	81	Caudate_L	12.0% Left_Caudate
85	49	-60	-4	5.6	68	Temporal_Inf_R	43.0% Right_Lateral_Occipital_Cortex_inferior_division; 12.0% Right_Inferior_Temporal_Gyrus_temporooccipital_part; 10.0% Right_Middle_Temporal_Gyrus_temporooccipital_part
86	-48	44	12	5.98	68	Frontal_Inf_Tri_L	44.0% Left_Frontal_Pole
87	-10	10	34	5.34	68	Cingulate_Mid_L	23.0% Left_Cingulate_Gyrus_anterior_division; 15.0% Left_Paracingulate_Gyrus
88	41	44	29	6.25	68	Frontal_Mid_2_R	75.0% Right_Frontal_Pole
89	37	34	29	5.61	68	Frontal_Mid_2_R	30.0% Right_Middle_Frontal_Gyrus; 24.0% Right_Frontal_Pole
90	25	5	63	5.44	68	Frontal_Sup_2_R	54.0% Right_Superior_Frontal_Gyrus; 6.0% Right_Middle_Frontal_Gyrus
91	-22	24	12	5.55	68	no_label	0% no_label

Table S3. Brain regions whose activation change was positive (red) or negative (blue) over time for the differential contrast “Task after regulate to SN > Task after regulate to ECN”. The X-, Y- and Z-coordinates are in MNI space and volume is in mm.

NR	X	Y	Z	Z-VALUE	VOLUME	AAL	HARVARD_OXFORD
1	-15	-72	58	-7.1	327	Parietal_Sup_L	65.0% Left_Lateral_Occipital_Cortex_superior_division
2	25	3	65	-6.67	286	Frontal_Sup_2_R	62.0% Right_Superior_Frontal_Gyrus; 6.0% Right_Middle_Frontal_Gyrus
3	44	1	-37	-6.29	273	Temporal_Inf_R	42.0% Right_Inferior_Temporal_Gyrus_anterior_division; 10.0% Right_Middle_Temporal_Gyrus_anterior_division
4	-3	27	0	6.62	232	no_label	6.0% Left_Subcallosal_Cortex
5	15	10	-13	-6.83	218	Olfactory_R	31.0% Right_Frontal_Orbital_Cortex; 6.0% Right_Putamen
6	29	65	-8	-7.71	150	no_label	53.0% Right_Frontal_Pole
7	27	67	0	-6.06	150	Frontal_Sup_2_R	42.0% Right_Frontal_Pole
8	-32	1	63	-6.85	136	Frontal_Mid_2_L	42.0% Left_Middle_Frontal_Gyrus; 5.0% Left_Superior_Frontal_Gyrus
9	-24	-56	70	-7.26	109	Parietal_Sup_L	28.0% Left_Superior_Parietal_Lobule; 19.0% Left_Lateral_Occipital_Cortex_superior_division
10	3	58	43	-7.62	95	no_label	0% no_label
11	-22	55	36	-6.5	81	no_label	8.0% Left_Frontal_Pole
12	-27	70	12	-5.94	81	no_label	0% no_label
13	-55	-68	3	-6.01	81	Temporal_Mid_L	63.0% Left_Lateral_Occipital_Cortex_inferior_division; 9.0% Left_Middle_Temporal_Gyrus_temporooccipital_part
14	-12	-63	67	-6.48	81	Precuneus_L	50.0% Left_Lateral_Occipital_Cortex_superior_division; 5.0% Left_Superior_Parietal_Lobule
15	15	72	15	-6.87	68	no_label	11.0% Right_Frontal_Pole
16	6	72	10	-6.47	68	Frontal_Sup_Medial_R	28.0% Right_Frontal_Pole
17	32	-1	63	-5.75	68	Frontal_Sup_2_R	36.0% Right_Middle_Frontal_Gyrus; 15.0% Right_Superior_Frontal_Gyrus; 12.0% Right_Precentral_Gyrus
18	-24	58	-11	-5.85	68	Frontal_Mid_2_L	76.0% Left_Frontal_Pole

19	-34	60	-11	-5.97	68	Frontal_Mid_2_L	71.0% Left_Frontal_Pole
----	-----	----	-----	-------	----	-----------------	-------------------------

Emotional Faces Oddball task

Table S4. Brain regions whose activation change was positive (red) or negative (blue) over time for the differential contrast “Task after regulate to SN > Task after rest”. The X-, Y- and Z-coordinates are in MNI space and volume is in mm.

NR	X	Y	Z	Z-VALUE	VOLUME	AAL	HARVARD_oxford
1	34	-22	67	10.07	18923	Precentral_R	52.0% Right_Precentral_Gyrus; 19.0% Right_Postcentral_Gyrus
1	1	-84	51	10.04	18923	no_label	0% no_label
1	3	-56	75	9.25	18923	no_label	0% no_label
1	6	-17	79	8.85	18923	Paracentral_Lobule_R	13.0% Right_Precentral_Gyrus
1	-5	-77	-16	8.37	18923	Cerebelum_6_L	21.0% Left_Lingual_Gyrus; 9.0% Left_Occipital_Fusiform_Gyrus
1	3	-91	27	7.69	18923	no_label	34.0% Right_Occipital_Pole; 10.0% Right_Cuneal_Cortex
1	10	-82	3	7.61	18923	Calcarine_R	45.0% Right_Intracalcarine_Cortex; 14.0% Right_Lingual_Gyrus
1	-1	-22	55	7.55	18923	Paracentral_Lobule_L	61.0% Left_Precentral_Gyrus
1	-29	-84	-25	6.44	18923	Cerebelum_Crus1_L	8.0% Left_Lateral_Occipital_Cortex_inferior_division
2	1	-60	-20	9.19	3675	Vermis_6	0% no_label
2	-1	-41	-6	7.94	3675	Vermis_4_5	0% no_label
3	-1	-72	-35	10.32	3251	Vermis_8	0% no_label
4	29	-84	-23	8.17	2650	Cerebelum_Crus1_R	7.0% Right_Lateral_Occipital_Cortex_inferior_division
5	3	13	70	9.25	2186	Supp_Motor_Area_R	18.0% Right_Superior_Frontal_Gyrus; 8.0% Right_Juxtapositional_Lobule_Cortex_(formerly_Supplementary_Motor_Cortex)
5	-3	39	53	7.38	2186	Frontal_Sup_Medial_L	50.0% Left_Superior_Frontal_Gyrus; 5.0% Left_Frontal_Pole
6	-53	17	-6	7.91	2063	no_label	8.0% Left_Inferior_Frontal_Gyrus_pars_opercularis; 6.0% Left_Temporal_Pole; 6.0% Left_Inferior_Frontal_Gyrus_pars_triangularis
6	-63	3	12	6.16	2063	Frontal_Inf_Oper_L	41.0% Left_Precentral_Gyrus
7	-10	-94	0	7.46	1393	Occipital_Mid_L	56.0% Left_Occipital_Pole; 5.0% Left_Intracalcarine_Cortex
8	-39	-63	53	7.35	1338	Parietal_Inf_L	67.0% Left_Lateral_Occipital_Cortex_superior_division
9	-51	-58	-25	6.8	1024	Cerebelum_Crus1_L	10.0% Left_Inferior_Temporal_Gyrus_temporooccipital_part
10	49	-70	-25	7.61	983	Cerebelum_Crus1_R	0% no_label
11	-10	-63	-16	6.41	929	Cerebelum_6_L	0% no_label
12	-44	44	0	6.55	929	Frontal_Mid_2_L	86.0% Left_Frontal_Pole
13	39	-8	19	7.52	847	Rolandic_Oper_R	36.0% Right_Central_Opercular_Cortex
14	44	15	-4	7.21	847	Insula_R	49.0% Right_Insular_Cortex; 15.0% Right_Frontal_Operculum_Cortex; 5.0% Right_Frontal_Orbital_Cortex
15	-39	1	3	6.7	819	Insula_L	79.0% Left_Insular_Cortex
16	-17	44	36	6.56	655	Frontal_Sup_2_L	75.0% Left_Frontal_Pole
17	-53	-48	39	6.44	573	Parietal_Inf_L	51.0% Left_Supramarginal_Gyrus_posterior_division; 17.0% Left_Angular_Gyrus
18	-29	58	19	6.76	546	Frontal_Sup_2_L	76.0% Left_Frontal_Pole
19	-1	-22	10	6.4	478	no_label	39.0% Left_Thalamus
20	58	5	3	6.33	464	Rolandic_Oper_R	23.0% Right_Precentral_Gyrus; 19.0% Right_Central_Opercular_Cortex; 14.0% Right_Planum_Polare; 10.0% Right_Temporal_Pole
21	-58	-27	51	7.08	437	no_label	23.0% Left_Supramarginal_Gyrus_anterior_division; 16.0% Left_Postcentral_Gyrus

22	-29	-37	70	8.36	423	Postcentral_L	44.0% Left_Postcentral_Gyrus; 15.0% Left_Superior_Parietal_Lobule
23	-12	41	15	5.95	396	Cingulate_Ant_L	32.0% Left_Paracingulate_Gyrus; 8.0% Left_Cingulate_Gyrus_anterior_division
24	-41	-15	19	7.62	396	Rolandic_Oper_L	60.0% Left_Central_Opercular_Cortex
25	60	-17	43	6.34	396	Postcentral_R	45.0% Right_Postcentral_Gyrus; 30.0% Right_Supramarginal_Gyrus_anterior_division
26	51	-32	55	6.96	396	Parietal_Inf_R	30.0% Right_Supramarginal_Gyrus_anterior_division; 30.0% Right_Postcentral_Gyrus; 10.0% Right_Supramarginal_Gyrus_posterior_division
27	-17	-13	27	6.31	368	no_label	17.0% Left_Lateral_Ventricular; 10.0% Left_Caudate
28	29	-80	-40	6.04	355	Cerebelum_Crus2_R	0% no_label
29	-22	-65	-20	6.66	341	Cerebelum_6_L	0% no_label
30	-27	17	63	6.05	327	Frontal_Mid_2_L	22.0% Left_Superior_Frontal_Gyrus; 11.0% Left_Middle_Frontal_Gyrus
31	-53	-63	24	5.96	327	Angular_L	60.0% Left_Lateral_Occipital_Cortex_superior_division; 25.0% Left_Angular_Gyrus
32	-15	27	58	6.27	327	Frontal_Sup_2_L	66.0% Left_Superior_Frontal_Gyrus
33	-58	-6	39	5.98	314	Postcentral_L	63.0% Left_Precentral_Gyrus; 24.0% Left_Postcentral_Gyrus
34	18	-1	27	6.66	300	no_label	6.0% Right_Caudate
35	-51	-15	41	5.66	259	Postcentral_L	54.0% Left_Postcentral_Gyrus; 24.0% Left_Precentral_Gyrus
36	-34	5	15	6.15	245	Rolandic_Oper_L	36.0% Left_Central_Opercular_Cortex
37	37	-37	63	6.58	232	Postcentral_R	50.0% Right_Postcentral_Gyrus; 23.0% Right_Superior_Parietal_Lobule
38	22	-25	-28	6.91	232	Cerebelum_3_R	26.0% Right_Parahippocampal_Gyrus_posterior_division; 14.0% Right_Parahippocampal_Gyrus_anterior_division
39	56	10	15	5.65	218	Frontal_Inf_Oper_R	47.0% Right_Inferior_Frontal_Gyrus_pars_opercularis; 27.0% Right_Precentral_Gyrus
40	39	5	-1	5.86	191	no_label	86.0% Right_Insular_Cortex
41	-5	58	24	5.48	191	Frontal_Sup_Medial_L	45.0% Left_Frontal_Pole; 24.0% Left_Superior_Frontal_Gyrus
42	-22	-75	-23	5.98	177	Cerebelum_Crus1_L	0% no_label
43	-27	-72	53	6.59	177	Parietal_Sup_L	61.0% Left_Lateral_Occipital_Cortex_superior_division
44	-22	-29	-40	5.84	163	Cerebelum_10_L	0% no_label
45	65	-20	29	6.16	163	SupraMarginal_R	54.0% Right_Supramarginal_Gyrus_anterior_division; 24.0% Right_Postcentral_Gyrus
46	39	1	15	6.23	136	Rolandic_Oper_R	67.0% Right_Central_Opercular_Cortex
47	-12	-96	19	6.34	136	Occipital_Sup_L	57.0% Left_Occipital_Pole
48	25	-34	-42	7.39	136	Cerebelum_10_R	0% no_label
49	63	-17	15	6.29	136	Rolandic_Oper_R	30.0% Right_Central_Opercular_Cortex; 23.0% Right_Planum_Temporale; 11.0% Right_Postcentral_Gyrus; 7.0% Right_Parietal_Operculum_Cortex; 7.0% Right_Supramarginal_Gyrus_anterior_division
50	-20	-22	22	5.85	136	Caudate_L	17.0% Left_Caudate
51	-46	-10	55	7.16	136	Postcentral_L	56.0% Left_Precentral_Gyrus; 17.0% Left_Postcentral_Gyrus
52	-24	53	29	6.37	122	Frontal_Sup_2_L	78.0% Left_Frontal_Pole
53	34	48	29	5.81	122	Frontal_Mid_2_R	80.0% Right_Frontal_Pole
54	53	-53	-35	6.13	122	Cerebelum_Crus1_R	0% no_label
55	46	39	7	5.41	122	Frontal_Inf_Tri_R	59.0% Right_Frontal_Pole; 13.0% Right_Inferior_Frontal_Gyrus_pars_triangularis
56	18	-60	-23	5.43	109	Cerebelum_6_R	0% no_label

57	-17	-48	75	5.78	109	Parietal_Sup_L	30.0% Left_Postcentral_Gyrus; Left_Superior_Parietal_Lobule	23.0%
58	-8	-32	5	6.2	109	Thalamus_L	90.0% Left_Thalamus	
59	37	-6	7	6.1	109	Insula_R	77.0% Right_Insular_Cortex	
60	13	-27	-25	6.38	95	no_label	99.0% Brain-Stem	
61	-3	36	27	5.4	95	Cingulate_Ant_L	73.0% Left_Paracingulate_Gyrus; Left_Cingulate_Gyrus_anterior_division	23.0%
62	6	-58	-6	5.54	95	Vermis_4_5	7.0% Right_Lingual_Gyrus	
63	-41	-80	-23	6.01	95	Cerebelum_Crus1_L	11.0% Left_Lateral_Occipital_Cortex_inferior_division	
64	-5	-8	46	5.54	95	Cingulate_Mid_L	37.0% Left_Juxtapositional_Lobule_Cortex_(formerly_Supplementary_Motor_Cortex); Left_Cingulate_Gyrus_anterior_division	35.0%
65	41	-60	-42	5.55	81	Cerebelum_Crus2_R	0% no_label	
66	34	55	22	5.81	81	Frontal_Sup_2_R	83.0% Right_Frontal_Pole	
67	51	46	-11	5.55	81	Frontal_Inf_Orb_2_R	42.0% Right_Frontal_Pole	
68	60	-41	41	5.8	81	SupraMarginal_R	63.0% Right_Supramarginal_Gyrus_posterior_division; 17.0% Right_Angular_Gyrus	
69	32	65	-1	6.91	81	no_label	45.0% Right_Frontal_Pole	
70	-17	53	-6	6.28	81	Frontal_Sup_2_L	10.0% Left_Frontal_Pole	
71	-39	-51	65	5.85	81	no_label	22.0% Left_Superior_Parietal_Lobule	
72	22	-56	-23	6.03	81	Cerebelum_6_R	0% no_label	
73	-34	-51	-23	5.96	81	Cerebelum_6_L	30.0% Left_Temporal_Occipital_Fusiform_Cortex	
74	-17	-22	17	5.86	81	no_label	18.0% Left_Thalamus; 5.0% Left_Caudate	
75	-32	-8	65	5.61	81	Frontal_Sup_2_L	46.0% Left_Precentral_Gyrus; Left_Middle_Frontal_Gyrus	5.0%
76	6	63	19	5.37	81	Frontal_Sup_Medial_R	80.0% Right_Frontal_Pole	
77	-15	-70	10	5.84	81	Calcarine_L	58.0% Left_Intracalcarine_Cortex; Left_Supracalcarine_Cortex	7.0%
78	-41	-58	29	5.42	68	Angular_L	33.0% Left_Angular_Gyrus; Left_Lateral_Occipital_Cortex_superior_division	18.0%
79	39	-3	0	5.67	68	Insula_R	90.0% Right_Insular_Cortex	
80	-32	-22	70	6.28	68	Precentral_L	43.0% Left_Precentral_Gyrus; Left_Postcentral_Gyrus	22.0%
81	-29	-6	34	5.66	68	no_label	0% no_label	
82	-1	-8	7	7.19	68	no_label	82.0% Left_Thalamus	
83	-3	-70	46	6.05	68	Precuneus_L	86.0% Left_Precuneous_Cortex	
84	-65	-1	0	5.85	68	no_label	5.0% Left_Superior_Temporal_Gyrus_anterior_division	

Table S5. Brain regions whose activation change was positive (red) or negative (blue) over time for the differential contrast “Task after regulate to ECN > Task after rest”. The X-, Y- and Z-coordinates are in MNI space and volume is in mm.

NR	X	Y	Z	Z-VALUE	VOLUME	AAL	HARVARD_OXFORD	
1	-1	-80	53	7.88	1161	no_label	12.0% Left_Precuneous_Cortex	
1	10	-94	29	6.46	1161	no_label	55.0% Right_Occipital_Pole	
2	3	-94	10	6.86	956	Calcarine_L	53.0% Right_Occipital_Pole; 8.0% Left_Occipital_Pole	
3	49	-29	27	6.52	819	no_label	43.0% Right_Parietal_Operculum_Cortex; Right_Supramarginal_Gyrus_anterior_division	15.0%
4	44	13	-1	6.74	437	Insula_R	41.0% Right_Insular_Cortex; Right_Frontal_Operculum_Cortex; Right_Central_Opercular_Cortex	19.0% 9.0%
5	-5	-60	72	8.11	327	Precuneus_L	7.0% Left_Lateral_Occipital_Cortex_superior_division	
6	3	-29	79	6.17	273	Paracentral_Lobule_R	13.0% Right_Precentral_Gyrus; Right_Postcentral_Gyrus	6.0%

7	1	-80	36	6.08	259	Cuneus_L	22.0% Left_Cuneal_Cortex; 18.0% Left_Precuneous_Cortex; 11.0% Right_Cuneal_Cortex; 9.0% Right_Precuneous_Cortex
8	20	-89	29	6.17	259	Occipital_Sup_R	52.0% Right_Occipital_Pole; 22.0% Right_Lateral_Occipital_Cortex_superior_division
9	-60	1	7	6.83	218	Rolandic_Oper_L	60.0% Left_Precentral_Gyrus
10	46	-72	-25	6.6	191	Cerebelum_Crus1_R	0% no_label
11	51	-56	-23	6.27	177	Temporal_Inf_R	39.0% Right_Inferior_Temporal_Gyrus_temporooccipital_part; 13.0% Right_Temporal_Occipital_Fusiform_Cortex
12	-39	-63	53	6.39	177	Parietal_Inf_L	67.0% Left_Lateral_Occipital_Cortex_superior_division
13	-10	-84	3	5.68	177	Calcarine_L	46.0% Left_Intracalcarine_Cortex; 8.0% Left_Lingual_Gyrus
14	-12	-96	17	5.87	150	Occipital_Sup_L	56.0% Left_Occipital_Pole
15	10	-82	3	5.63	136	Calcarine_R	45.0% Right_Intracalcarine_Cortex; 14.0% Right_Lingual_Gyrus
16	8	-13	46	5.89	122	Cingulate_Mid_R	37.0% Right_Juxtapositional_Lobule_Cortex_(formerly_Supplementary_Motor_Cortex); 19.0% Right_Cingulate_Gyrus_posterior_division; 18.0% Right_Cingulate_Gyrus_anterior_division; 14.0% Right_Precentral_Gyrus
17	-12	-77	29	5.96	109	Cuneus_L	40.0% Left_Cuneal_Cortex; 18.0% Left_Precuneous_Cortex; 5.0% Left_Lateral_Occipital_Cortex_superior_division
18	53	13	7	5.96	109	Frontal_Inf_Oper_R	66.0% Right_Inferior_Frontal_Gyrus_pars_opercularis; 9.0% Right_Precentral_Gyrus
19	37	1	15	6.4	109	Insula_R	54.0% Right_Central_Opercular_Cortex; 19.0% Right_Insular_Cortex
20	-17	-65	-13	5.64	95	Cerebelum_6_L	25.0% Left_Lingual_Gyrus; 22.0% Left_Occipital_Fusiform_Gyrus; 8.0% Left_Temporal_Occipital_Fusiform_Cortex
21	63	-20	19	5.75	95	SupraMarginal_R	23.0% Right_Postcentral_Gyrus; 22.0% Right_Central_Opercular_Cortex; 22.0% Right_Supramarginal_Gyrus_anterior_division; 15.0% Right_Parietal_Operculum_Cortex; 7.0% Right_Planum_Temporale
22	3	-51	75	5.67	95	no_label	7.0% Right_Postcentral_Gyrus
23	1	-72	-32	5.55	81	Vermis_7	0% no_label
24	1	-68	60	6.08	81	Precuneus_R	5.0% Left_Precuneous_Cortex
25	-39	-15	19	6.01	81	Rolandic_Oper_L	74.0% Left_Central_Opercular_Cortex; 6.0% Left_Parietal_Operculum_Cortex
26	13	-72	-6	5.59	81	Lingual_R	53.0% Right_Lingual_Gyrus; 12.0% Right_Occipital_Fusiform_Gyrus
27	-8	-37	77	5.95	68	Paracentral_Lobule_L	42.0% Left_Postcentral_Gyrus; 8.0% Left_Precentral_Gyrus
28	-10	-91	0	6.16	68	no_label	42.0% Left_Occipital_Pole; 12.0% Left_Intracalcarine_Cortex; 7.0% Left_Lingual_Gyrus
29	15	-37	75	5.72	68	Postcentral_R	52.0% Right_Postcentral_Gyrus
30	6	-17	79	7.26	68	Paracentral_Lobule_R	13.0% Right_Precentral_Gyrus
31	-48	-58	-23	6.29	68	Cerebelum_Crus1_L	33.0% Left_Inferior_Temporal_Gyrus_temporooccipital_part; 18.0% Left_Temporal_Occipital_Fusiform_Cortex; 8.0% Left_Lateral_Occipital_Cortex_inferior_division
32	-55	-60	-18	6.21	68	Temporal_Inf_L	45.0% Left_Inferior_Temporal_Gyrus_temporooccipital_part; 24.0% Left_Lateral_Occipital_Cortex_inferior_division;

							6.0% Left_Middle_Temporal_Gyrus_temporooccipital_part
--	--	--	--	--	--	--	--

Table S6. Brain regions whose activation change was positive (red) or negative (blue) over time for the differential contrast “Task after regulate to SN > Task after regulate to ECN”. The X-, Y- and Z-coordinates are in MNI space and volume is in mm.

NR	X	Y	Z	Z-VALUE	VOLUME	AAL	HARVARD_OXFORD
1	-1	-41	-6	6.52	519	Vermis_4_5	0% no_label
2	1	-70	-40	6.64	450	Vermis_8	0% no_label
3	-20	46	41	6.9	245	Frontal_Sup_2_L	70.0% Left_Frontal_Pole
4	41	39	10	5.86	136	Frontal_Mid_2_R	62.0% Right_Frontal_Pole; Right_Inferior_Frontal_Gyrus_pars_triangularis 8.0%
5	34	-22	67	7.52	136	Precentral_R	52.0% Right_Precentral_Gyrus; Right_Postcentral_Gyrus 19.0%
6	-12	8	72	8.04	122	Frontal_Sup_2_L	32.0% Left_Superior_Frontal_Gyrus
7	-20	55	15	6.11	122	Frontal_Sup_2_L	49.0% Left_Frontal_Pole
8	32	39	0	6.09	109	no_label	0% no_label
9	13	36	10	5.6	109	Cingulate_Ant_R	11.0% Right_Cingulate_Gyrus_anterior_division
10	20	44	34	5.54	95	Frontal_Sup_2_R	53.0% Right_Frontal_Pole
11	10	46	-1	5.68	95	Frontal_Med_Orb_R	60.0% Right_Paracingulate_Gyrus; Right_Cingulate_Gyrus_anterior_division; 9.0% Right_Frontal_Medial_Cortex 9.0%
12	-1	-58	-23	5.93	95	Vermis_6	0% no_label
13	-8	46	15	5.8	95	Cingulate_Ant_L	72.0% Left_Paracingulate_Gyrus; Left_Cingulate_Gyrus_anterior_division 14.0%
14	13	53	-11	5.85	81	Frontal_Sup_2_R	0% no_label
15	3	13	70	7.14	81	Supp_Motor_Area_R	18.0% Right_Superior_Frontal_Gyrus; Right_Juxtapositional_Lobule_Cortex_(formerly_Suppl ementary_Motor_Cortex) 8.0%
16	-41	55	-4	5.8	68	Frontal_Mid_2_L	82.0% Left_Frontal_Pole